

AD A132 443

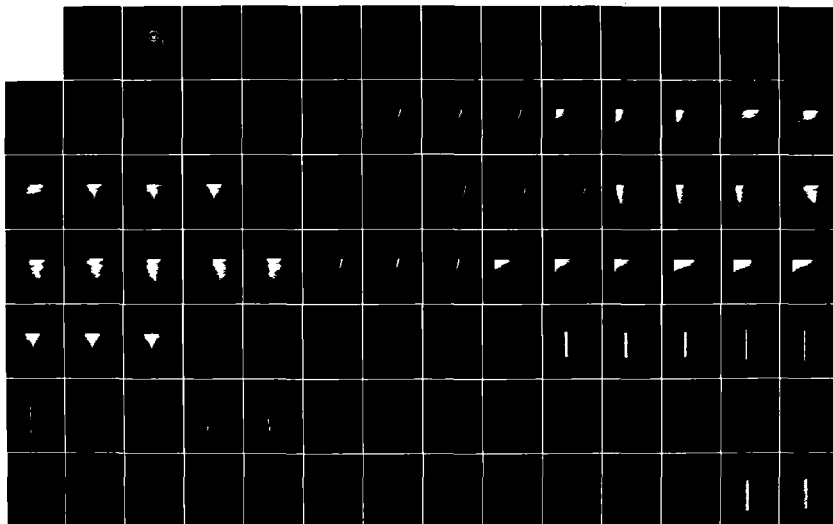
AN ANALYSIS OF A PC-3 MICROPULSATION IN THE GEOMAGNETIC  
FIELD(U) NAVAL POSTGRADUATE SCHOOL MONTEREY CA  
K B STEVENS JUN 83

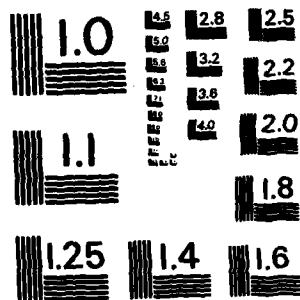
1/2

UNCLASSIFIED

F/G 8/14

NL





MICROCOPY RESOLUTION TEST CHART  
NATIONAL BUREAU OF STANDARDS-1963-A

ADA 132443

2

# NAVAL POSTGRADUATE SCHOOL

Monterey, California



DTIC  
ELECTE  
SEP 15 1983  
S B

## THESIS

AN ANALYSIS OF A PC-3 MICROPULSATION IN  
THE GEOMAGNETIC FIELD

by

Kurt B. Stevens

June 1983

Thesis Advisor:

A. Ochadlick

Approved for public release; distribution unlimited

83 09 14 062

DTIC FILE COPY

Unclassified

SECURITY CLASSIFICATION OF THIS PAGE (When Data Entered)

REPORT DOCUMENTATION PAGE		READ INSTRUCTIONS BEFORE COMPLETING FORM
1. REPORT NUMBER	2. GOVT ACCESSION NO.	3. RECIPIENT'S CATALOG NUMBER
	AD A132	443
4. TITLE (and Subtitle)		5. TYPE OF REPORT & PERIOD COVERED
An Analysis of a PC-3 Micropulsation in the Geomagnetic Field		Master's Thesis June 1983
		6. PERFORMING ORG. REPORT NUMBER
7. AUTHOR(s)		8. CONTRACT OR GRANT NUMBER(s)
Kurt B. Stevens		
9. PERFORMING ORGANIZATION NAME AND ADDRESS		10. PROGRAM ELEMENT, PROJECT, TASK AREA & WORK UNIT NUMBERS
Naval Postgraduate School Monterey, California 93940		
11. CONTROLLING OFFICE NAME AND ADDRESS		12. REPORT DATE
Naval Postgraduate School Monterey, California 93940		June 1983
		13. NUMBER OF PAGES
		141
14. MONITORING AGENCY NAME & ADDRESS (if different from Controlling Office)		15. SECURITY CLASS. (of this report)
		Unclassified
		15a. DECLASSIFICATION/DOWNGRADING SCHEDULE
16. DISTRIBUTION STATEMENT (of this Report)		
Approved for public release; distribution unlimited		
17. DISTRIBUTION STATEMENT (of the abstract entered in Block 20, if different from Report)		
18. SUPPLEMENTARY NOTES		
19. KEY WORDS (Continue on reverse side if necessary and identify by block number)		
Micropulsation Coherence Degree of Polarization Ellipticity		
20. ABSTRACT (Continue on reverse side if necessary and identify by block number)		
<p>The Naval Postgraduate School has an ongoing effort to study geomagnetic noise and micropulsations in the ULF frequency range (<math>.05 &lt; f &lt; 10</math> Hz). Data is collected by three orthogonally mounted coils at a remote land site and telemetered to the laboratory for computer analysis.</p> <p>To isolate data containing a micropulsation event, time series plots of the magnetic field were generated. The</p> <p>(continued).</p>		

DD FORM 1 JAN 73 1473

EDITION OF 1 NOV 65 IS OBSOLETE  
S/N 0102- LF-014-6601

1

Unclassified

SECURITY CLASSIFICATION OF THIS PAGE (When Data Entered)

Unclassified

SECURITY CLASSIFICATION OF THIS PAGE (When Data Entered)

Item 20. (continued)

development of a double running average routine made possible the isolation of micropulsations in large data sets. A type PC-3 micropulsation was found and the coherence, ellipticity and polarization properties were determined as follows: Coherence = 0.99, Degree of Polarization = 0.99 and the micropulsation was elliptically polarized.

Power spectral density (PSD) plots summarizing data segments about two hours long occasionally contained structures found to be artificial and not representative of natural phenomena in the geomagnetic field. Methods to avoid this anomalous behavior in PSD plots are suggested.

Accession For	
NTIS GRA&I	<input checked="checked" type="checkbox"/>
DTIC TAB	<input type="checkbox"/>
Unannounced	<input type="checkbox"/>
Justification	
By	
Distribution/	
Availability Codes	
Dist	Avail and/or Special
A	



Unclassified

SECURITY CLASSIFICATION OF THIS PAGE (When Data Entered)

Approved for public release; distribution unlimited

An Analysis of a PC-3 Micropulsation in the Geomagnetic Field

by

Kurt B. Stevens  
Captain, United States Air Force  
B.S., United States Air Force Academy, 1979

Submitted in partial fulfillment of the  
requirements for the degree of

MASTER OF SCIENCE IN PHYSICS

from the

NAVAL POSTGRADUATE SCHOOL  
June 1983

Author:

Kurt B. Stevens

Approved by:

Arthur R. Ochallish, Jr.

Thesis Advisor

Otto Reitz

Second Reader

Y. E. Schacher

Chairman, Department of Physics

John Dyer

Dean of Science and Engineering

# ABSTRACT

→ The Naval Postgraduate School has an ongoing effort to study geomagnetic noise and micropulsations in the ULF frequency range ( $0.05 \leq f \leq 10$  Hz). Data is collected by three orthogonally mounted coils at a remote land site and telemetered to the laboratory for computer analysis.

To isolate data containing a micropulsation event, time series plots of the magnetic field were generated. The development of a double running average routine made possible the isolation of micropulsations in large data sets. A type PC-3 micropulsation was found and the coherence, ellipticity and polarization properties were determined as follows: Coherence = 0.99, Degree of Polarization = 0.99 and the micropulsation was elliptically polarized.

Power spectral density (PSD) plots summarizing data segments about two hours long occasionally contained structures found to be artificial and not representative of natural phenomena in the geomagnetic field. Methods to avoid this anomalous behavior in PSD plots are suggested. ↗

## TABLE OF CONTENTS

I.	INTRODUCTION -----	8
II.	BACKGROUND -----	10
	A. COLLECTION SYSTEM -----	10
	1. System Calibration -----	11
	B. PREVIOUS SOFTWARE -----	13
	C. ANALYSIS OF INITIAL DATA PLOTS -----	17
III.	TIME SERIES DATA -----	59
	A. TIME SERIES VOLTAGE DATA -----	59
	1. Voltage Software -----	59
	2. Time Series Voltage Data Analysis -----	61
	B. TIME SERIES MAGNETIC FIELD DATA -----	69
	1. Magnetic Field Software -----	69
	2. Smoothed Magnetic Field Data Analysis -----	79
IV.	SYSTEM AND SOFTWARE VALIDATION -----	88
	A. EXPERIMENTAL APPARATUS -----	88
	B. EXPERIMENT RESULTS -----	90
	1. Voltage -----	90
	2. Magnetic Field -----	97
V.	MICROPULSATIONS -----	110
	A. THEORY -----	110
	B. MICROPULSATION DATA ANALYSIS -----	112
VI.	CONCLUSIONS -----	118
	APPENDIX A: VOLTR COMPUTER PROGRAM -----	120
	APPENDIX B: VOLTS COMPUTER PROGRAM -----	126



APPENDIX C: LFVTC1 COMPUTER PROGRAM -----	131
LIST OF REFERENCES -----	139
INITIAL DISTRIBUTION LIST -----	140

#### ACKNOWLEDGEMENTS

Special thanks to my wife Kathy, without whom I might still be doing figures. Also, thanks to my advisor, Professor Andrew Ochadlick for his patience and advice. And thanks to the Naval Air Development Center for the loan of a fluxgate magnetometer.

## I. INTRODUCTION

This thesis is part of an ongoing effort at the Naval Postgraduate School to analyze ULF geomagnetic noise and micropulsations. The results of the Naval Postgraduate School studies could impact communications systems or systems in which geomagnetic noise and/or micropulsations introduce operational difficulties.

An objective of this thesis was to develop the software necessary for obtaining computer generated plots of geomagnetic field versus time. Then, with the plots, sections of data containing obvious geomagnetic micropulsations were located. Those sections were analyzed to determine the power spectral density (PSD), coherence, degree of polarization and ellipticity of the micropulsation using already developed software [Ref. 1].

After analyzing some of the plots (PSD, coherence, etc.) produced by the software documented in [Ref. 1], it was demonstrated that problems existed in the software. New software was developed to obtain times series raw voltage and geomagnetic field plots. Validation of the software required an on-site experiment. Documented within this thesis is the software to produce time series voltage and geomagnetic field plots and the questions the validation experiment raised concerning the sensing system and software.

Using the newly developed software, a micropulsation event was located. A double running average software routine accentuated the micropulsation to permit the determination of its frequency and amplitude. The micropulsation event was further analyzed to obtain information on coherence, degree of polarization and ellipticity.

## II. BACKGROUND

### A. COLLECTION SYSTEM

The Naval Postgraduate School has two operating geomagnetic sensing systems. The land site is located at the La Mesa Village Housing Area and has three orthogonally mounted induction coils. The second operating system contains two orthogonally mounted induction coils that can be placed on the bottom of Monterey Bay. When both systems are operating, the data is collected simultaneously. The ground work has been laid for a third system located at Chew's Ridge. Three orthogonal and simultaneous measurements can be taken only between two sites since the School has only five induction coils and a sixth just calibrated. This thesis used data from the La Mesa Village site and the software associated with it.

An induction coil senses the geomagnetic field fluctuations based on Faraday's Law of induction, induced emf  $= -N \frac{d\Phi}{dt}$ , which describes the relation between the induced emf and the time rate of change of magnetic flux through the coil.  $N$  is the number of turns in the coil.

The voltage induced in the coils is sampled 32 or 64 times/second and is amplified approximately one million times. The voltage data undergoes pulse-code-modulation (PCM) for noiseless VHF radio link transmission from the La Mesa Village site, to the recording system in the Geophysics Signal

Processing Laboratory located in Spanagel 531. Data reduction on the Naval Postgraduate School's IBM 3033 computer follows digitization of the PCM data. A block diagram of the system is provided in Figure 2.1. A more detailed description of the system is given in Reference 2.

#### 1. System Calibration

For purposes of documentation, the calibration of the third coil for either the Chew's Ridge or Monterey Bay system is being included in this thesis. The general method of induction coil calibration will be covered here. For a more indepth explanation, see Reference 1.

The sensing coil and its associated electronics are calibrated using a Helmholtz coil apparatus to establish a uniform magnetic field. By placing the sensing coil into the field produced by the Helmholtz coil, one can establish a relationship between the Helmholtz coil magnetic field magnitude and frequency and the coil system voltage. Once the response of the coil system is known for the frequency band of interest, it can be included in the system transfer function used in data reduction.

The experiment to determine the sixth coil system transfer function was done at the La Mesa Village site. A Wavetek Model 142 signal generator supplied a sinusoidal current to a 1.22 meter diameter, 0.61 meter high Helmholtz coil. The current was measured across a 996 ohm resistor in series with the Helmholtz coil. A Hewlett Packard HP-3582A spectrum

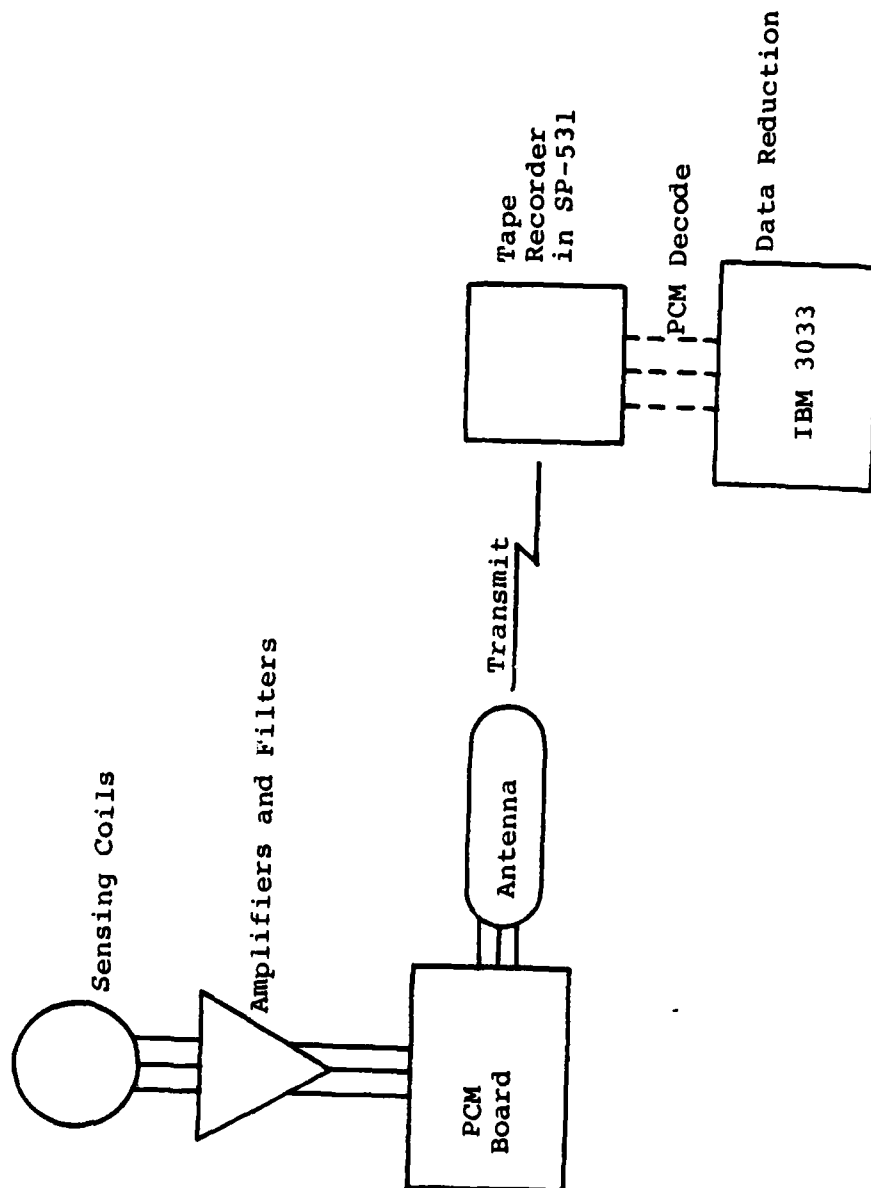


Figure 2.1. System Data Flow

analyzer measured the output voltage of the coil system as a function of frequency.

The experiment measured the response of the coil system in the frequency band .05 hertz to 20 hertz for applied fields of 0.02, 0.2 and 1.0 nanoteslas. The coil system response is shown in Figure 2.2. The transfer function of this coil system corresponds closely to those of coil systems previously calibrated. The only noticable difference is that the 0.02 nanotesla response at 15 hertz is approximately 15 volts/nanotesla higher than those measured before [Ref. 1]. It should be noted that this difference will not influence data analysis in the frequency range of interest. The transfer function algorithm is listed in Table 2.1.

#### B. PREVIOUS SOFTWARE

Software has been developed (see References 1 and 3), to extract power spectral densities for each coil, coherence between the coils, degree of polarization in the three measurement planes, ellipticity in the three measurement planes and a variety of Stokes parameters. The following is a basic description of the computer code that produces the above mentioned plots. First, the voltage data is read off the digital tape using a subroutine called RD provided by Dr. Tim Stanton of the Oceanography Department. A parameter ISEC, representing the number of seconds one wishes to advance the tape, is frequently used. ISEC establishes the number of



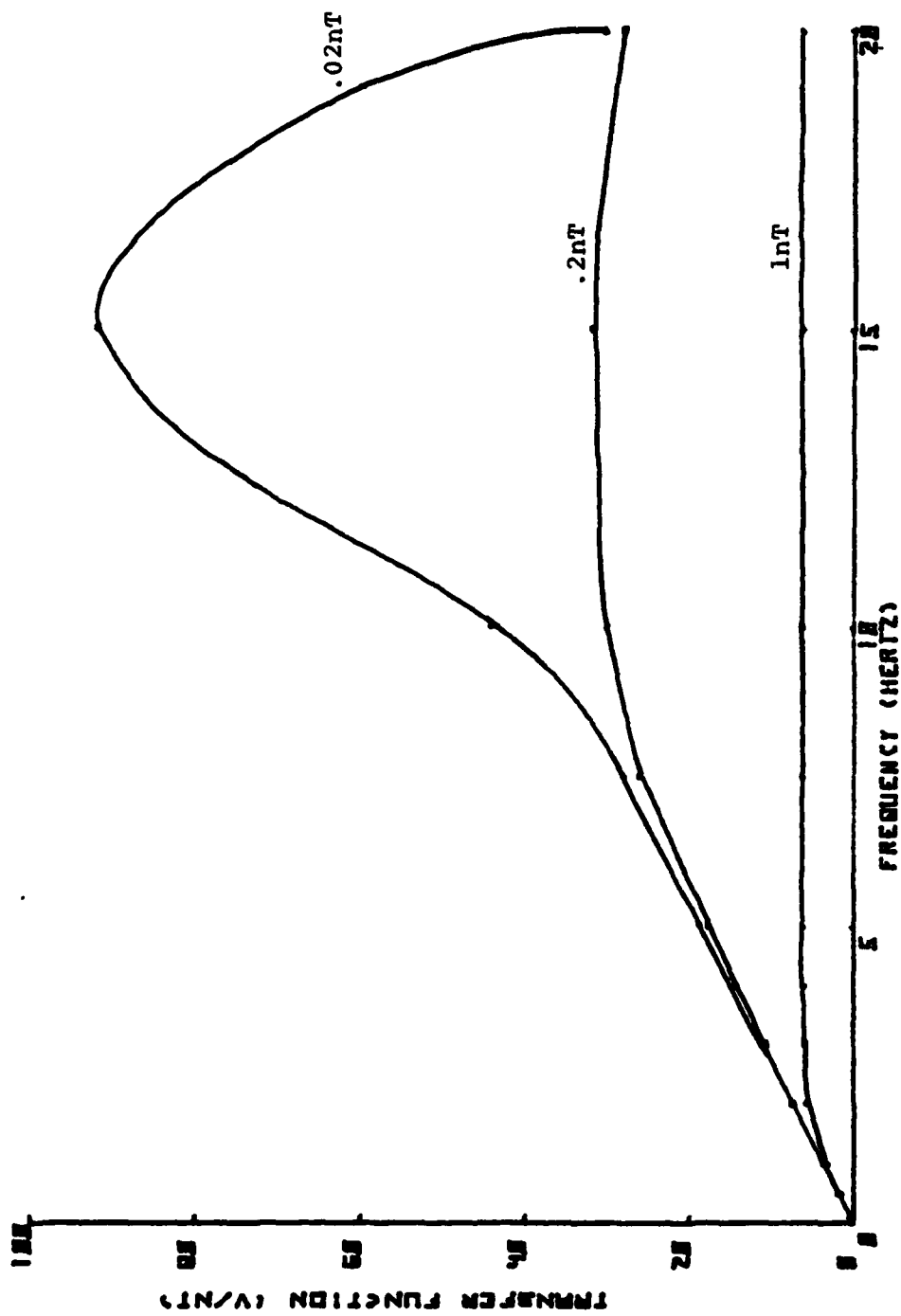


Figure 2.2. Coil Transfer Function

Table 2.1. System Transfer Function Algorithm

```

DC 9 L=1,N
FFQ=FRQ(L)
IF(FRQ.LE.25.)GO TO 1
XX(L)=XX(L)/28.
GC TO 8
1 IF(FRQ.LE.15.)GO TO 2
XX(L)=XX(L)/(105.5-3.14*FRQ)
YY(L)=YY(L)/(181.32-7.588*FRQ)
ZZ(L)=ZZ(L)/(177.26-7.484*FRQ)
GC TO 8
2 IF(FRQ.LE.10.)GO TO 3
XX(L)=XX(L)/(5.958*FRQ-30.97)
YY(L)=YY(L)/(7.166*FRQ-39.99)
ZZ(L)=ZZ(L)/(6.49*FRQ-32.35)
GC TO 8
3 IF(FRQ.LE.7.5)GO TO 4
XX(L)=XX(L)/(3.492*FRQ-6.31)
YY(L)=YY(L)/(4.252*FRQ-10.85)
ZZ(L)=ZZ(L)/(4.044*FRQ-7.89)
GC TO 3
4 IF(FRQ.LE.5.)GO TO 5
XX(L)=XX(L)/(2.6311*FRQ+0.14667)
YY(L)=YY(L)/(3.012*FRQ-1.55)
ZZ(L)=ZZ(L)/(3.184*FRQ-1.44)
GC TO 8
5 IF(FRQ.LE.3.)GO TO 6
XX(L)=XX(L)/(2.6311*FRQ+0.14667)
7 YY(L)=YY(L)/(2.702*FRQ)
ZZ(L)=ZZ(L)/(2.92*FRQ)
GC TO 8
8 XX(L)=XX(L)/(2.72*FRQ)
GC TO 7
8 CONTINUE
TF(L)=(XX(L)*COS0 + YY(L)*COS01)*COS00 + ZZ(L)*COS30
9 CONTINUE

```

times RD is called and the data not stored. Previously, tape advances of approximately 30 seconds or ISEC = 30 were used. Once the tape is advanced the desired amount, data analysis can begin. Each digital tape contains about 90 minutes or  $1.728 \times 10^5$  pieces of data per axis resulting from the sampling rate of 32 samples/second. Because of the large amount of data, the analysis has to be accomplished in blocks. Data analysis takes place on 256 seconds or 8192 frames of data at a time. RD is called 8192 times and places the voltages for each coil in an array. The voltages are integer values from 0 to 4096 representing -5 volts to +5 volts. Ideally the value 2048 represents 0 volts. The integers between 0-4096 are normalized to  $\pm 5$  volts and placed in new complex arrays. These arrays containing 8192 pieces of data are Fourier transformed to the frequency domain where the system transfer function is applied. After applying the transfer function, the calculations begin for a determination of PSD's, coherence, ellipticity, etc. for the first block. After they are complete, the next block of 8192 pieces of data starts through the program. Once the desired amount of data has been processed, a NONIMSL subroutine called DRAWP plots the data. For a more complete description of this software, see Reference 1, Reference 3 and Reference 4.

### C. ANALYSIS OF INITIAL DATA PLOTS

Many of the PSD's, coherences, ellipticities and degree of polarization plots produced by the software of Reference 1 and Reference 3 have unexpected characteristics. The PSD's show "humps" that are shown in Figures 2.3-2.5. These "humps" are not characteristic in "normal" PSD's. The coherence plots show a coherence of essentially one degrading to hash in the frequencies greater than 2 hertz, Figures 2.6-2.8. We see a similar behavior in the plots of degree of polarization. These plots indicate a very highly polarized field from 0.02 hertz to 1.0 hertz. Figures 2.9-2.11. The ellipticity plots show a very linearly polarized field for these frequencies in Figures 2.12-2.14.

After examining the time series magnetic field plots, we noted a section of very large magnitude fluctuations (about one to three orders of magnitude greater than the general background) at the beginning of the digital tapes Figures 2.15-2.17. We found that if the digital tape was advanced past these large fluctuations the output (PSD, coherence, etc.) appeared "normal", Figures 2.18-2.29. If the program was executed on just the section containing the large fluctuations, the PSD's had the "humped" characteristic, the coherences were one, the degree of polarization was very high and the ellipticity was linear, Figures 2.30-2.41. This demonstrates that these large fluctuations dominate the output of an analysis in the frequency domain. A tape advance of 300 seconds or ISEC = 300 is

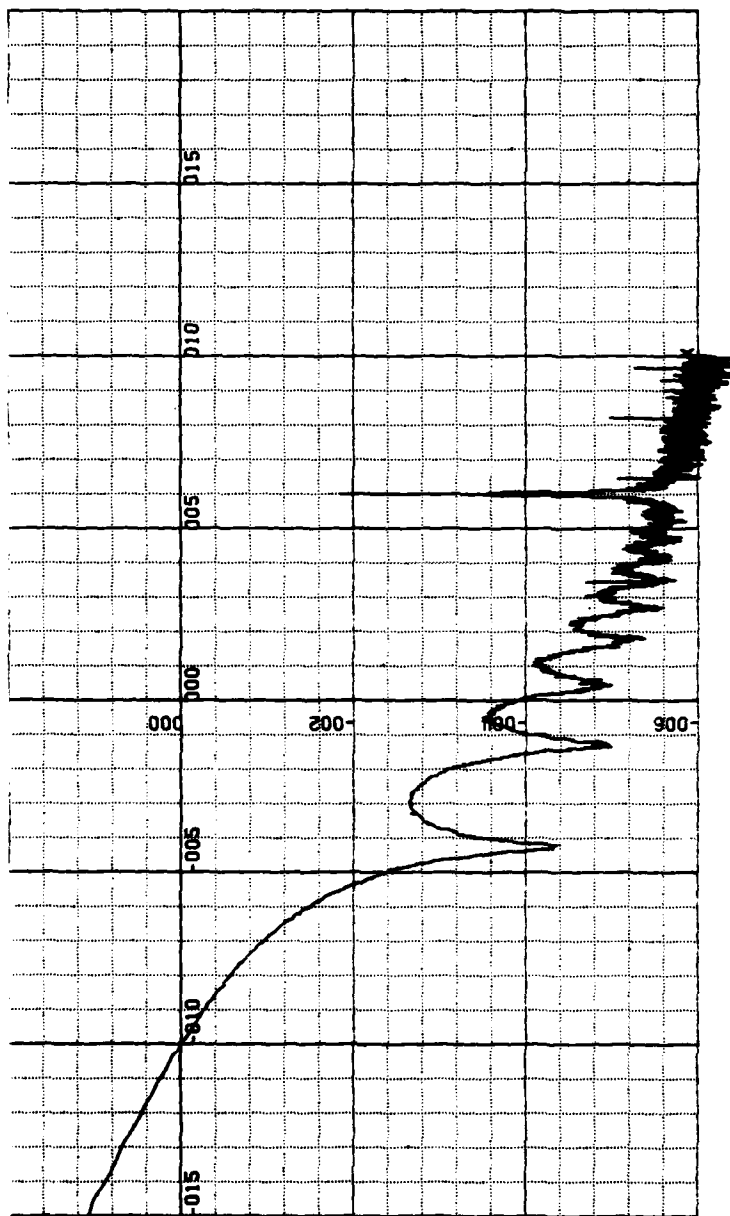


Figure 2.3. PSD X-Coil, 17 August 82, 2240-2348 Local.  
Amplitude in dB (REF nT\*\*2/Hz) (20 units/in) vs. Log  
Frequency (Hz) (0.5 units/in), 16 Averages

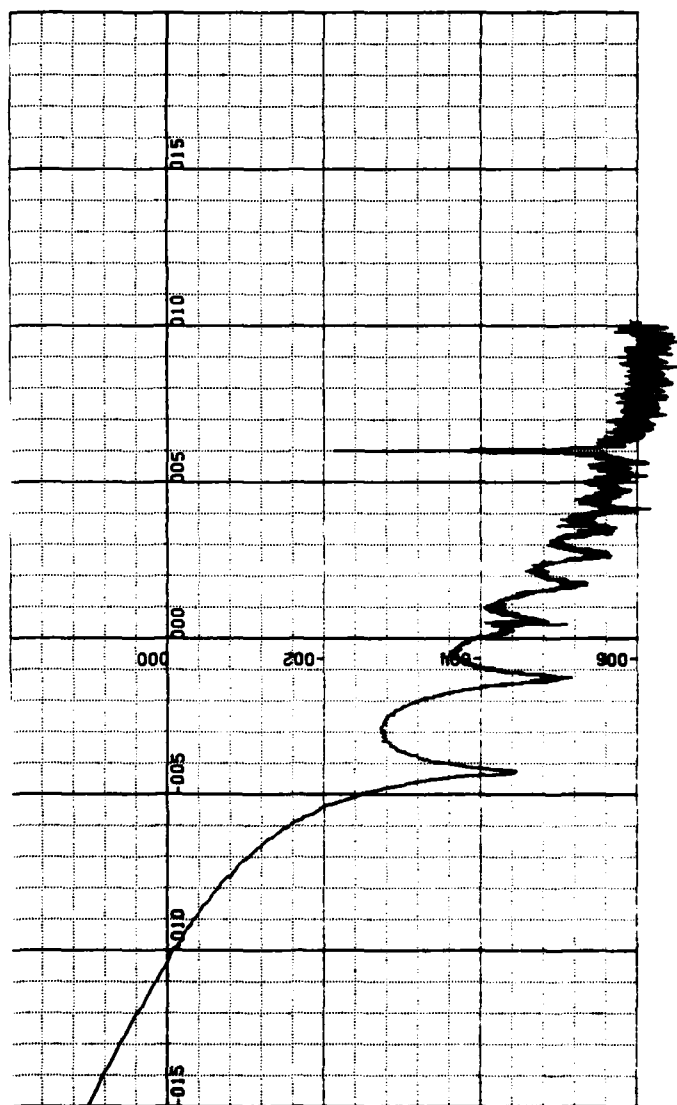


Figure 2.4. PSD Y-Coil, 17 August 82, 2240-2348 Local.  
Amplitude in dB (REF nT\*\*2/Hz) (20 units/in)  
vs. Log Frequency (Hz) (0.5 units/in), 16 Averages

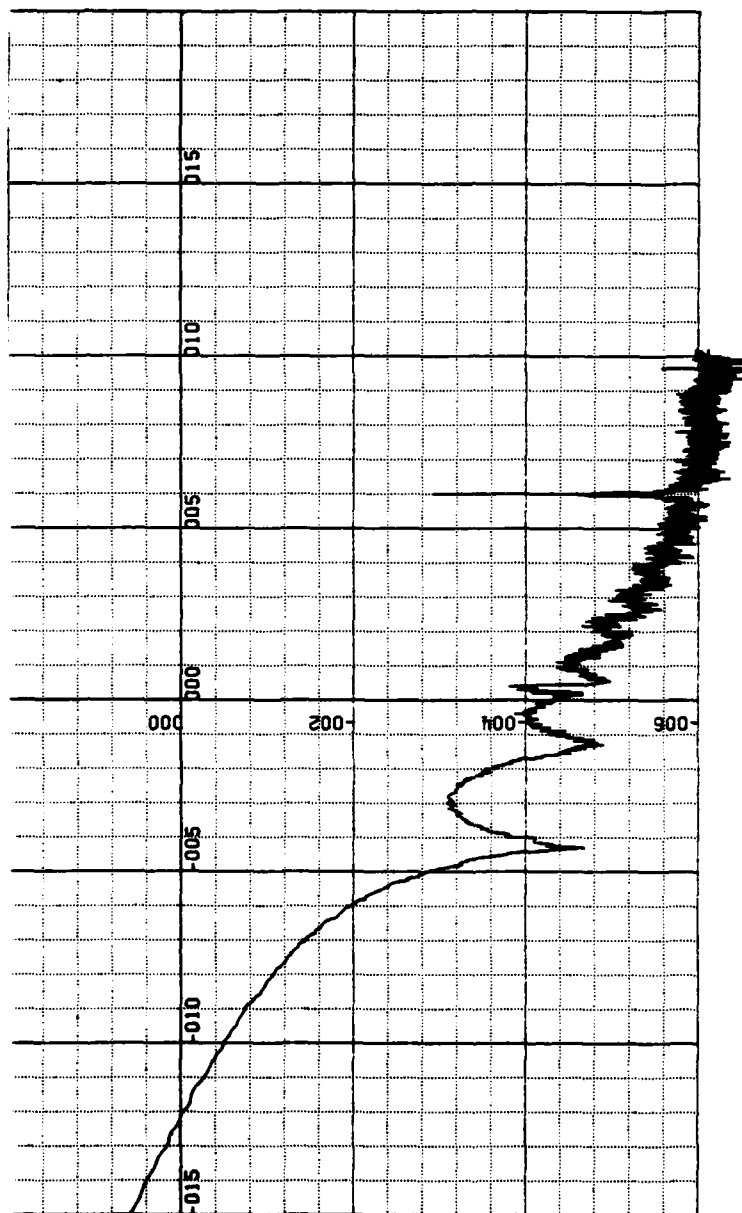


Figure 2.5. PSD Z-Coil, 17 August 82, 2240-2348 Local.  
Amplitude in dB (REF nT\*\*2/Hz) (20 units/in) vs.  
Log Frequency (Hz) (0.5 units/in), 16 Averages

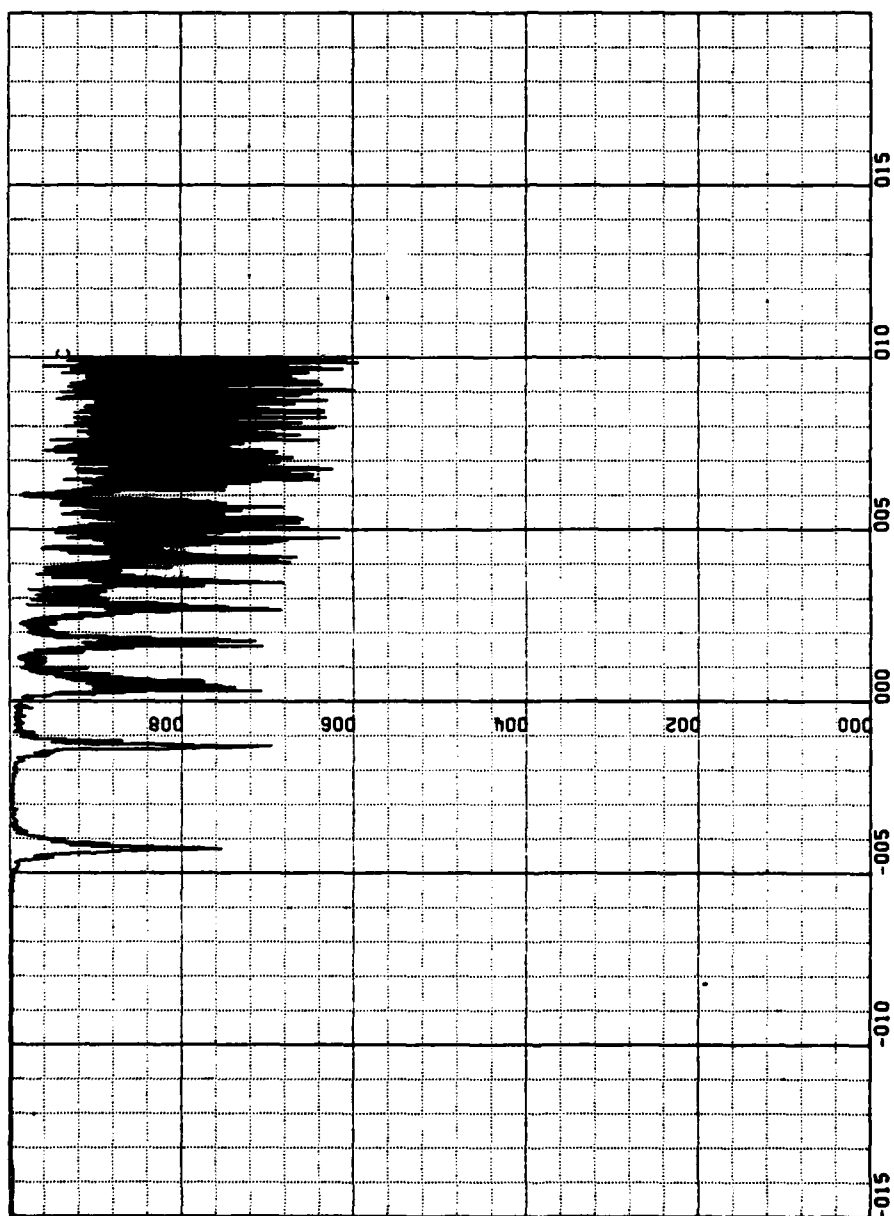


Figure 2.6. Coherence X and Y coils, 17 August 82, 2240-2348 Local.  
Coherence X and Y Coil (0.2 units/in) vs. Log Frequency  
(Hz) (0.5 units/in), 16 Averages



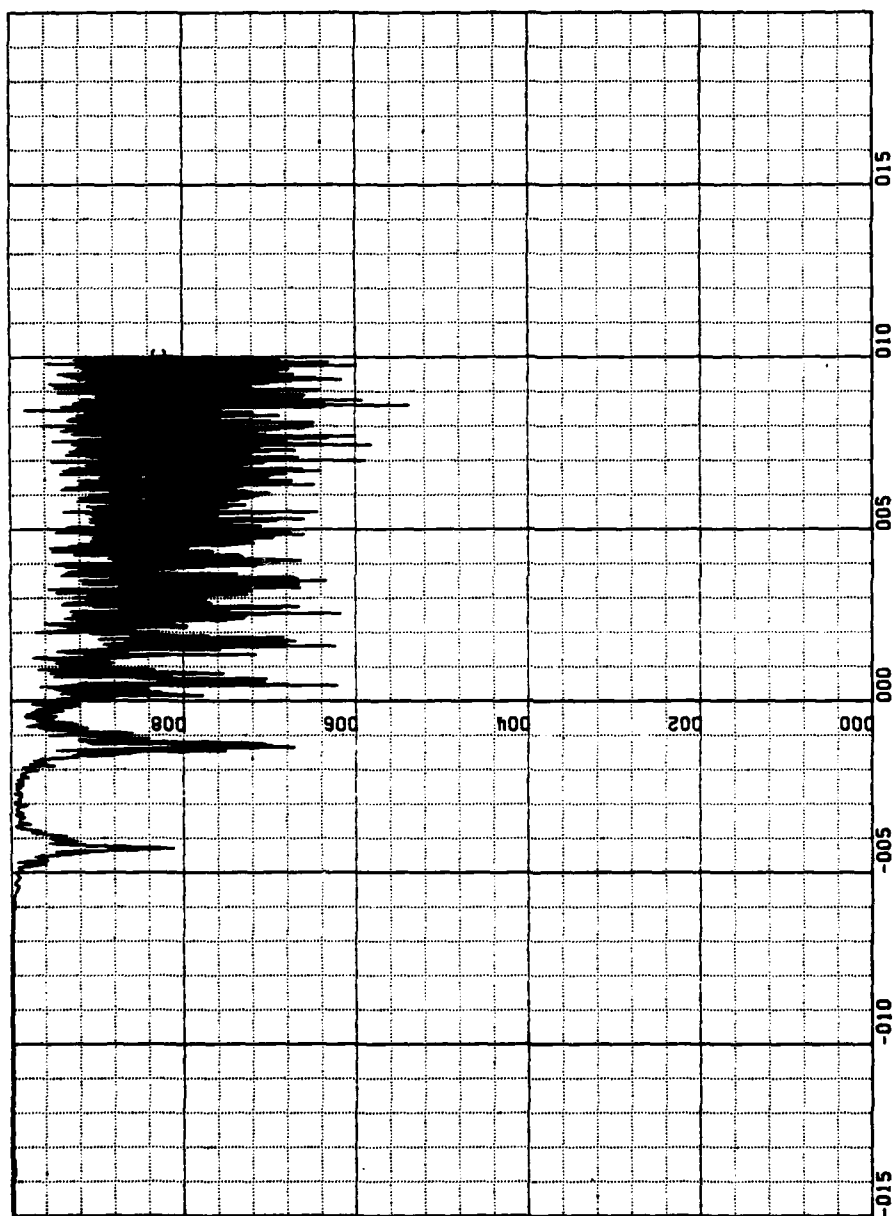


Figure 2.7. Coherence Y and Z Coils, 17 August 82, 2240-2348 Local.  
Coherence Y and Z Coils (0.2 units/in) vs. Log Frequency  
(Hz) (0.5 units/in), 16 Averages

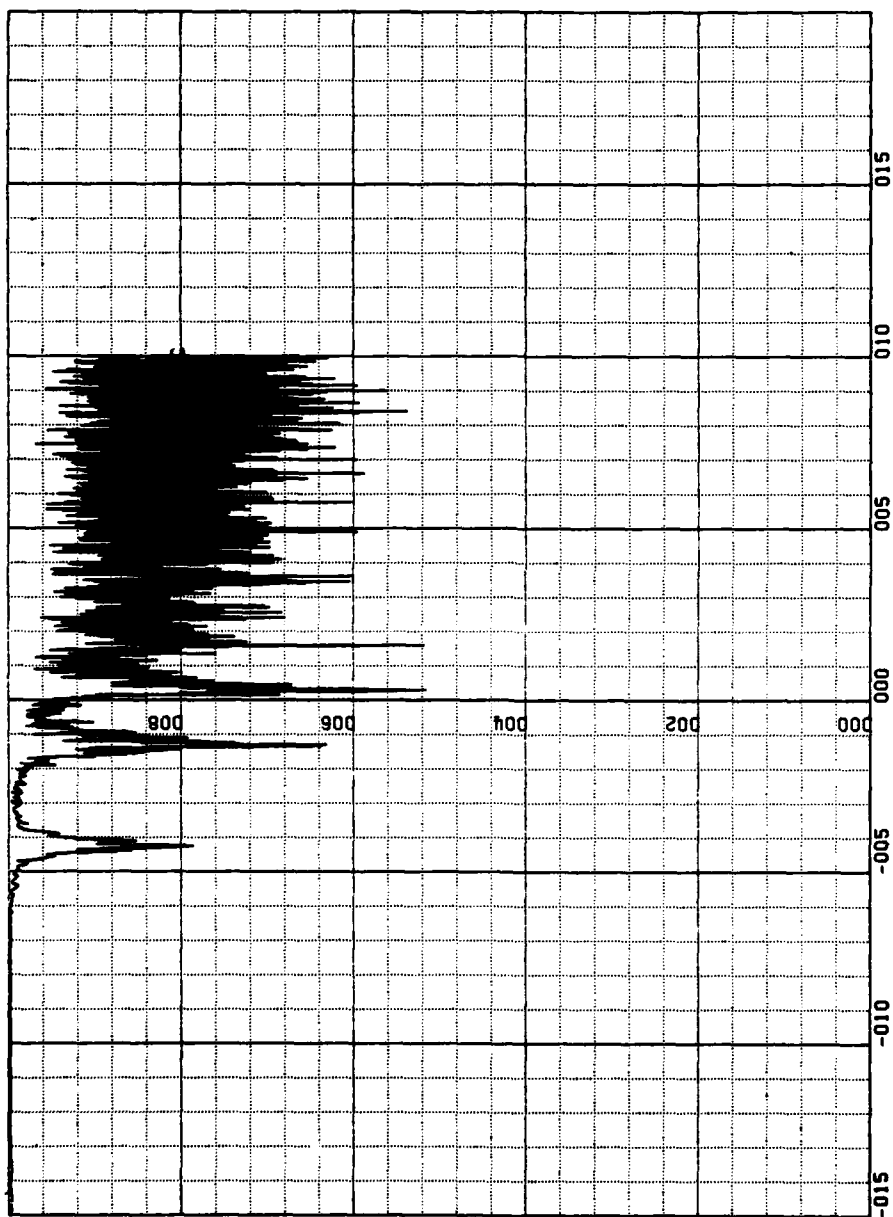


Figure 2.8. Coherence Z and Z Coils, 17 August 82, 2240-2348 Local.  
Coherence Z and X Coils (0.2 units/in) vs. Log Frequency  
(Hz) (0.5 units/in), 16 Averages

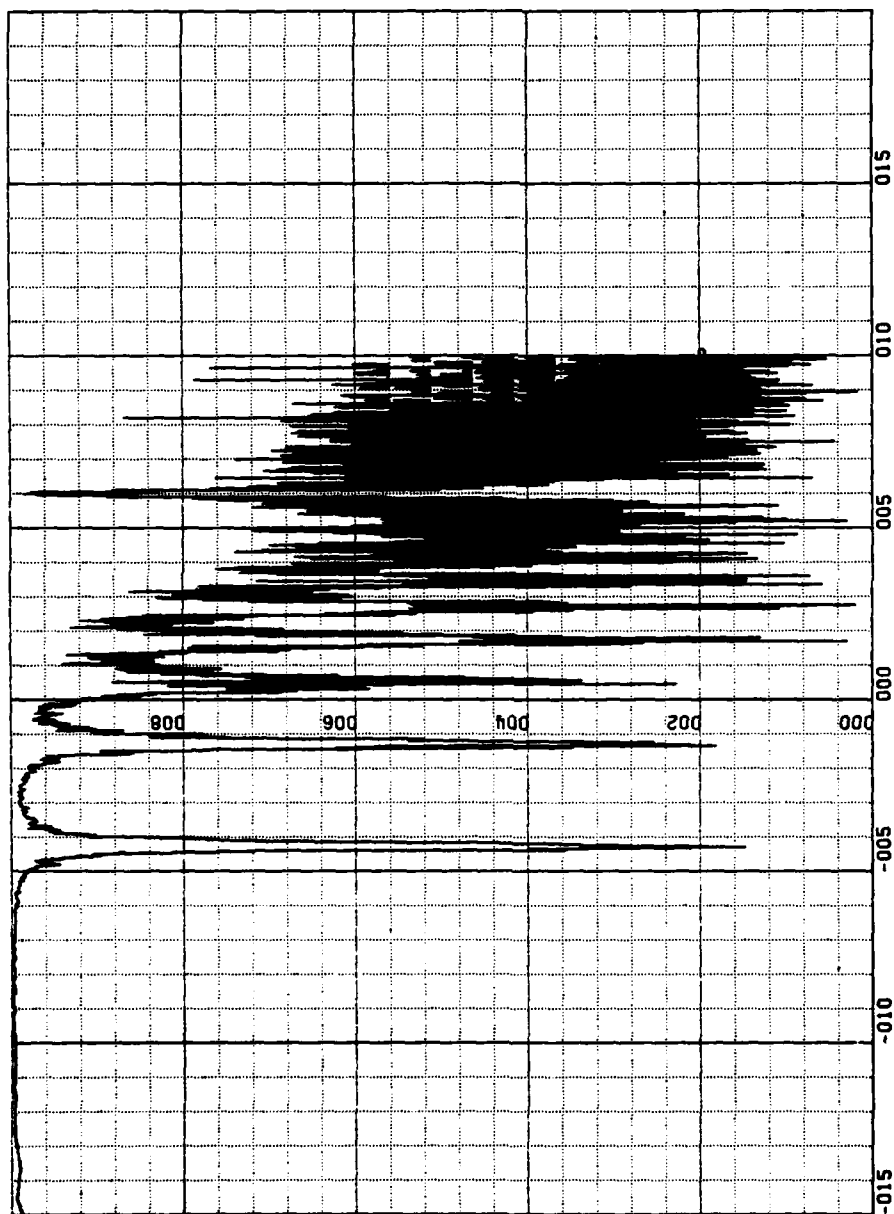


Figure 2.9. Degree of Polarization X-Y Plane, 17 August 82, 2240-2348 Local.  
 Degree of Polarization (0.2 units/in) vs. Log Frequency (Hz)  
 (0.5 units/in), 16 Averages

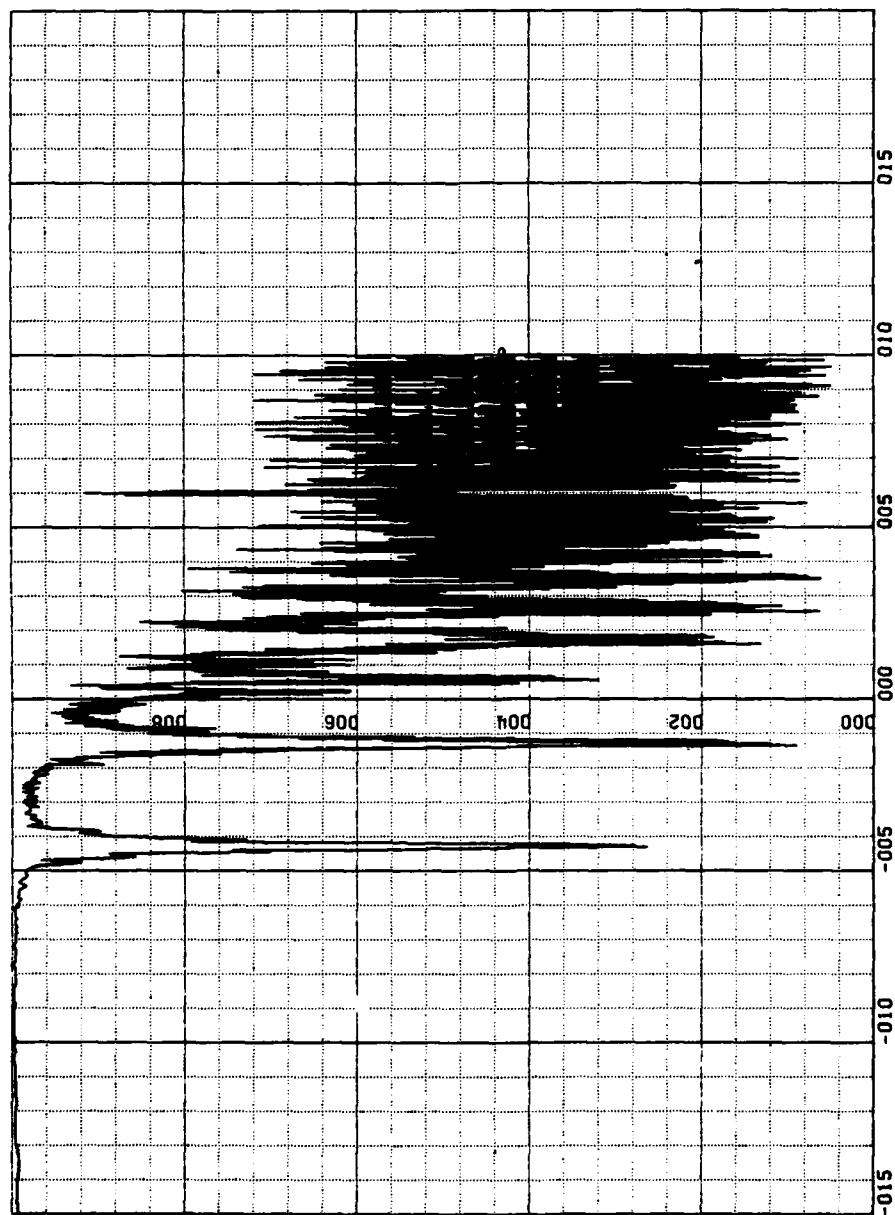


Figure 2.10. Degree of Polarization Y-Z Plane, 17 August 82, 2240-2348 Local.  
 Degree of Polarization (0.2 units/in) vs. Log  
 Frequency (Hz) (0.5 units/in), 16 Averages

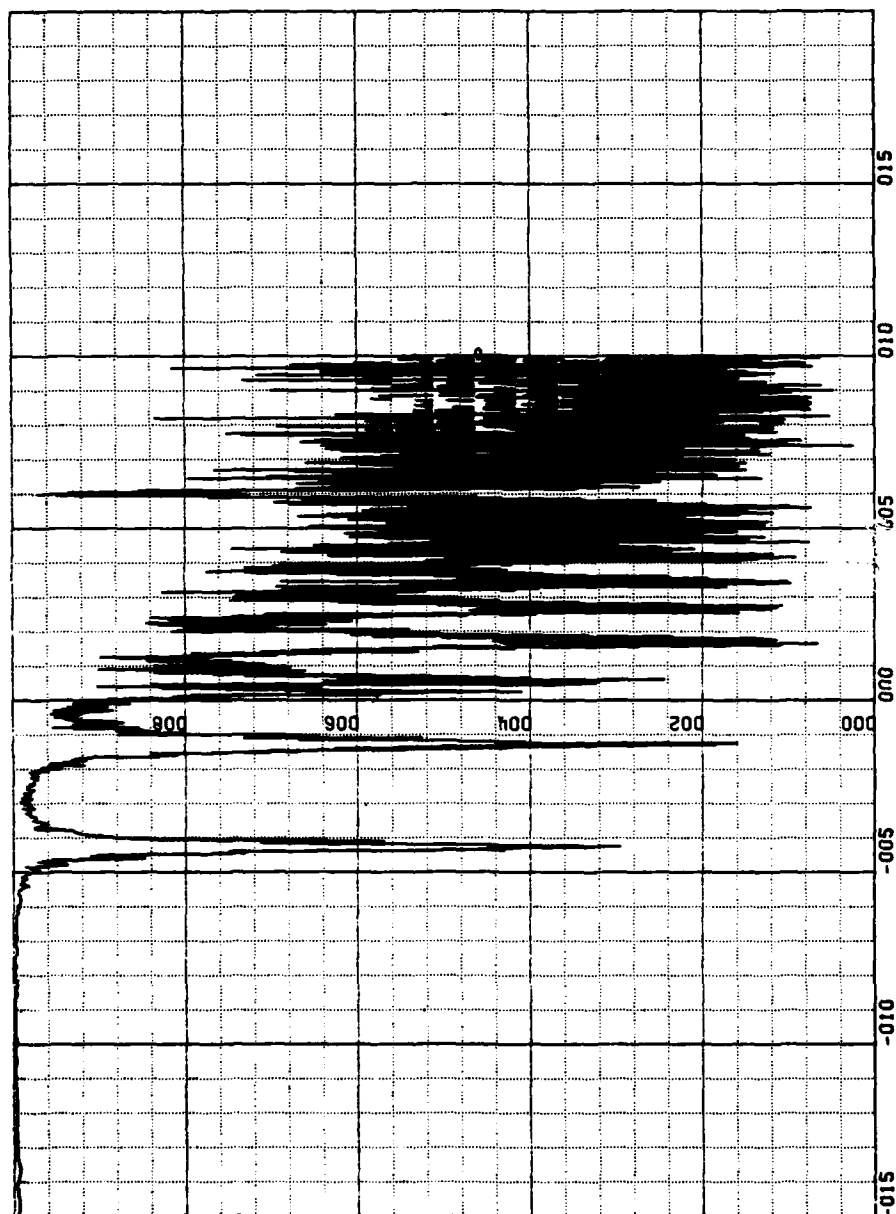


Figure 2.11. Degree of Polarization Z-X Plane, 17 August 82, 2240-2348 Local.  
 Degree of Polarization (0.2 units/in) vs. Log Frequency  
 (Hz) (0.5 units/in), 16 Averages

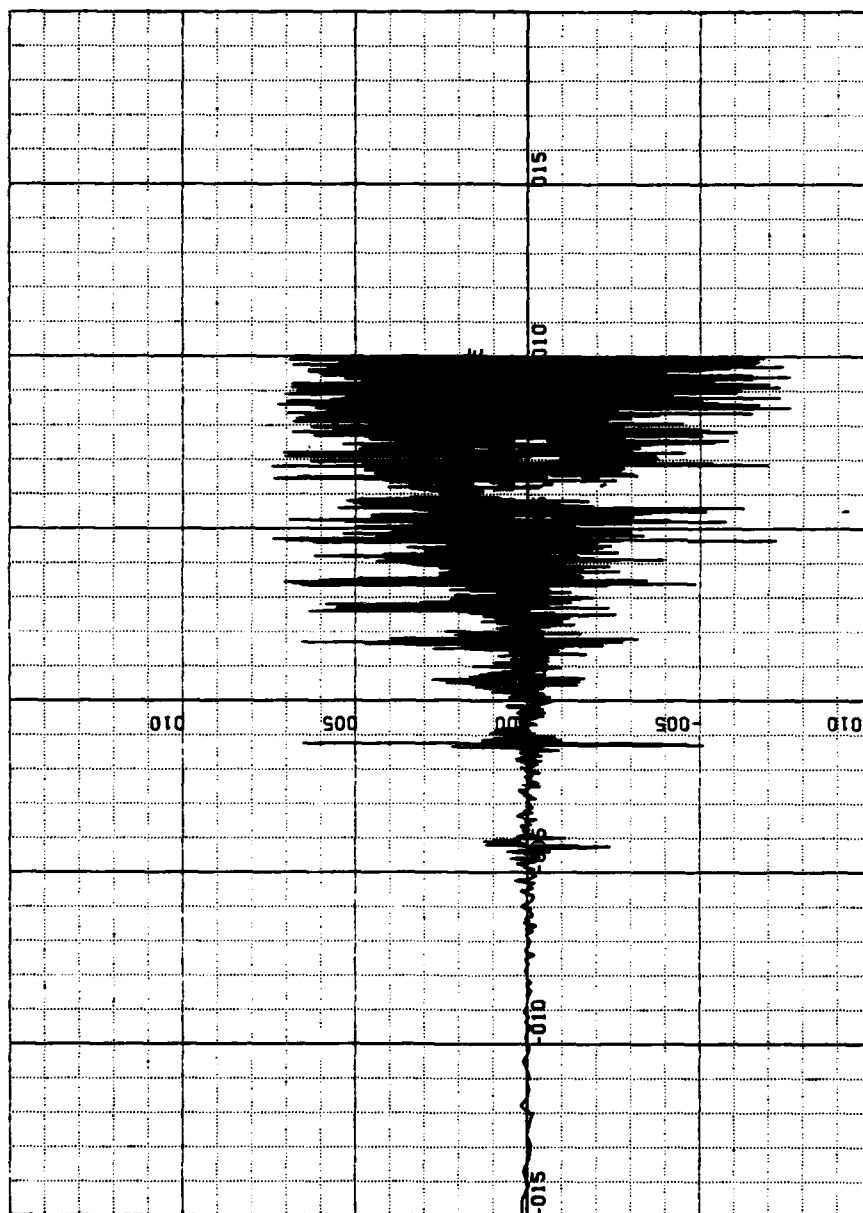


Figure 2.12. Ellipticity X-Y Plane, 17 August 82, 2240-2348 Local.  
 Ellipticity (0.5 unit/in) vs. Log Frequency (Hz) (0.5 unit/in)  
 16 Averages

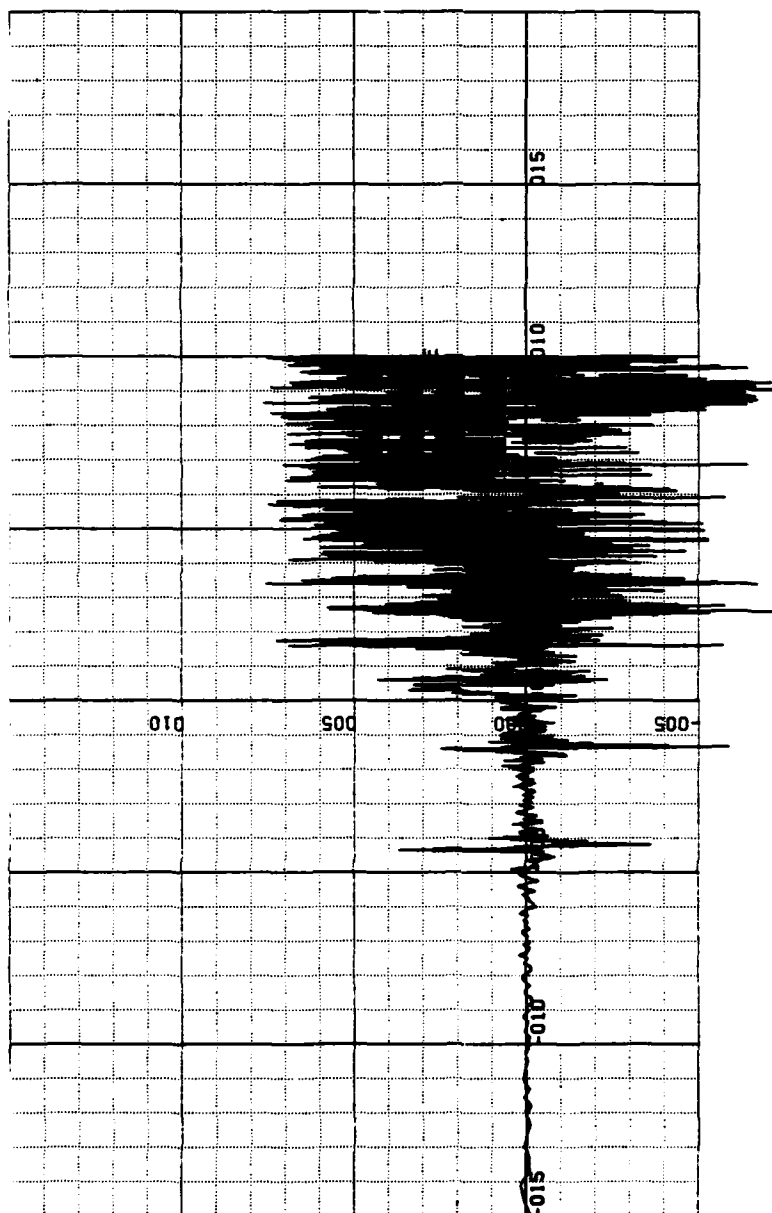


Figure 2.13. Ellipticity Y-Z Plane, 17 August 82, 2240-2348 Local.  
 Ellipticity (0.5 units/in) vs. Log Frequency (Hz) (0.5 units/in)  
 16 Averages

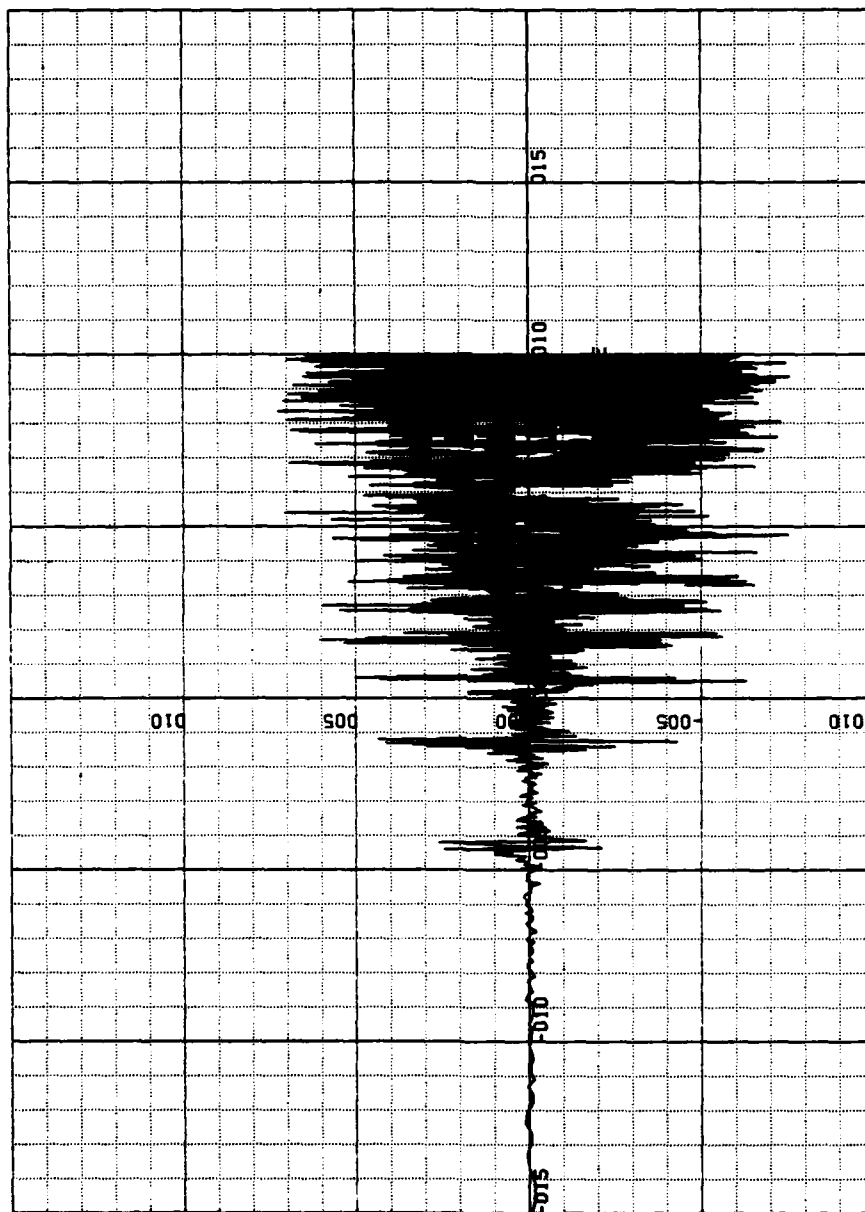


Figure 2.14. Ellipticity Z-X Plane, 17 August 82, 2240-2348 Local.  
 Ellipticity (0.5 units/in) vs. Log Frequency (Hz) (0.5 units/in)  
 16 Averages



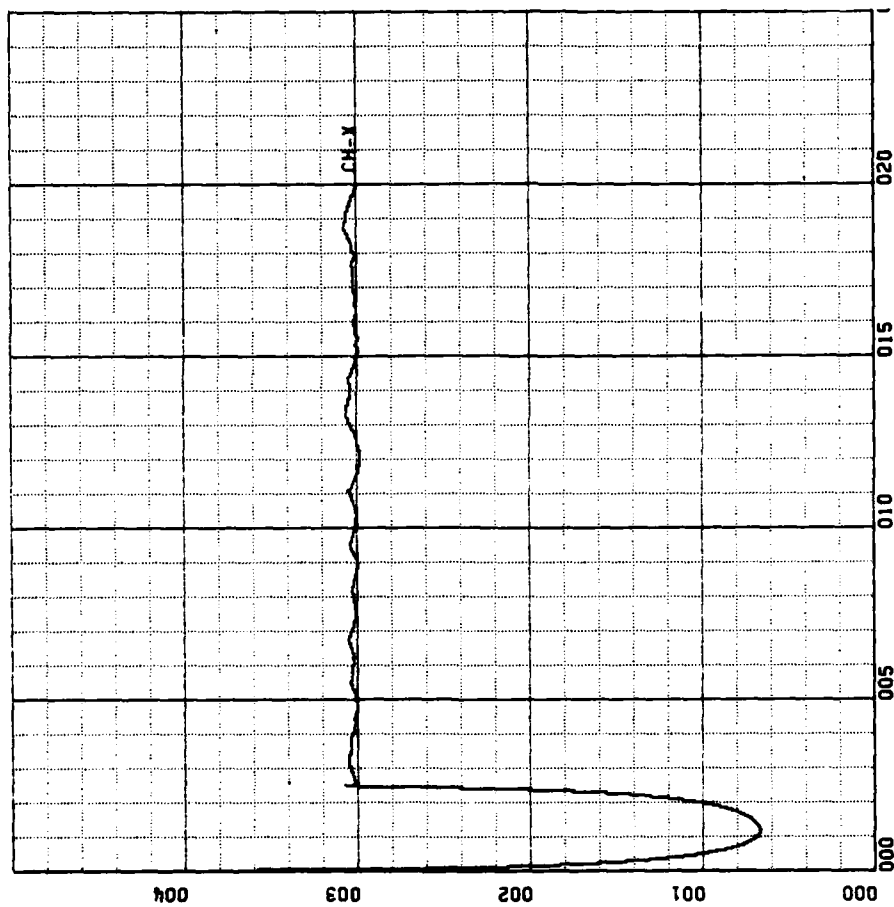


Figure 2.15. X-Coil Magnetic Field, 17 August 82, 2240-2348- Local.  
 Amplitude (nanoteslas : 10 units/in) vs. Time (seconds : 500 units/in)  
 16 Averages

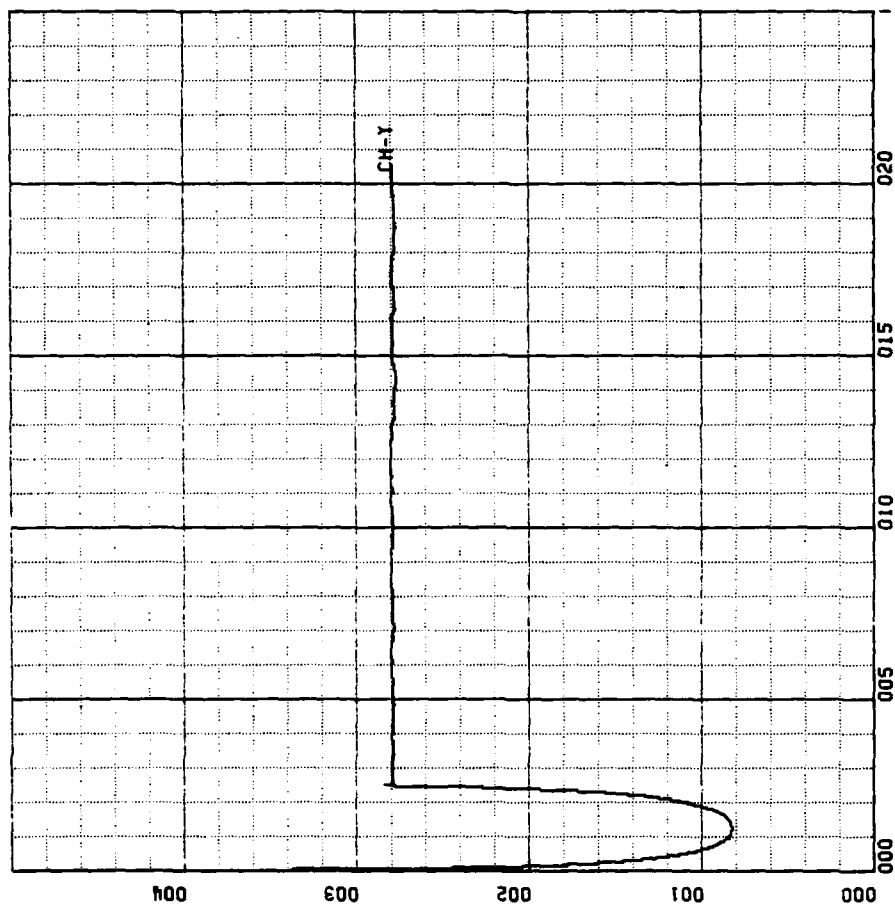


Figure 2.16. Y-Coil Magnetic Field, 17 August 82, 2240-2348 Local.  
 Amplitude (nanoteslas : 10 units/in) vs. Time (seconds : 500 units/in)  
 16 Averages

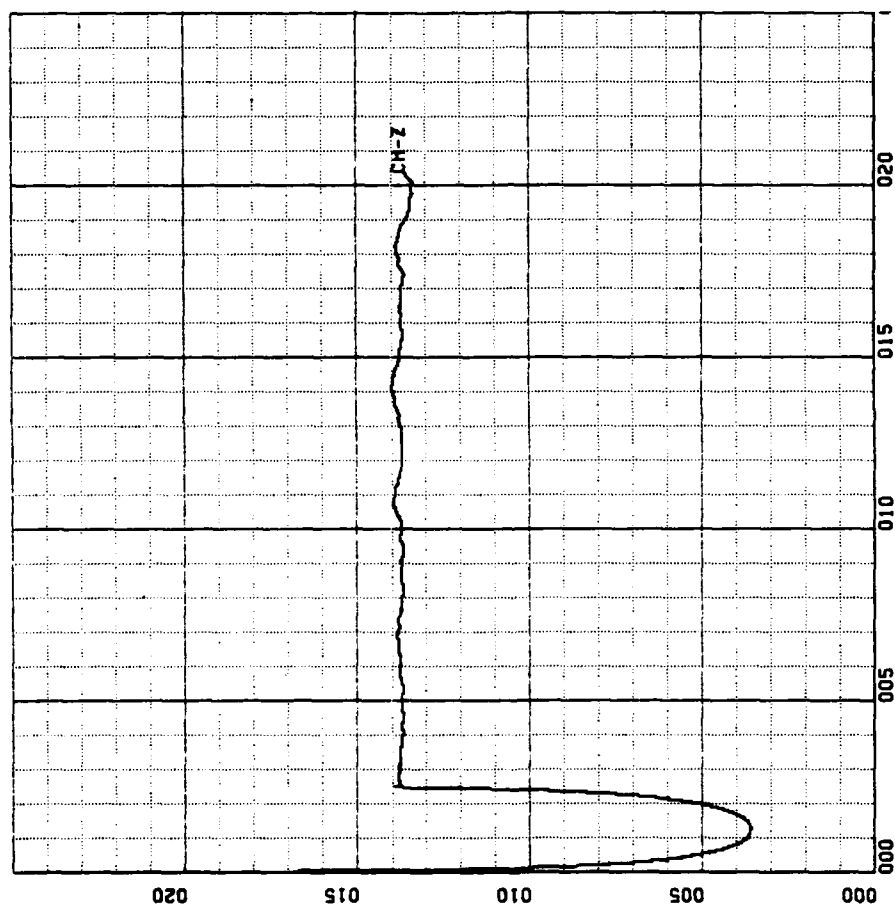


Figure 2.17. Z-Coil Magnetic Field, 17 August 82, 2240-2348 Local.  
 Amplitude (nanoteslas : 5 units/in) vs. Time (seconds : 500 units/in)  
 16 Averages

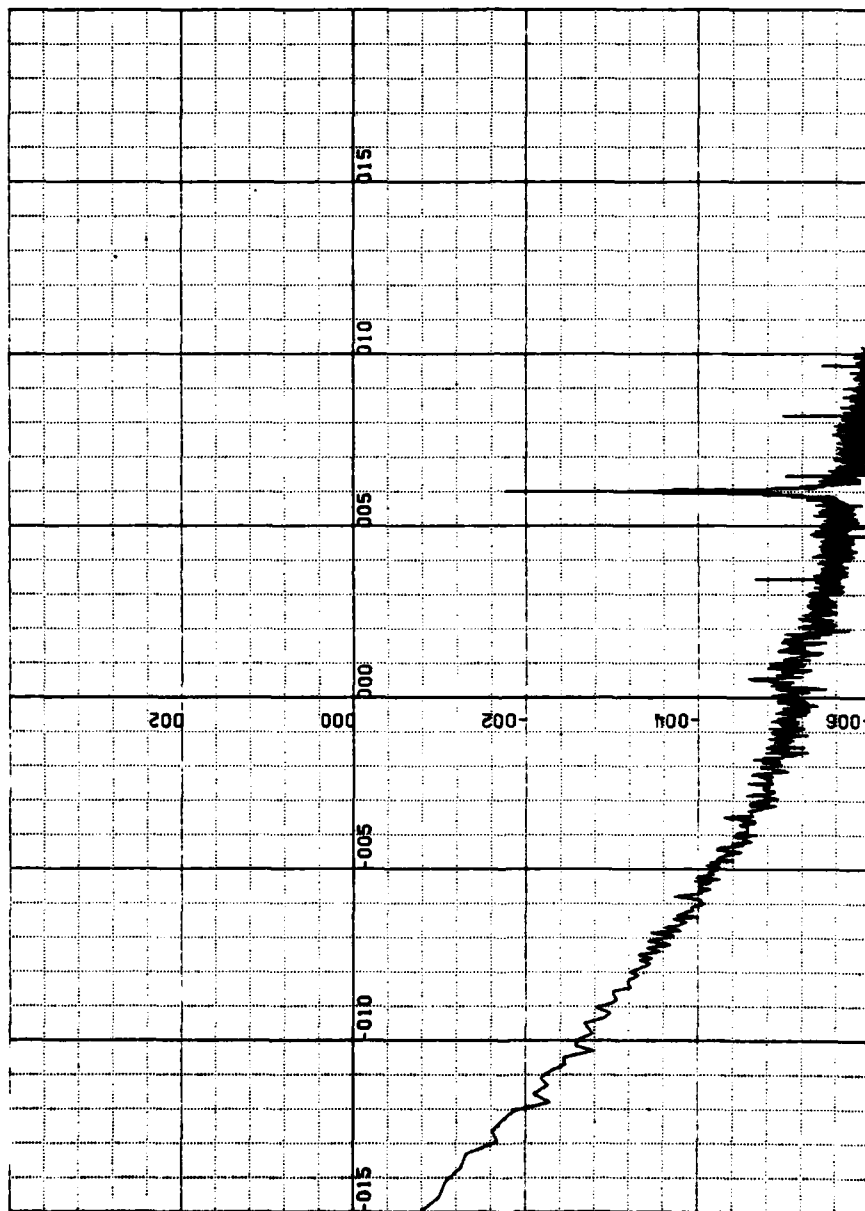


Figure 2.18. PSD X Coil, 17 August 82, 2245-2353 Local.  
 Amplitude in dB (REF nT\*\*2/Hz) (20 units/in) vs. Log  
 Frequency (Hz) (0.5 units/in), 16 Averages

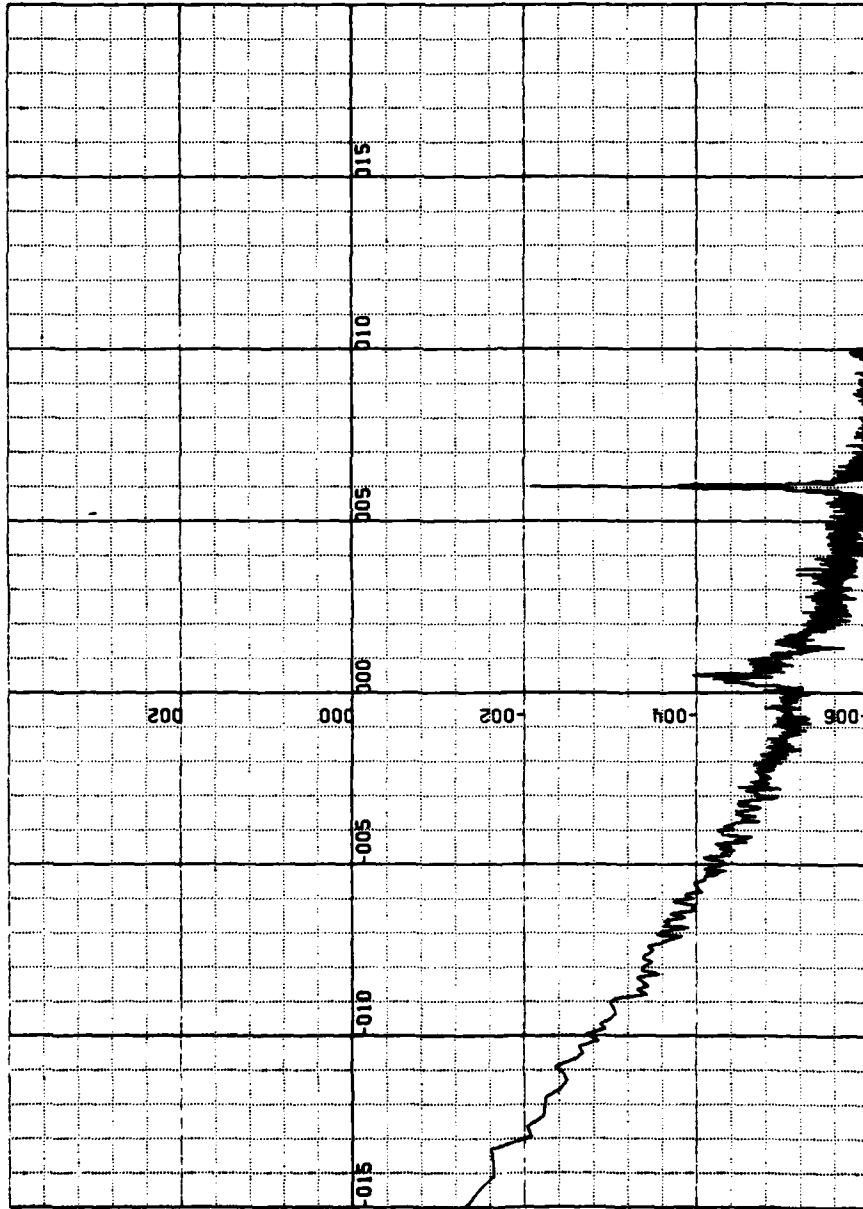


Figure 2.19. PSD Y Coil, 17 August 82, 2245-2353 Local.  
 Amplitude in dB (REF nT\*\*2/Hz) (20 units/in) vs. Log  
 Frequency (Hz) (0.5 units/in), 16 Averages

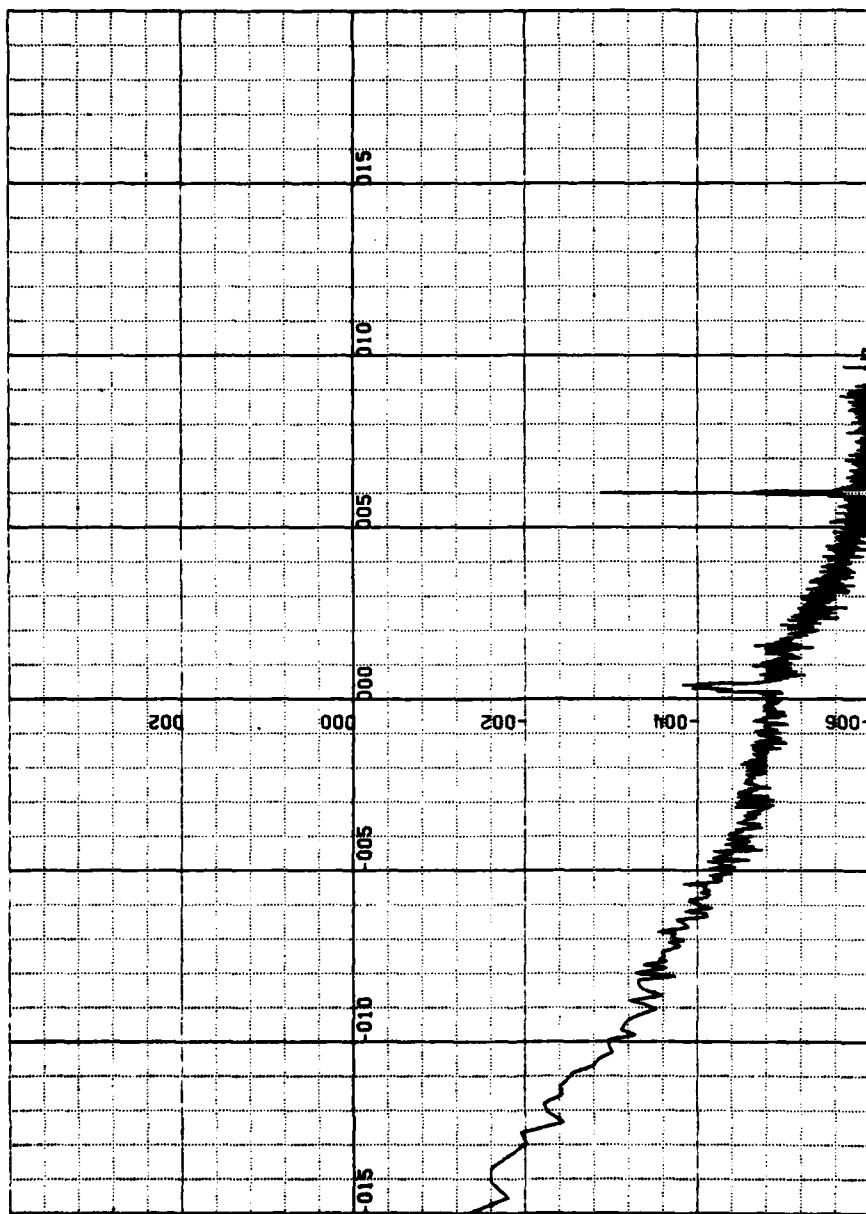


Figure 2.20. PSD Z Coil, 17 August 82, 2245-2353 Local.  
Amplitude in dB (REF nT\*\*2/Hz) (20 units/in) vs. Log  
Frequency (Hz) (0.5 units/in), 16 Averages

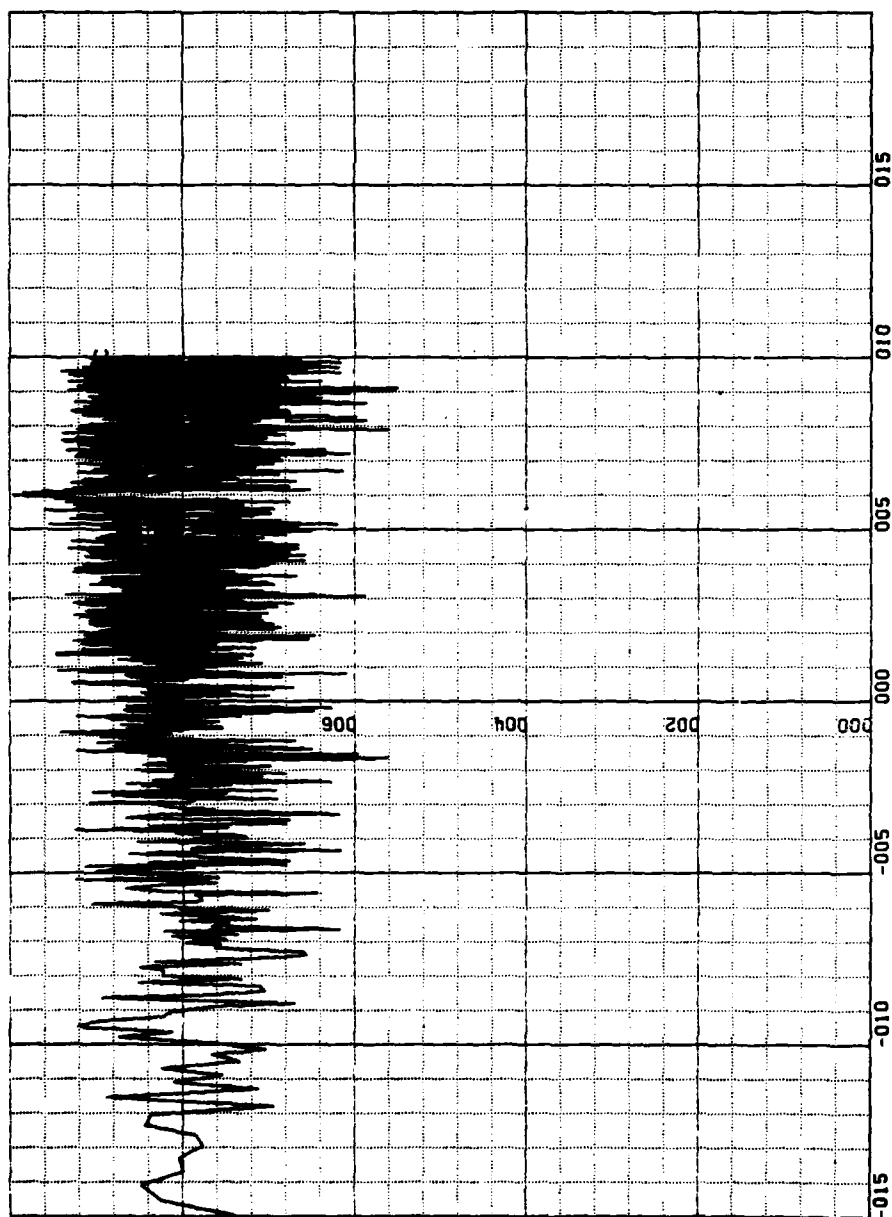


Figure 2.21. Coherence X-Y coils, 17 August 82, 2245-2353 Local.  
 Coherence X-Y Coils (0.2 units/in) vs. Log Frequency (Hz)  
 (0.5 units/in), 16 Averages

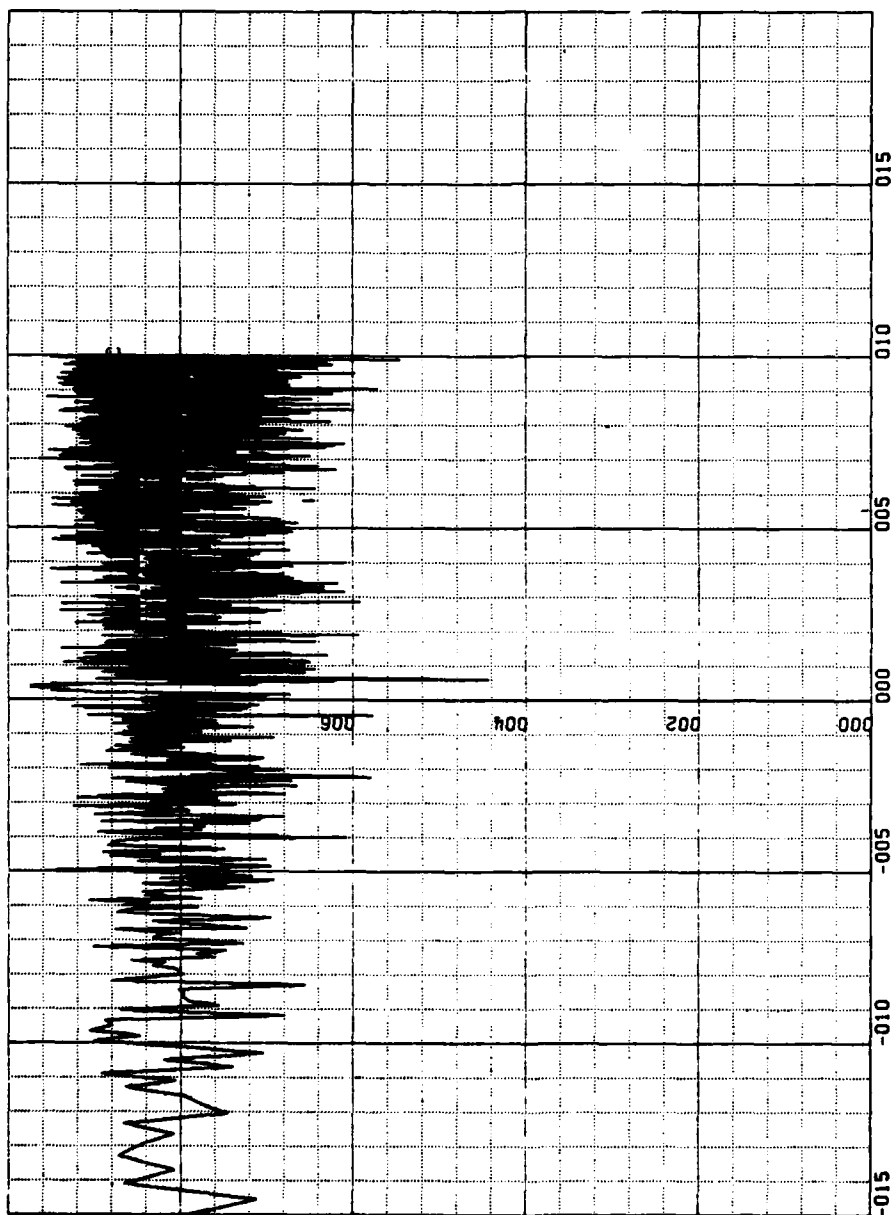


Figure 2.22. Coherence Y-Z Coils, 17 August 82, 2245-2353 Local  
 Coherence X-Y Coils (0.2 units/in) vs. Log Frequency (Hz)  
 (0.5 units/in), 16 Averages



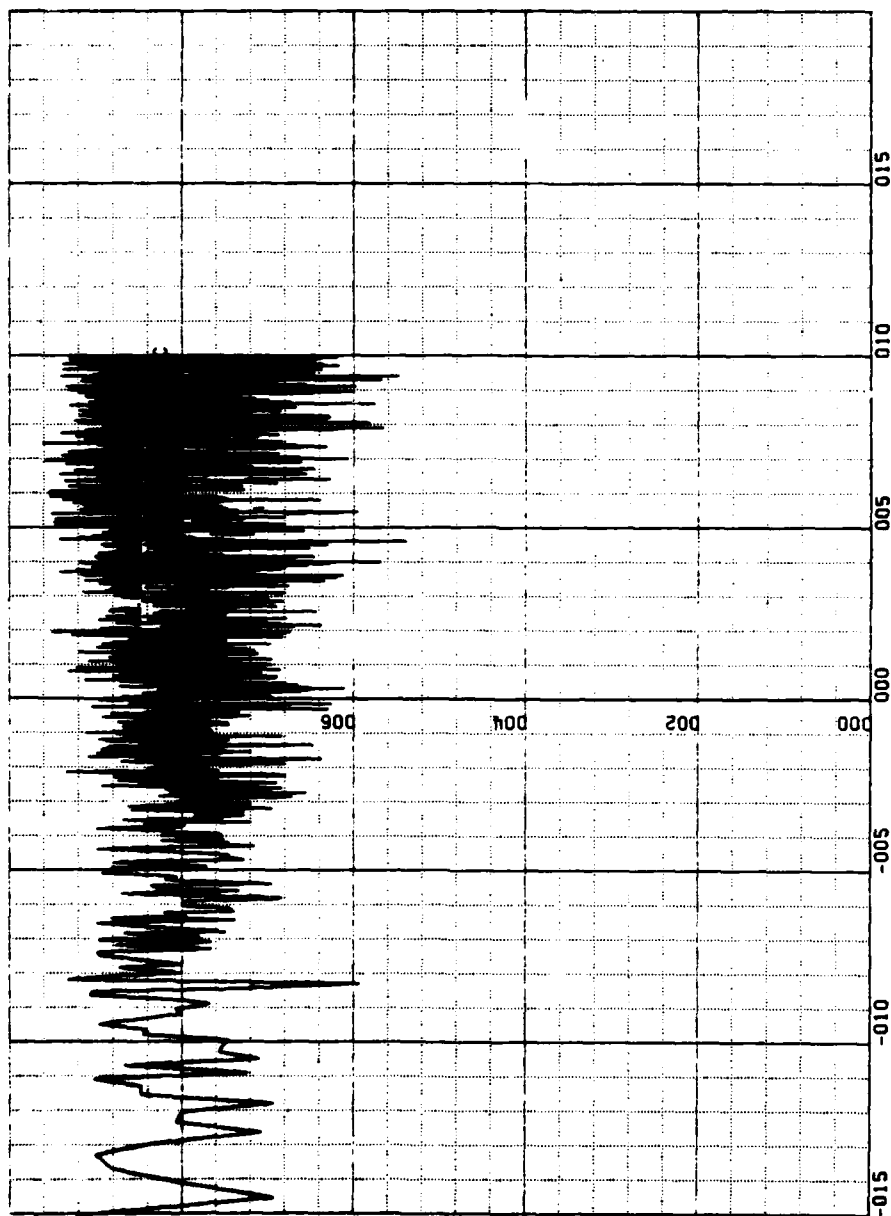


Figure 2.23. Coherence Z-X Coils, 17 August 82, 2245-2353 Local.  
Coherence Z-X Coils (0.2 units/in) vs. Log Frequency (Hz)  
(0.5 units/in), 16 Averages

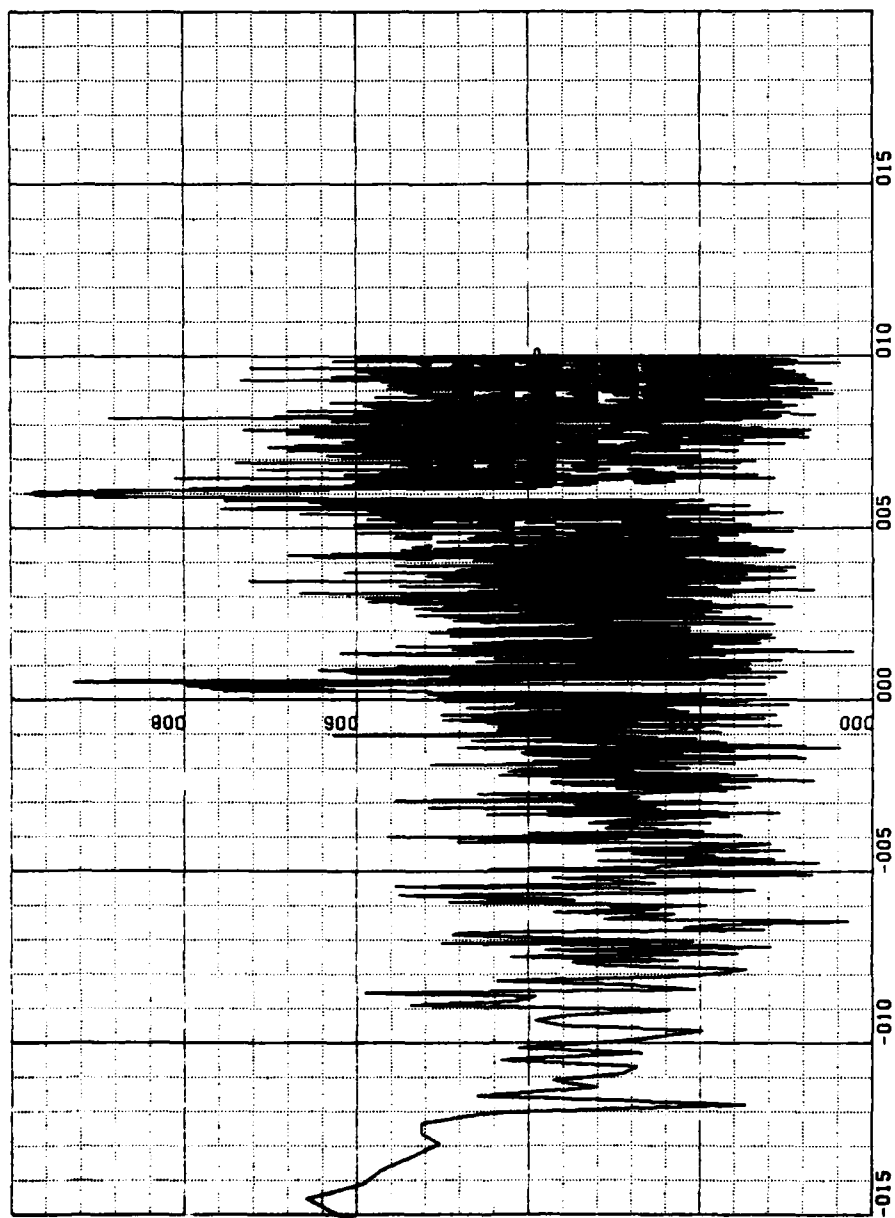


Figure 2.24. Degree of Polarization X-Y Plane, 17 August 82, 2245-2353 Local.  
 Degree of Polarization (0.2 units/in) vs. Log Frequency (Hz)  
 (0.5 units/in), 16 Averages

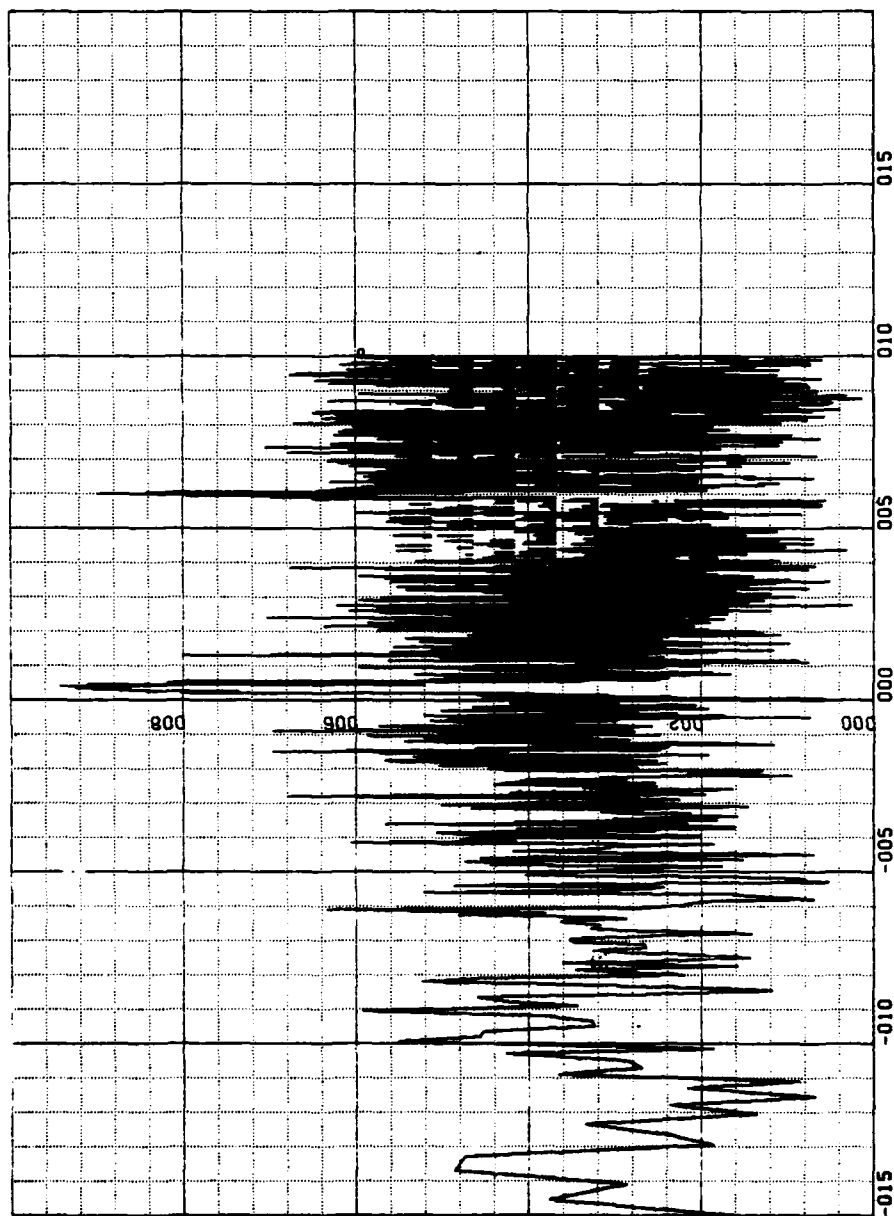


Figure 2.25. Degree of Polarization Y-Z Plane, 17 August 82, 2245-2353 Local.  
 Degree of Polarization (0.2 units/in) vs. Log Frequency (Hz)  
 (0.5 units/in), 16 Averages

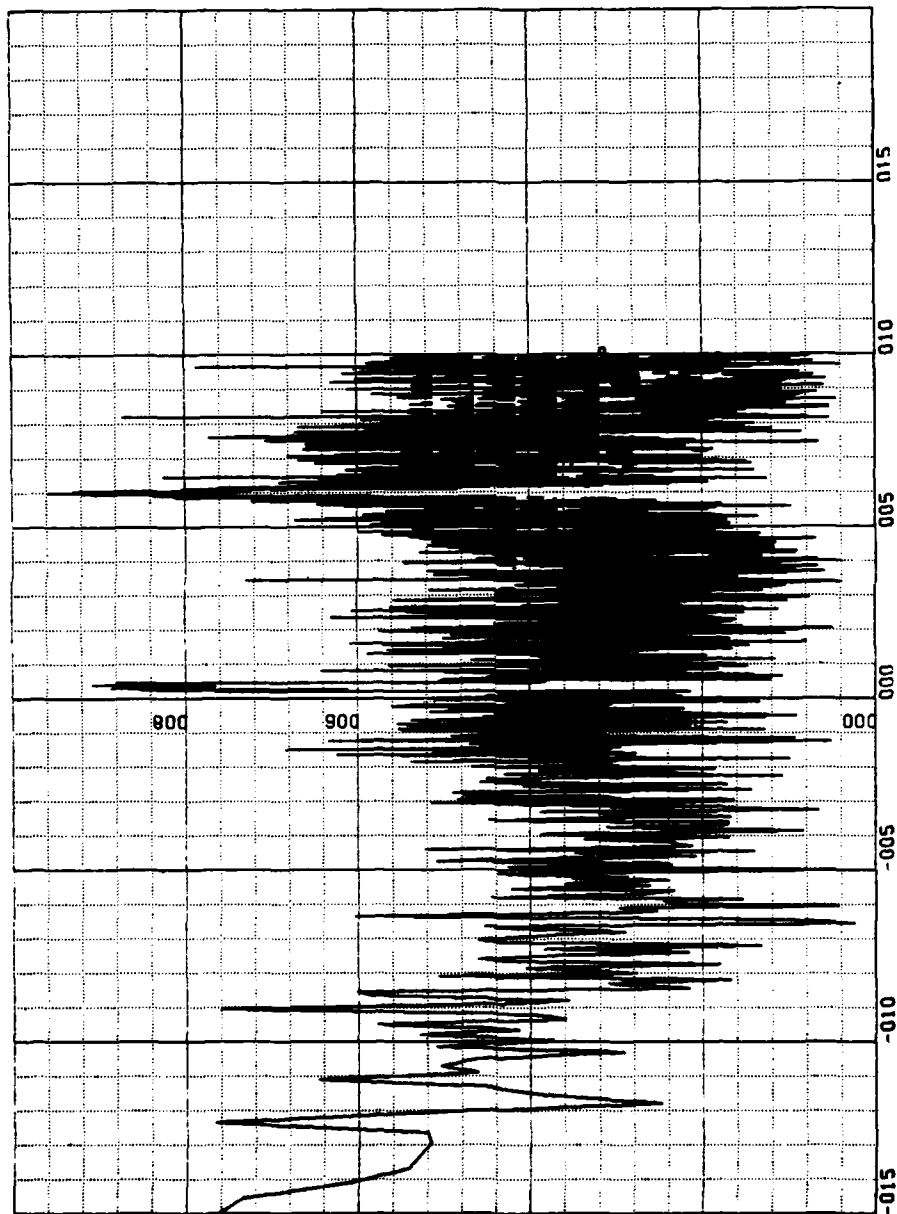


Figure 2.26. Degree of Polarization Z-X Plane, 17 August 82, 2245-2353 Local.  
 Degree of Polarization (0.2 units/in) vs. Log Frequency (Hz)  
 (0.5 units/in), 16 Averages

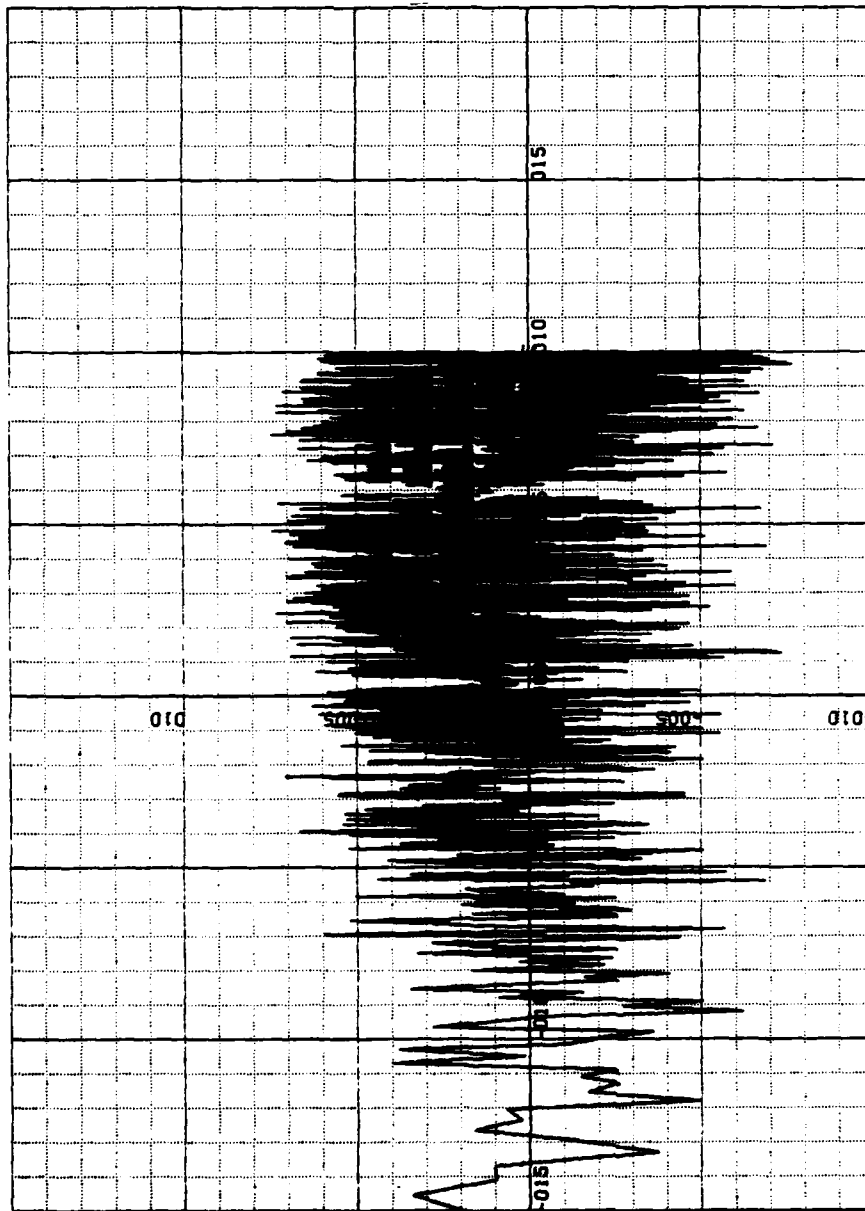


Figure 2.27. Ellipticity X-Y Plane, 17 August 82, 2245-2353 Local.  
 Ellipticity (0.5 units/in) vs. Log Frequency (Hz)  
 (0.5 units/in), 16 Averages

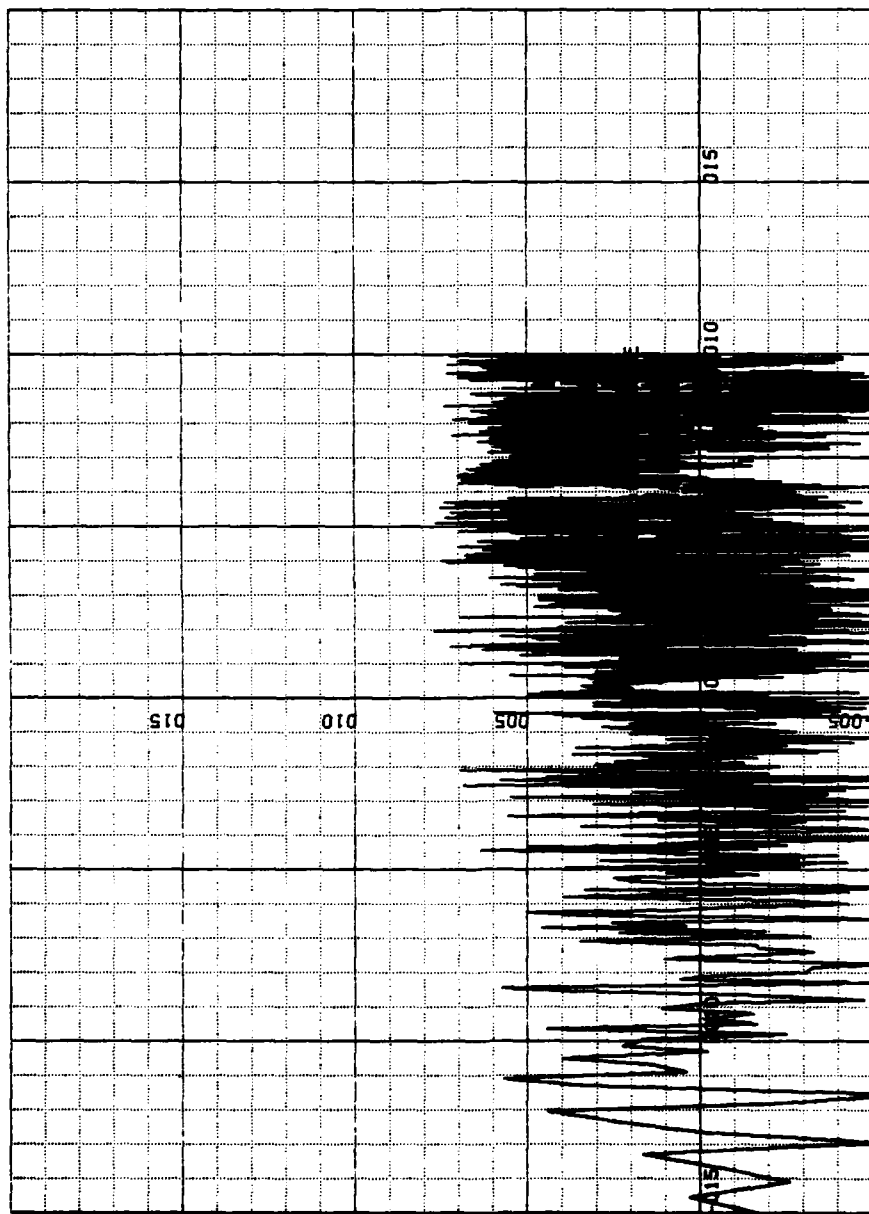


Figure 2.28. Ellipticity Y-Z Plane, 17 August 82, 2245-2353 Local.  
 Ellipticity (0.5 units/in) vs. Log Frequency (Hz) (0.5 units/in)  
 16 Averages

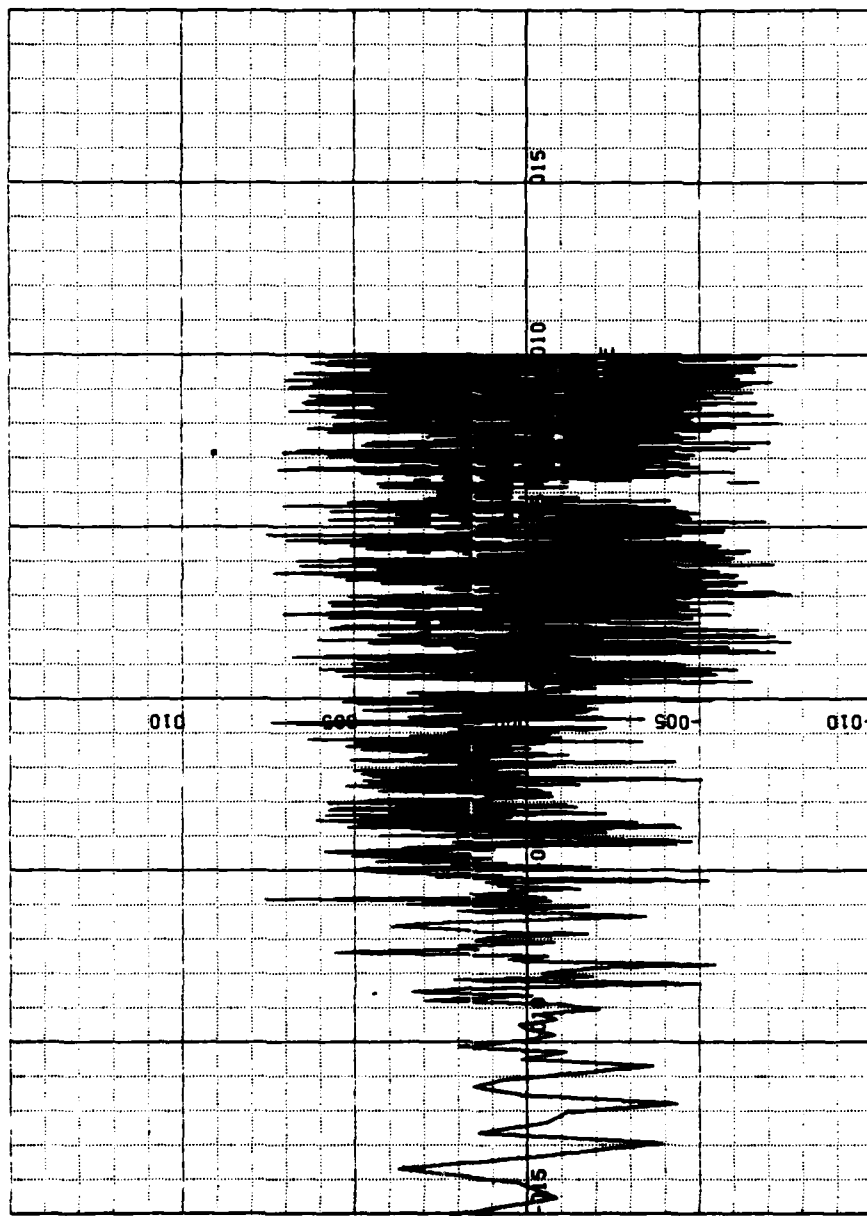


Figure 2.29. Ellipticity 2-X Plane, 17 August 82, 2245-2353 Local.  
 Ellipticity (0.5 units/in) vs. Log Frequency (Hz)  
 (0.5 units/in), 16 Averages

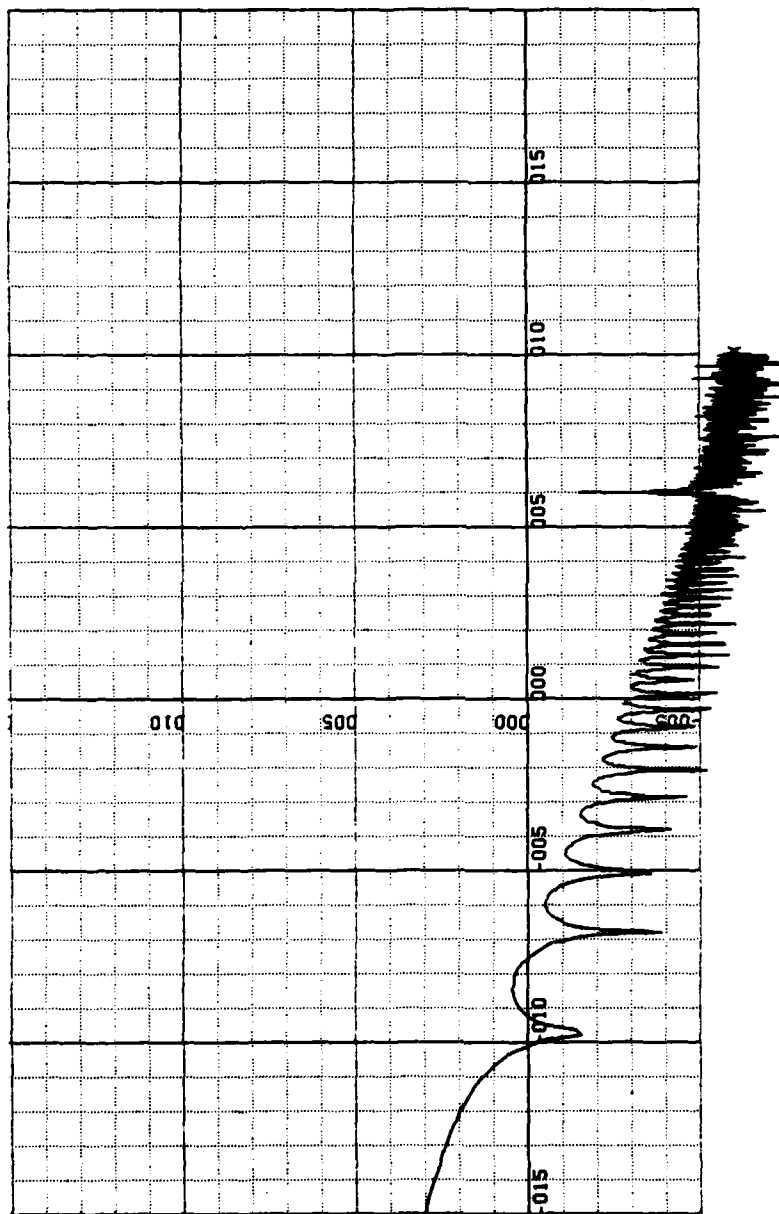


Figure 2.30. PSD X Coil, 17 August 82, 2240-2250 Local.  
Amplitude in dB (REF  $nT^{**}2/Hz$ ) (50 units/in) vs. Log  
Frequency (Hz) (0.5 units/in), 2 Averages



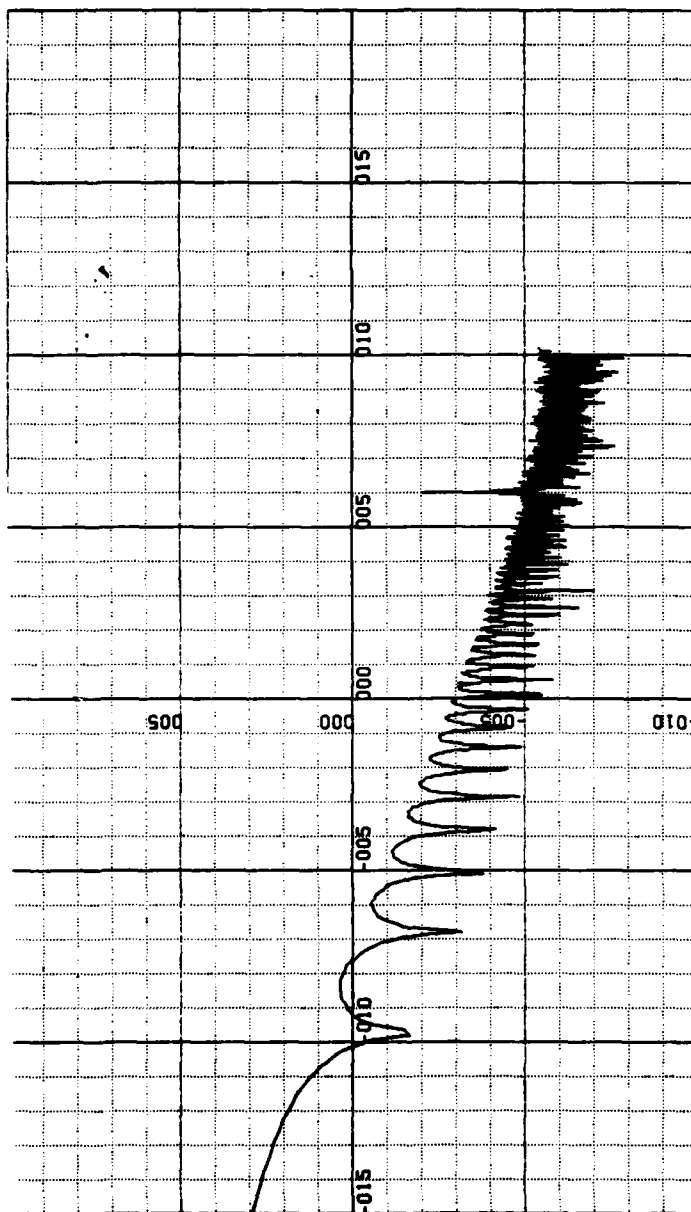


Figure 2.31. PSD Y Coil, 17 August 82, 2240-2250 Local.  
 Amplitude in dB (REF nT\*\*2/Hz) (50 units/in) vs. Log  
 Frequency (Hz) (0.5 units/in), 2 Averages

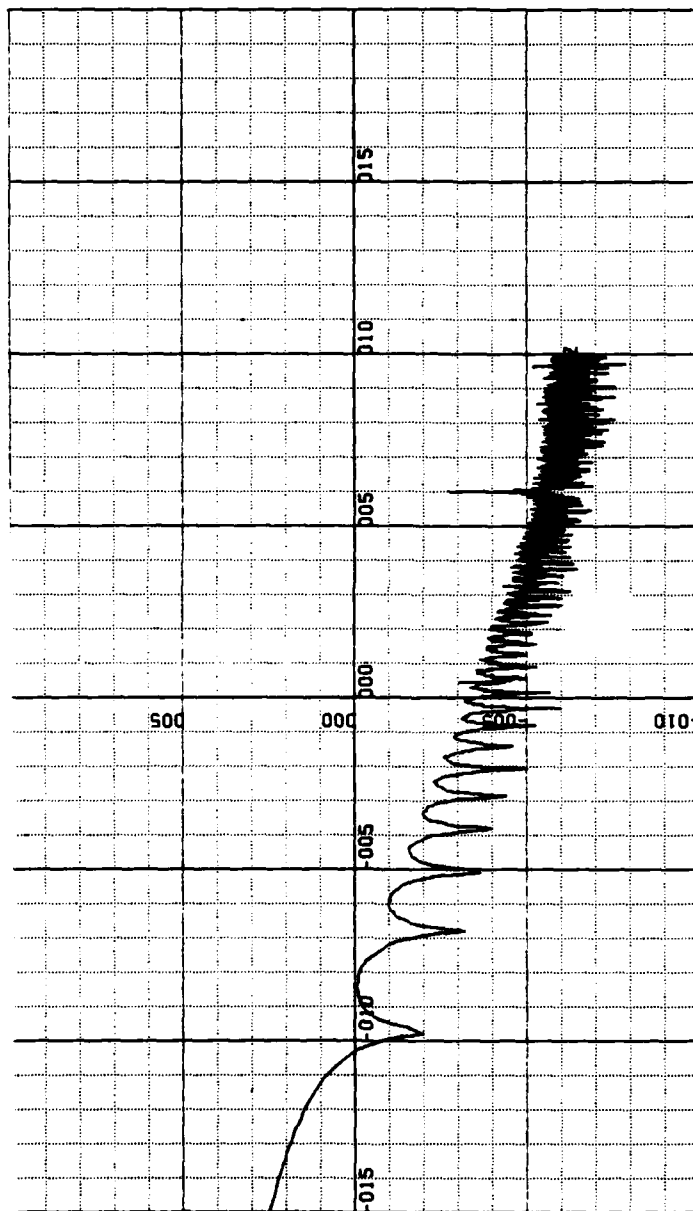


Figure 2.32. PSD Z Coil, 17 August 82, 2240-2250 Local.  
Amplitude in dB (REF nT\*\*2/Hz) (50 units/in) vs. Log  
Frequency (Hz) (0.5 units/in), 2 Averages

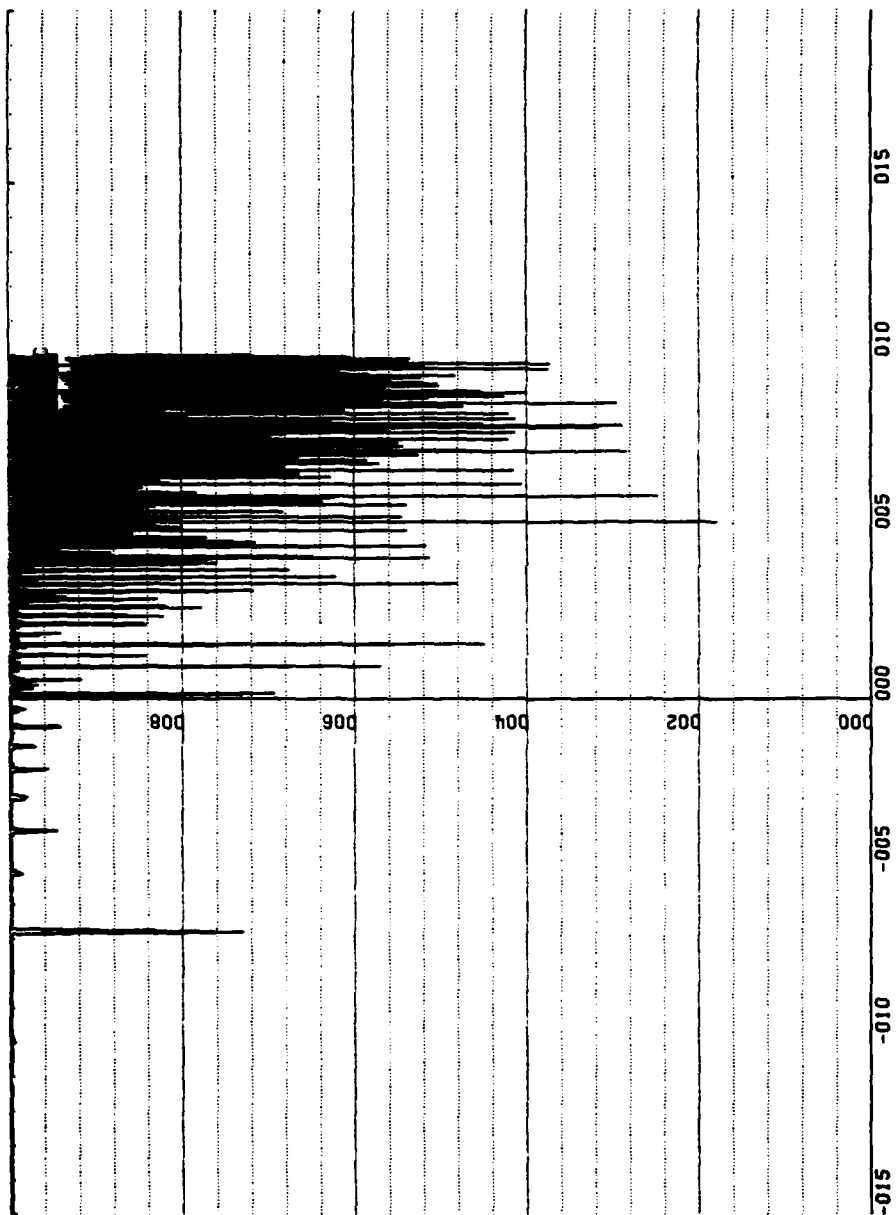


Figure 2.33. Coherence X-Y Coils, 17 August 82, 2240-2250 Local.  
Coherence X-Y Coils (0.2 units/in) vs. Log Frequency (Hz)  
(0.5 units/in), 2 Averages

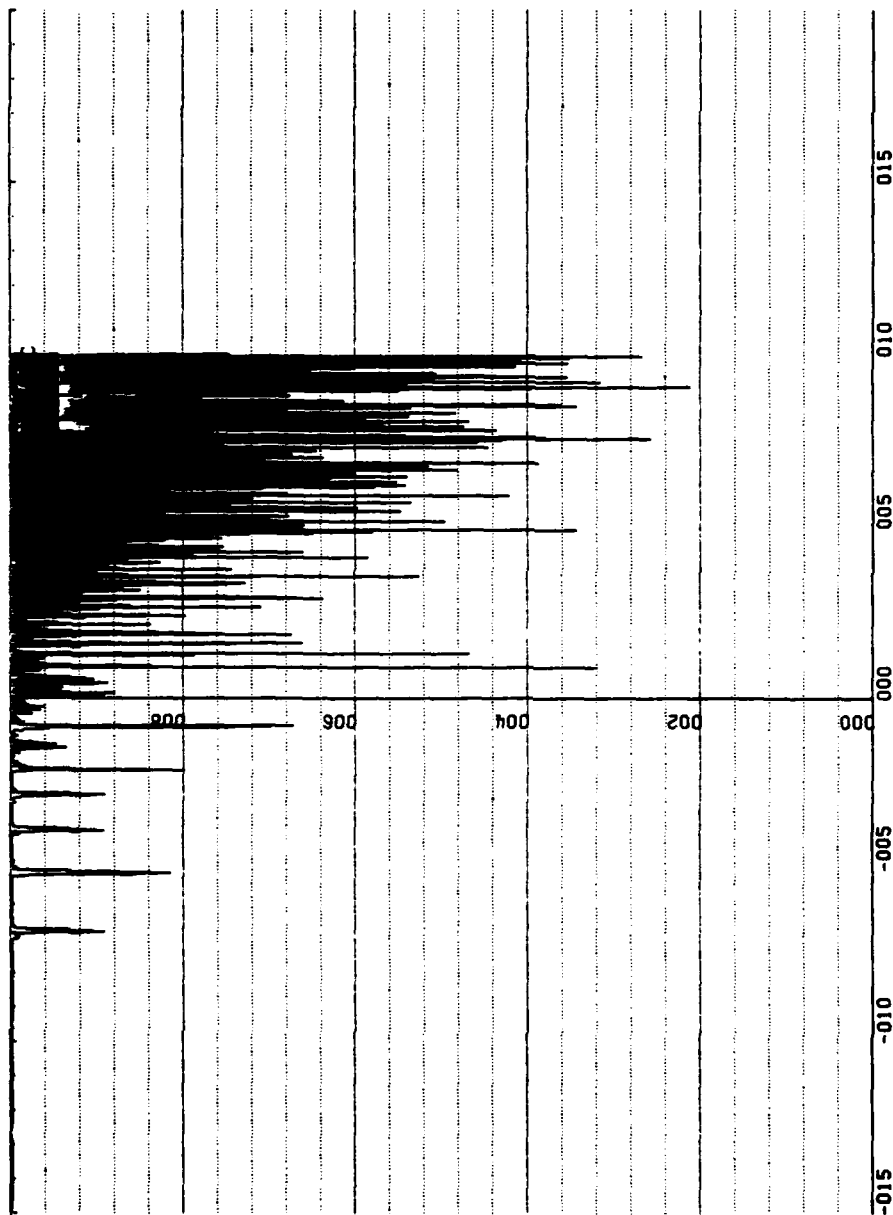


Figure 2.34. Coherence Y-Z Coils, 17 August 82, 2240-2250 Local.  
Coherence Y-Z Coils (0.2 units/in) vs. Log Frequency (Hz)  
(0.5 units/in), 2 Averages

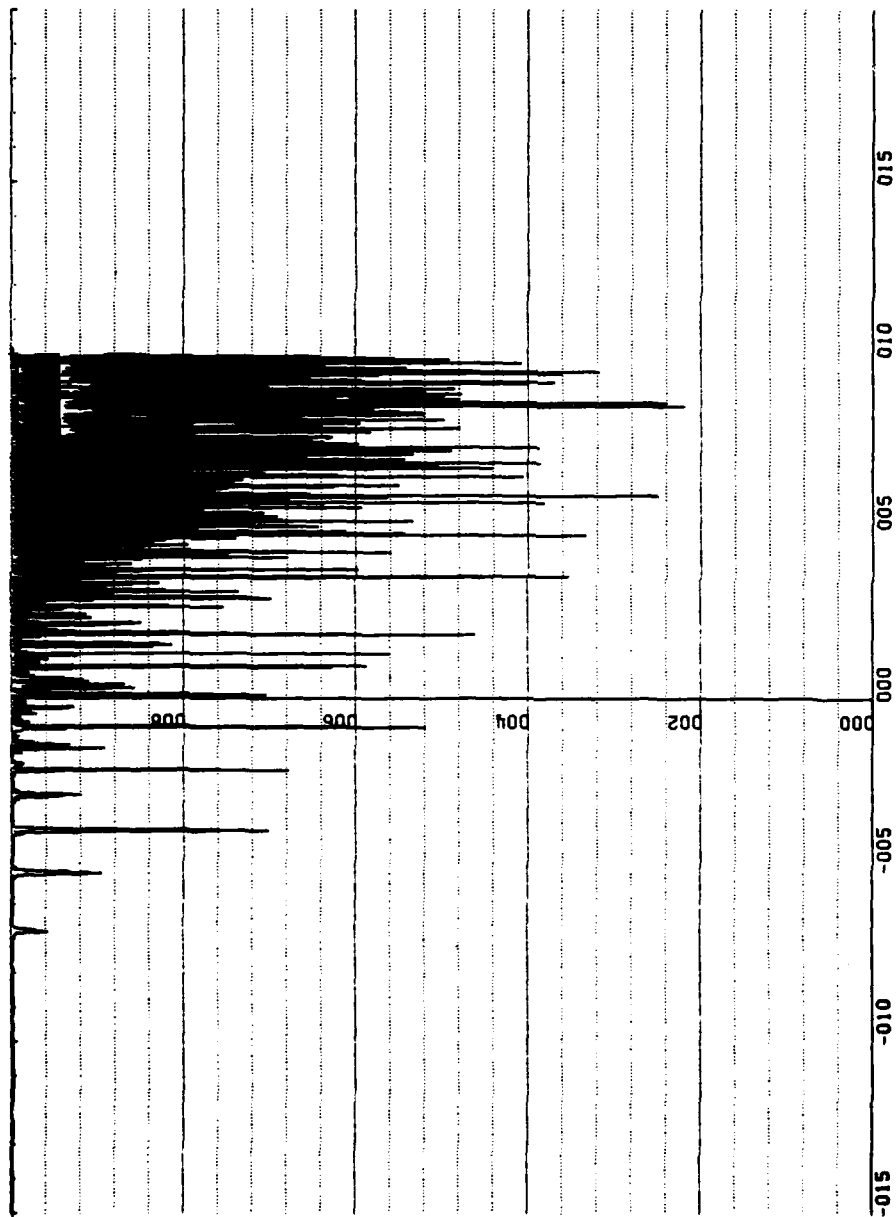


Figure 2.35. Coherence Z-X Coils, 17 August 82, 2240-2250 Local.  
Coherence Z-X Coils (0.2 units/in) vs. Log Frequency (Hz)  
(0.5 units/in), 2 Averages

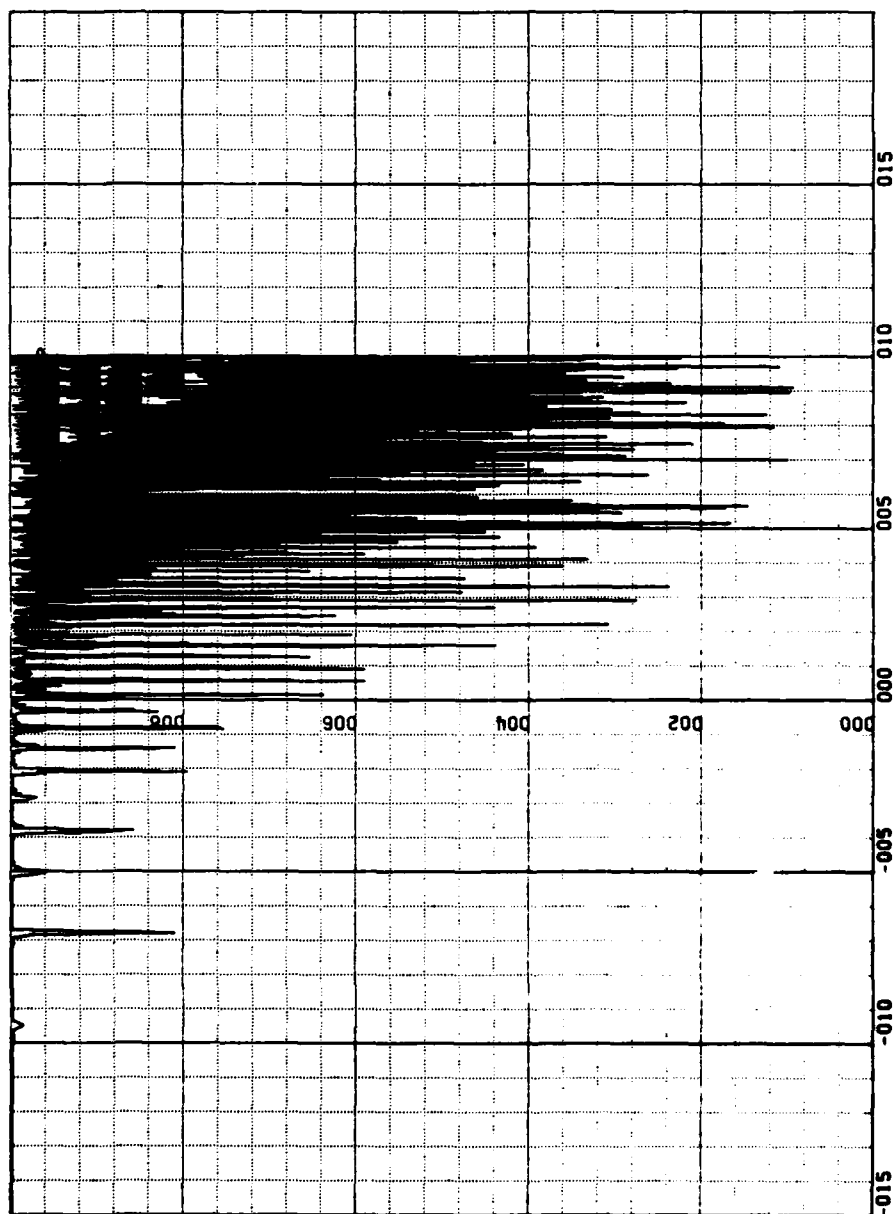


Figure 2.36. Degree of Polarization X-Y Plane, 17 August 82, 2240-2250 Local.  
 Degree of Polarization (0.2 units/in) vs. Log Frequency (Hz)  
 (0.5 units/in), 2 Averages

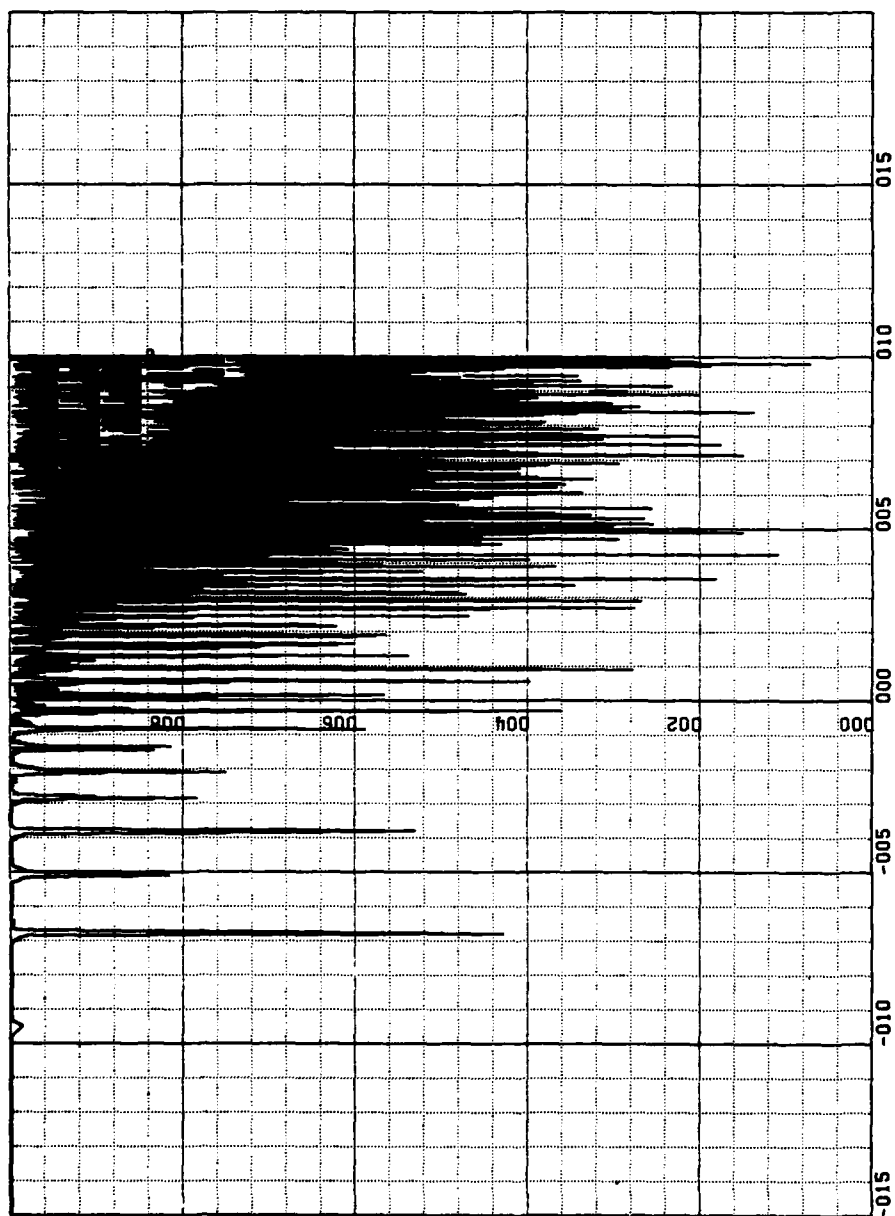


Figure 2.37. Degree of Polarization Y-X Plane, 17 August 82, 2240-2250 Local.  
 Degree of Polarization (0.2 units/in) vs. Log Frequency (Hz)  
 (0.5 units/in), 2 Averages

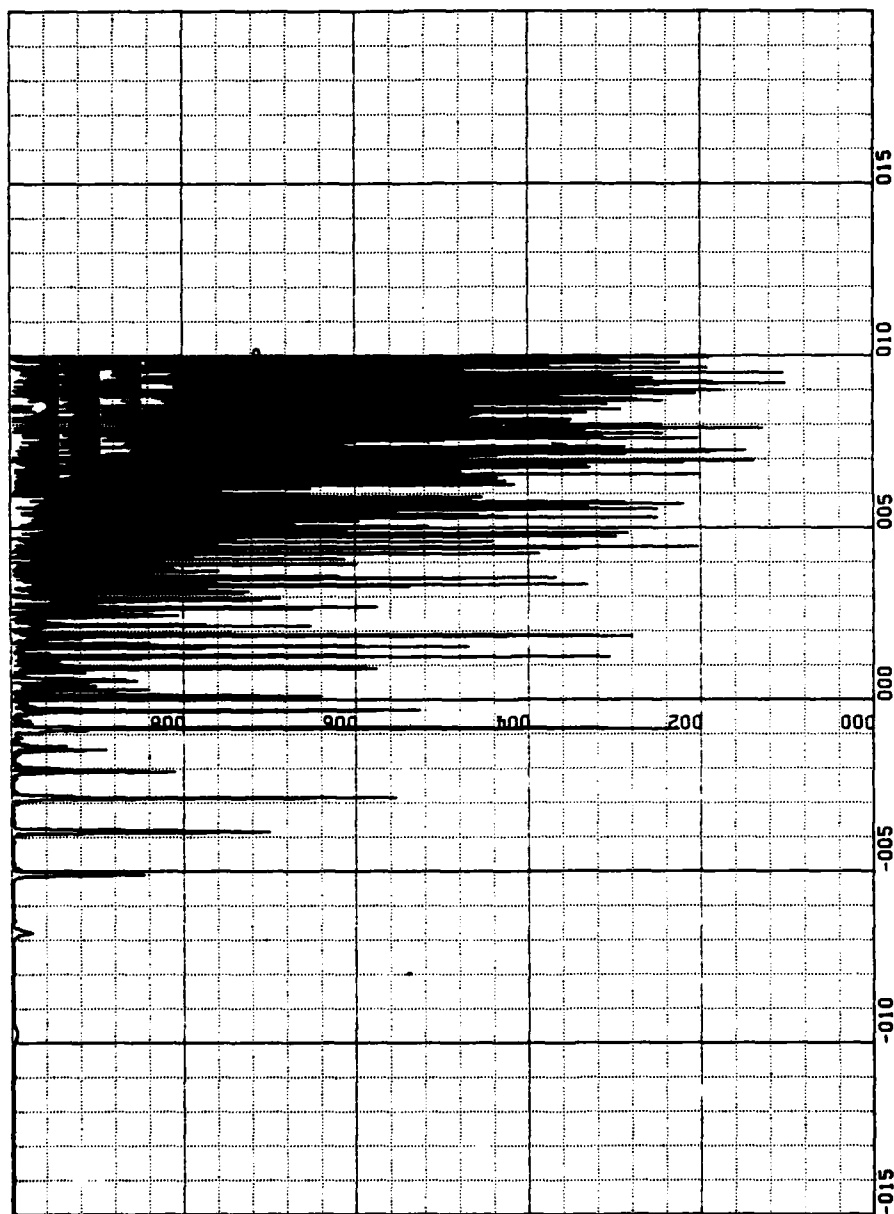


Figure 2.38. Degree of Polarization Z-X Plane, 17 August 82, 2240-2250 Local.  
 Degree of Polarization (0.2 units/in) vs. Log Frequency (Hz)  
 (0.5 units/in), 2 Averages



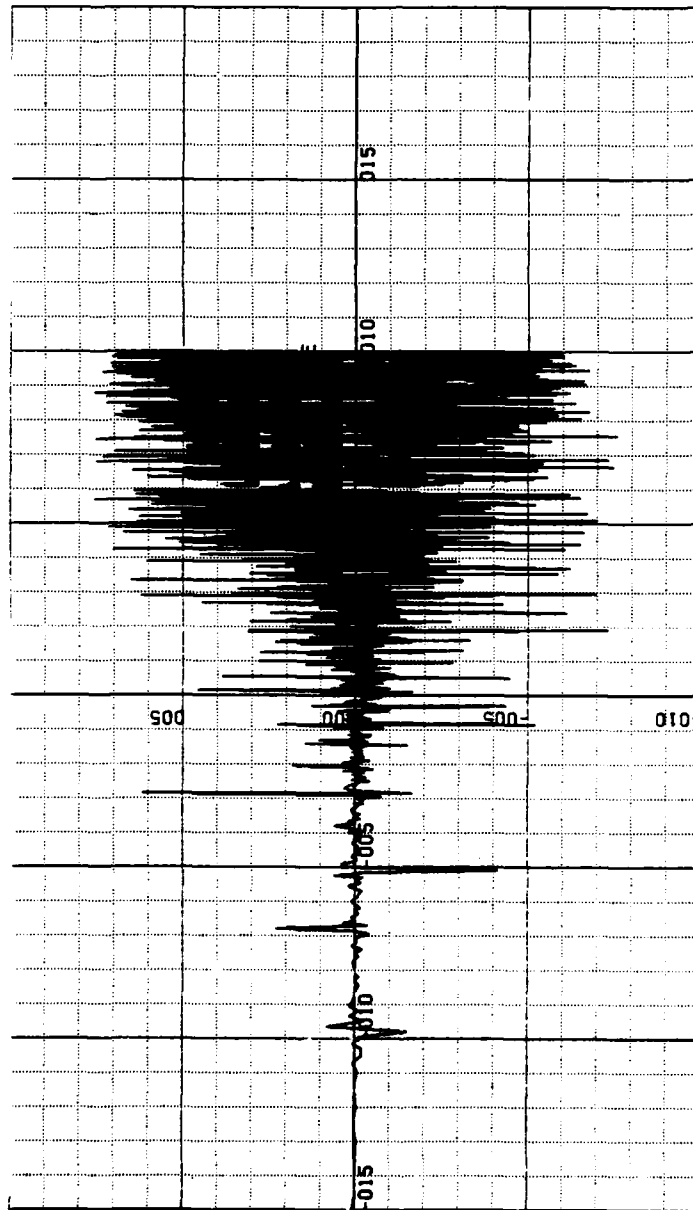


Figure 2.39. Ellipticity X-Y Plane, 17 August 82, 2240-2250 Local.  
 Ellipticity (0.5 units/in) vs. Log Frequency (Hz) (0.5 units/in)  
 2 Averages

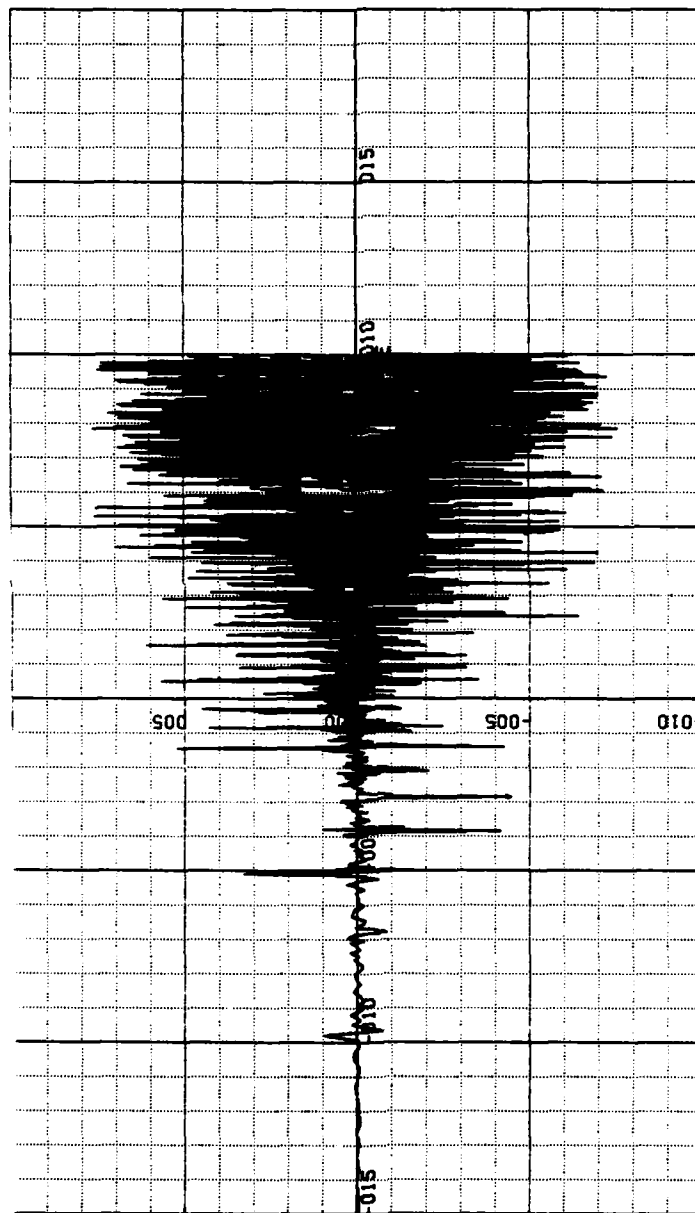


Figure 2.40. Ellipticity Y-Z Plane, 17 August 82, 2240-2250 Local.  
 Ellipticity (0.5 units/in) vs. Log Frequency (Hz) (0.5 units/in)  
 2 Averages

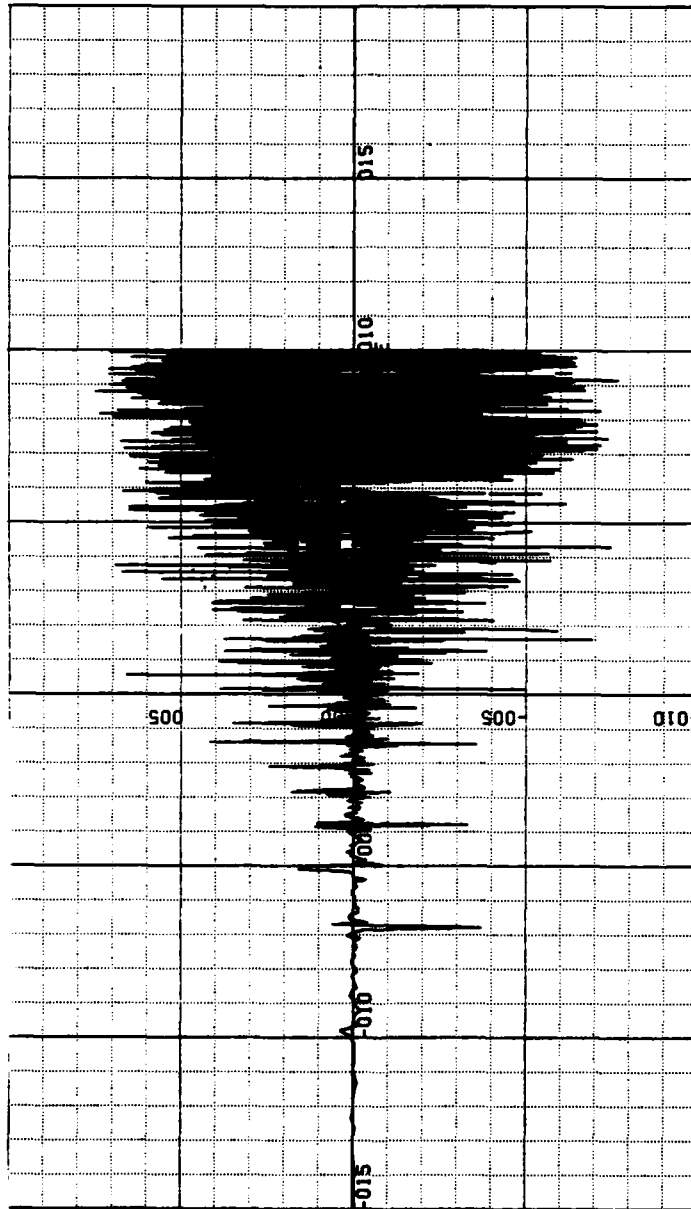


Figure 2.41. Ellipticity Z-X Plane, 17 August 82, 2240-2250 Local.  
 Ellipticity (0.5 units/in) vs. Log Frequency (Hz)  
 (0.5 units/in), 2 Averages

recommended at the beginning of the programs producing the above mentioned plots. Time series plots should also be made to provide a further check.

An explanation of the source of the large fluctuations is that the PCM to digital conversion begins before the actual PCM data starts on the tape. The decoding equipment considers the noise on the section of tape before the PCM data starts as signal.

The above analysis clearly proves that the "hump" like structure in the PSD's and the "nice" behavior observed in the corresponding coherence, ellipticity and degree of polarization are artificial and do not represent any real phenomena in the geomagnetic field. Thus, the data in Figures 2.3-2.14 and Figures 2.30-2.41 does not appear to be reliable. Unfortunately, this artificially induced, and therefore unphysical, behavior of the polarization has been published recently [Ref. 7]. The conclusion found in Reference 7 that

Geomagnetic fluctuations in land are well polarized below 1.0 Hz and that the polarization is quite frequently, though not consistently, linear. The situation under the sea is similar. Furthermore, a land-sea coherence study in the horizontal plane showed very high coherence below 1.0 Hz.

are not substantiated by the physical data. Plots of the artificially induced behavior are published in References 1, 2, and 3.

The 4 Hz peak present in the PSD's shown in Figures 2.18-2.20 is the result of 60 Hz aliasing. 60 Hz magnetic fields generated by local power lines exist at the measurement site. Digitization at a 32 Hz or 64 Hz rate of the analog voltages from the sensing coils shifts the true frequency of the power line signals down at 4 Hz. The 60 Hz aliasing results in the anomalous behavior at 4 Hz seen in the coherence, degree of polarization and ellipticity plots shown in Figures 2.21-2.29.

Another peak is present at about 1.2 Hz for the PSD's in Figures 2.18-2.20. For this data set, the 1.2 Hz signal correlates with a 1.2 Hz signal identified in the time series data. The origin of the 1.2 Hz signal is unknown. The 4 Hz and 1.2 Hz peaks are of little concern in this study since both are well above the frequency of the micropulsation analyzed.

Another "suspicious" feature of the PSD's is the large amount of hash appearing from 2 to 10 hertz. We will gain further insight into this problem in analyzing the time series voltage data.

From the analysis of the abnormal behavior in the PSD's, coherence, etc., future coil data sets should receive a balanced treatment between the time domain and the frequency domain to avoid misinterpretation.

### III. TIME SERIES DATA

#### A. TIME SERIES VOLTAGE DATA

##### 1. Voltage Software

The importance of time series data as a check became evident when we uncovered the problem with the initial PSD's, coherences, etc. Computer code was developed to produce both unsmoothed and smoothed times series voltage plots. The reason for producing both smoothed and unsmoothed voltage plots will become apparent in the time series voltage analysis section. Time series voltage plots could provide a means of monitoring the data for system "glitches" which might later produce erroneous PSD's, etc., and suspicious features on time series magnetic field plots.

The Fortran computer program that produces the voltage plots is compiled and run on the Naval Postgraduate School IBM 3033 VM or "batch" system. Both the unsmoothed voltage program (VOLTR) and the smoothed voltage program (VOLTS) require 2.048 megabytes of core memory and approximately 15 minutes of central processor unit (CPU) time to run. These figures provide a comfortable margin to insure that the program does not "bomb" due to lack of core or run time.

The design of both VOLTR and VOLTS is the same with the exception that a smoothing algorithm is applied to the data in the case of VOLTS. Both programs have incorporated in them the digital tape advance package using ISEC as the number of

seconds one wishes to advance the tape. Data is read off the digital tape in blocks of 8192 frames by the subroutine RD referenced earlier. As before, this data is in integer form and represents voltages between +5 volts by numbers between 0 and 4096. The integer representing 0 volts is ideally 2048, however, I found that the "real" zero values wander. The reason for this "wander" is not understood. For good results, the following values worked well for the respective coils.

X-coil : zero = 1966

Y-coil : zero = 2085

Z-coil : zero = 2539

The voltage values normalized to +5 volts are placed in new real arrays. At this point the next block of data is read off the digital tape and goes through the same process. VOLTR and VOLTS analyze eight blocks or 34 minutes of data. The linear arrays holding the voltage data are dimensioned to 65,536 elements given a sampling rate of 32 samples/second. For every one of the 65,536 voltage values there is a time value in another array. Thus four arrays are required to handle the data, three arrays containing voltage data and one that contains the respective times for each of the measurements. At this point, the VOLTR program calls the NONIMSL subroutine DRAWP to plot the data. The VOLTS program uses a smoothing algorithm to reduce the amount of high frequency hash.

The smoothing algorithm is a double running point average executed on all three axes of data. Since I was

interested in periods of approximately 10-45 seconds, I averaged over 144 points. With a running average over 23 percent of the oscillation, the unwanted background can be removed without destroying the oscillations. Averages greater than 50 percent of the period would partially remove the oscillation of interest. The construction of the algorithm makes changing the number of points averaged over trivial. One need only change a loop index and three divisors to obtain a different average. The smoothing algorithm is provided as Table 3.1. The computer code for both VOLTR and VOLTS is attached in Appendix A and Appendix B.

## 2. Time Series Voltage Data Analysis

One can gain a great deal of insight into the contents of the data by looking at the smoothed and unsmoothed voltage products. Figures 3.1-3.3 are unsmoothed voltage plots representing the first 34 minutes of the digital data tape GMDT 11 recorded 17 August 82, 1301-1408 local time. A one minute tape advance was used in producing this data. Immediately one notices the large amount of 60 hertz aliasing in the time series unsmoothed voltage. The 60 hertz aliasing appears as 4 hertz because of the 32 sample/second sampling rate. The sensing system has a low pass filter that should be improved to remove the aliasing problem. The 4 hertz background can be seen more clearly in Figures 3.4-3.6. Above the 60 hertz aliasing background, we see voltage spikes ranging in magnitude from 1 volt to over 4 volts. Expanding the time scale to 50



Table 3.1. Smoothing Algorithm

```

DC 73 L2=1,2
Q=0
DC 74 IS=1,65318
SUMX=0.0
SUMY=0.0
SUMZ=0.0
DC 75 J=1,144
SUMX=ZZX1(Q+J)+SUMX
SUMY=ZZY1(Q+J)+SUMY
SUMZ=ZZV1(Q+J)+SUMZ
75 CCNTINUE
ZZX1(IS)=SUMX/144.
ZZY1(IS)=SUMY/144.
ZZV1(IS)=SUMZ/144.
C=Q+1
74 CCNTINUE
73 CCNTINUE

```

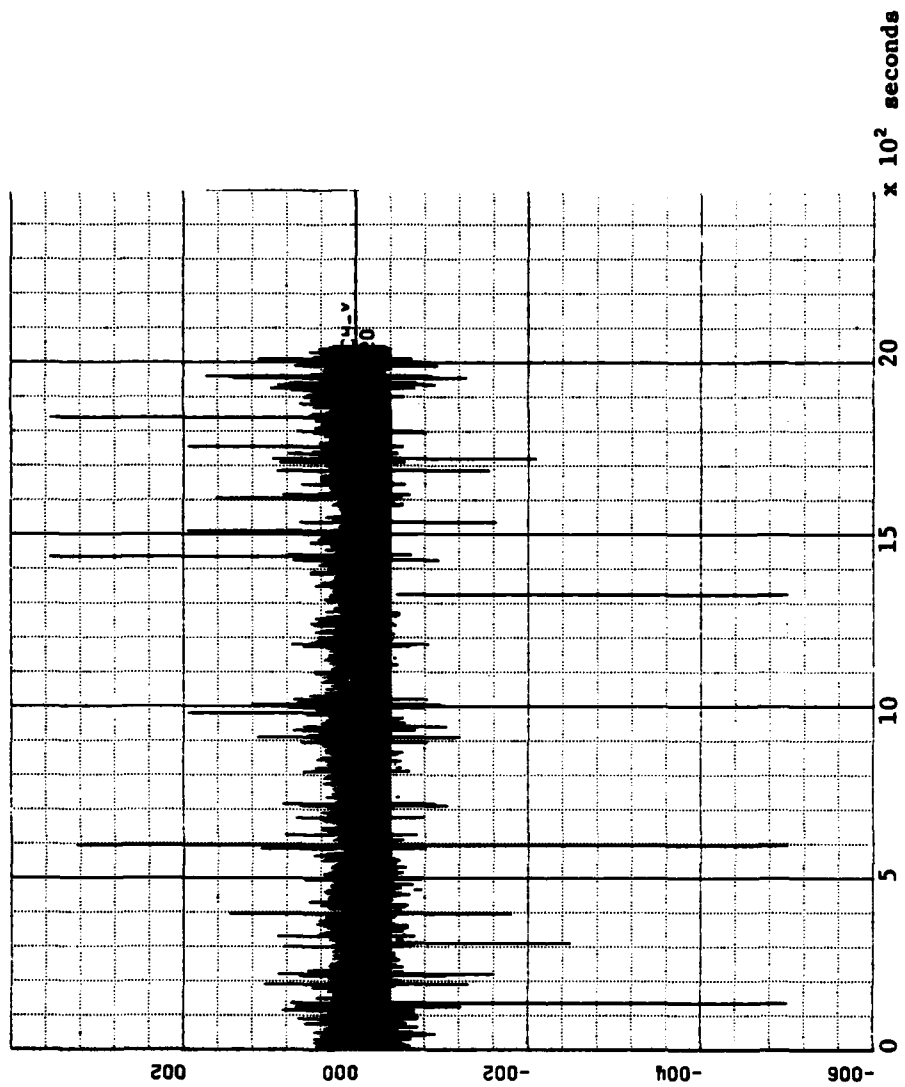


Figure 3.1. X Coil Voltage, 17 August 82, 1302-1336 Local.  
Amplitude (volts : 2 units/in) vs. Time (seconds : 500 units/in)

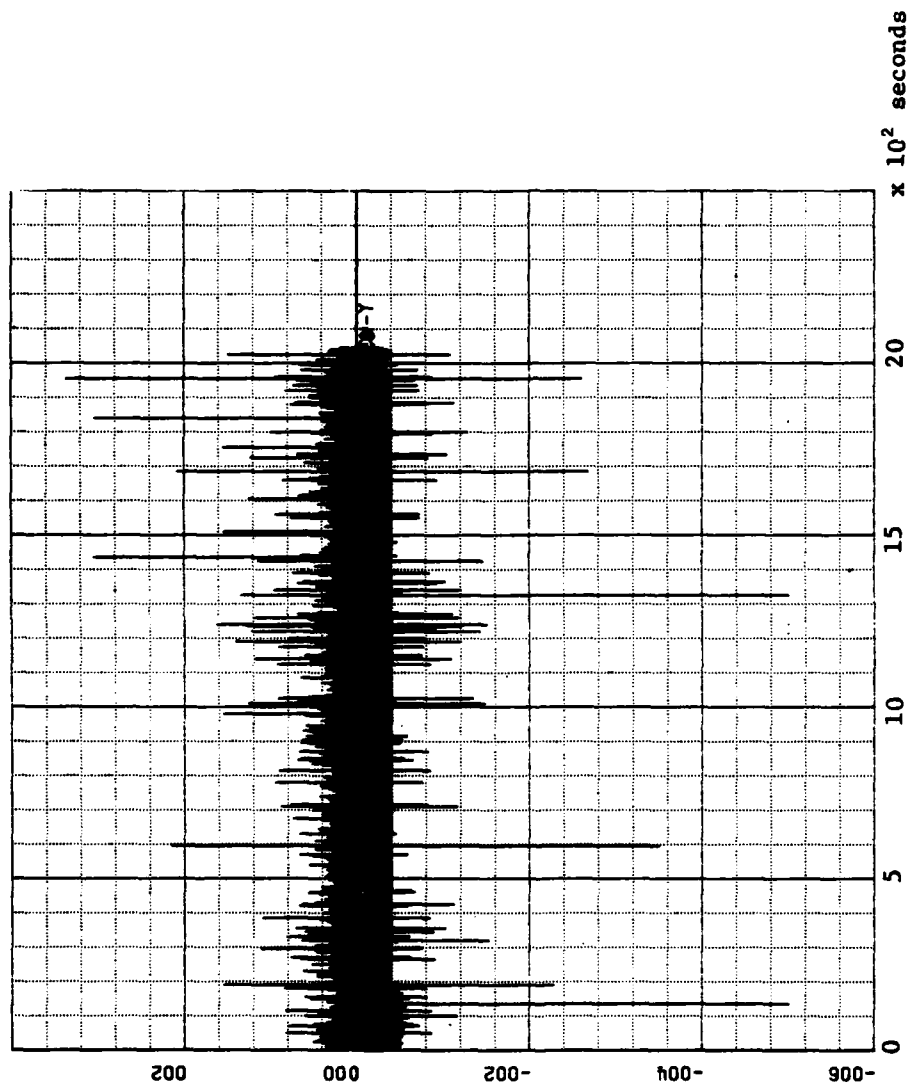


Figure 3.2. Y Coil Voltage, 17 August 82, 1302-1336 Local.  
Amplitude (volts : 2 units/in) vs. Time (seconds : 500 units/in)

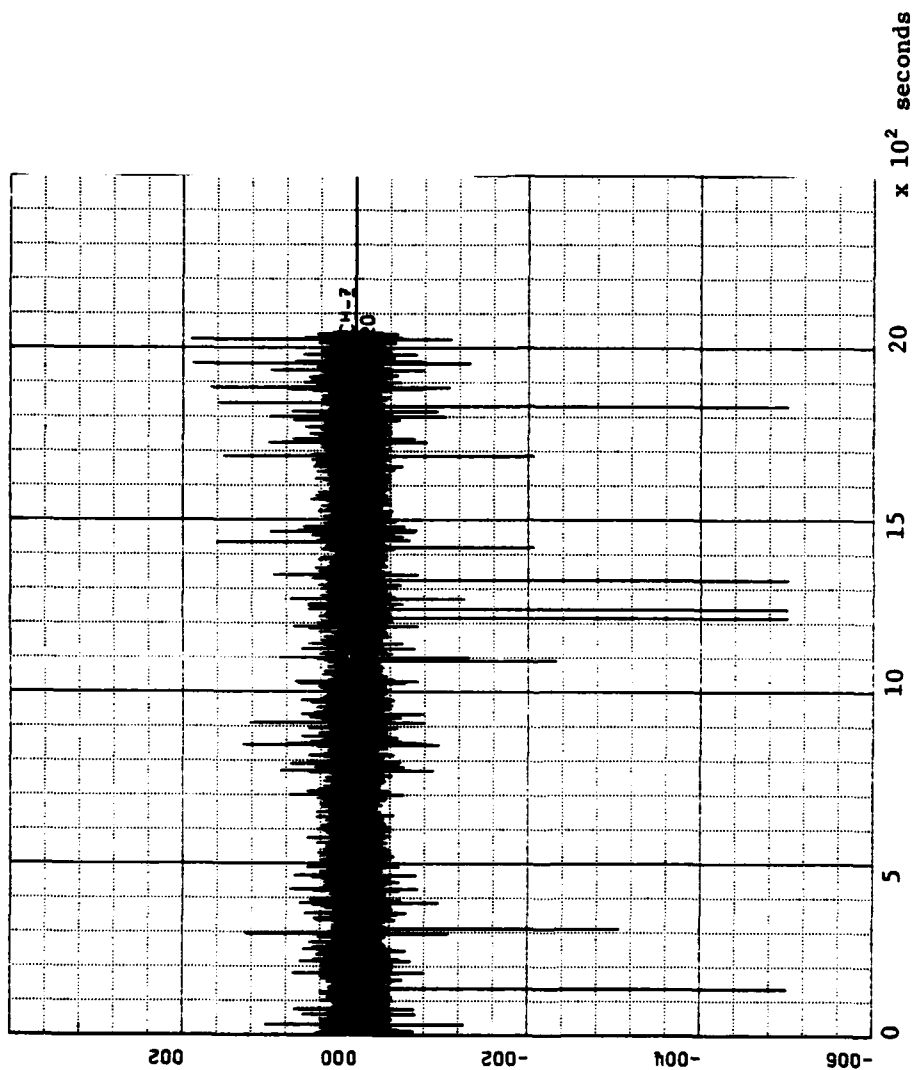


Figure 3.3. Z Coil Voltage, 17 August 82, 1302-1336 Local.  
Amplitude (volts : 2 units/in) vs. Time (seconds : 500 units/in)

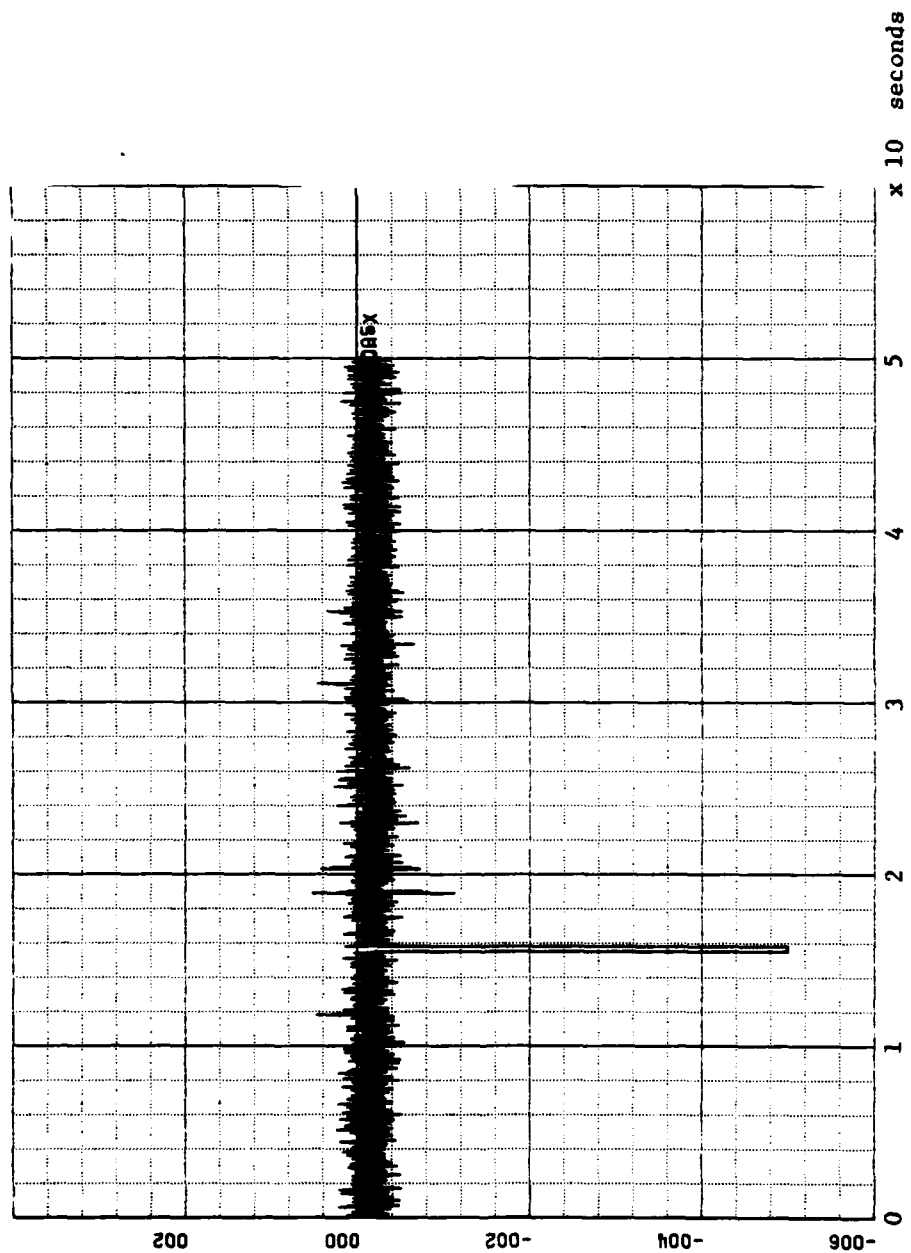


Figure 3.4. X-Coil Voltage, 17 August 82, 1322-1323 Local.  
Amplitude (Volts: 2 units/in) vs. Time (seconds : 10 units/in)

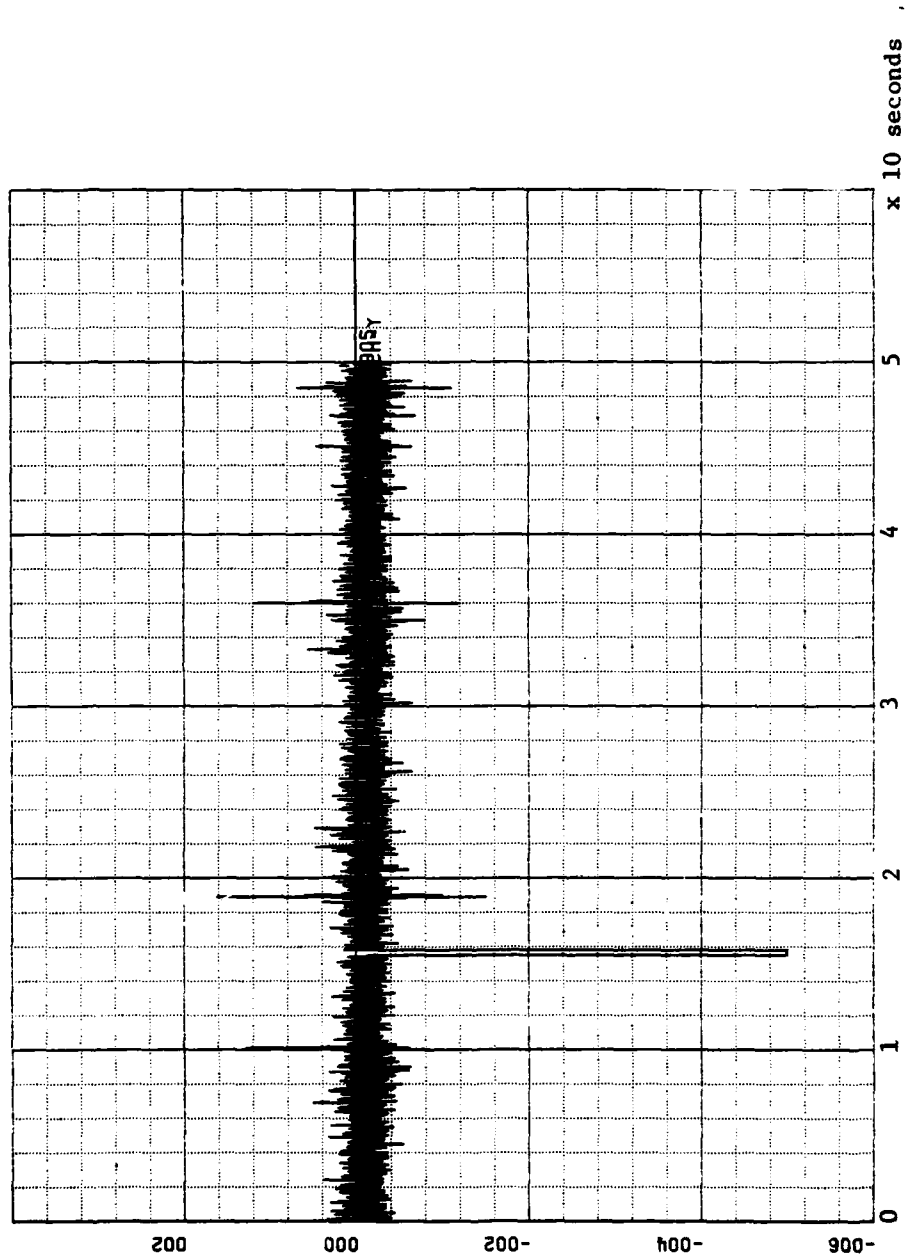


Figure 3.5. Y-Coil Voltage, 17 August 82, 1322-1323 Local.  
Amplitude (volts : 2 units/in) vs. Time (seconds : 10 units/in)

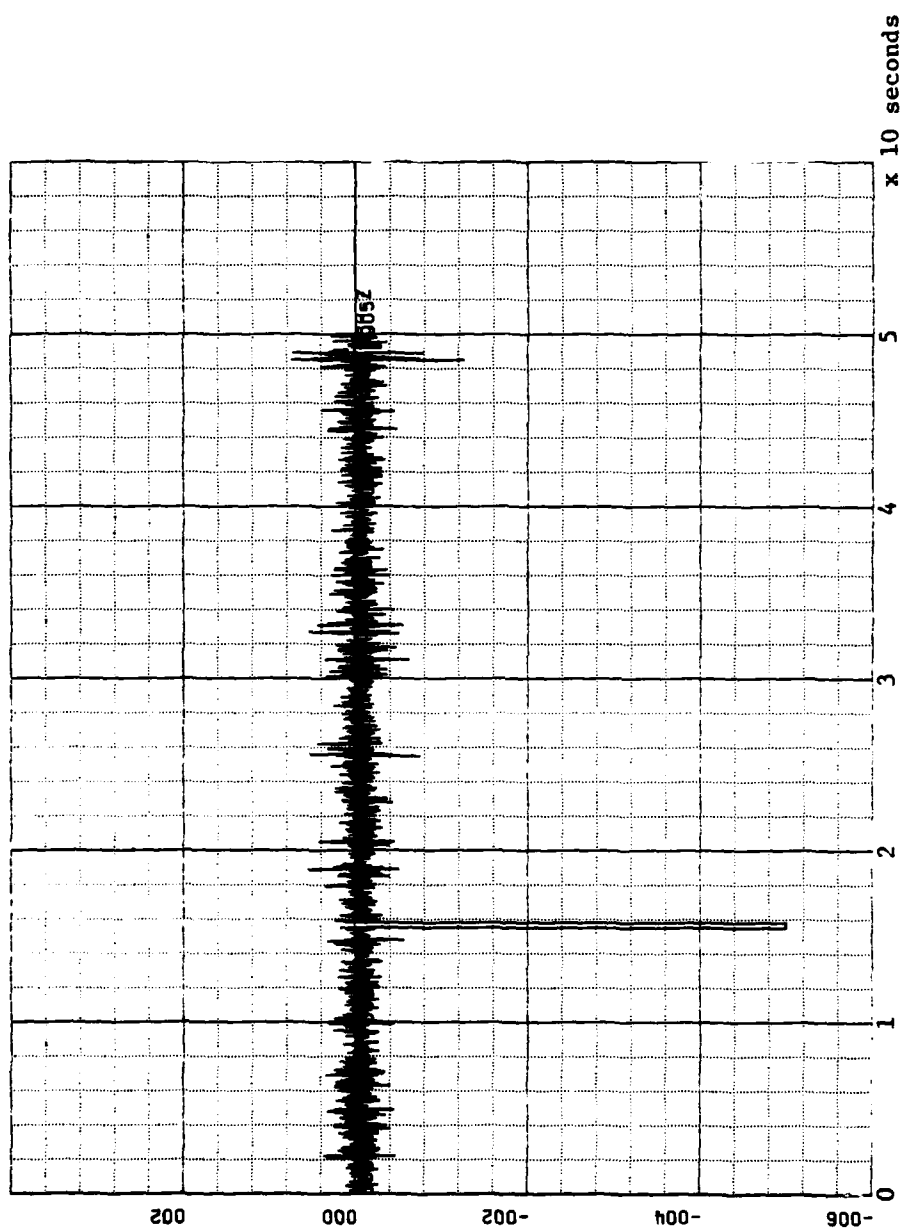


Figure 3.6. Z-Coil Voltage, 17 August 82, 1322-1323 Local.  
Amplitude (volts : 2 units/in) vs. Time (seconds : 10 units/in)

seconds of data, the structure of the voltage spikes becomes apparent in Figures 3.4-3.6. The "square well" shape is characteristic of PCM dropouts or instances during the PCM to digital conversion synchronization is lost between the tape recorder containing the PCM tape and the decoding unit. We do not know whether PCM dropouts always occur on all three channels, but current evidence suggests dropouts are simultaneous on all channels.

Figures 3.7-3.9 again show the first 34 minutes of GMDT 11 only smoothed by the 144 point running average. The smoothing algorithm removes the 60 hertz aliasing. The PCM dropouts appear as "glitches" in the otherwise quasi sinusoid characteristic of a micropulsation.

We should note that the unusually large amount of hash present between 2 hertz and 10 hertz in the PSD's and the average slope of the PSD curve for those frequencies may in part be due to the PCM dropouts that occur on the tapes. A "deglitching" algorithm could be developed to remove the sudden large amplitude structures injected by the system into the voltage data if hardware modifications fail.

## B. TIME SERIES MAGNETIC FIELD DATA

### 1. Magnetic Field Software

The time series magnetic field software is basically the same as that which produces the PSD's, etc. [Ref. 1 and Ref. 3]. The differences begin after the forward Fourier transform and the application of the transfer function. We



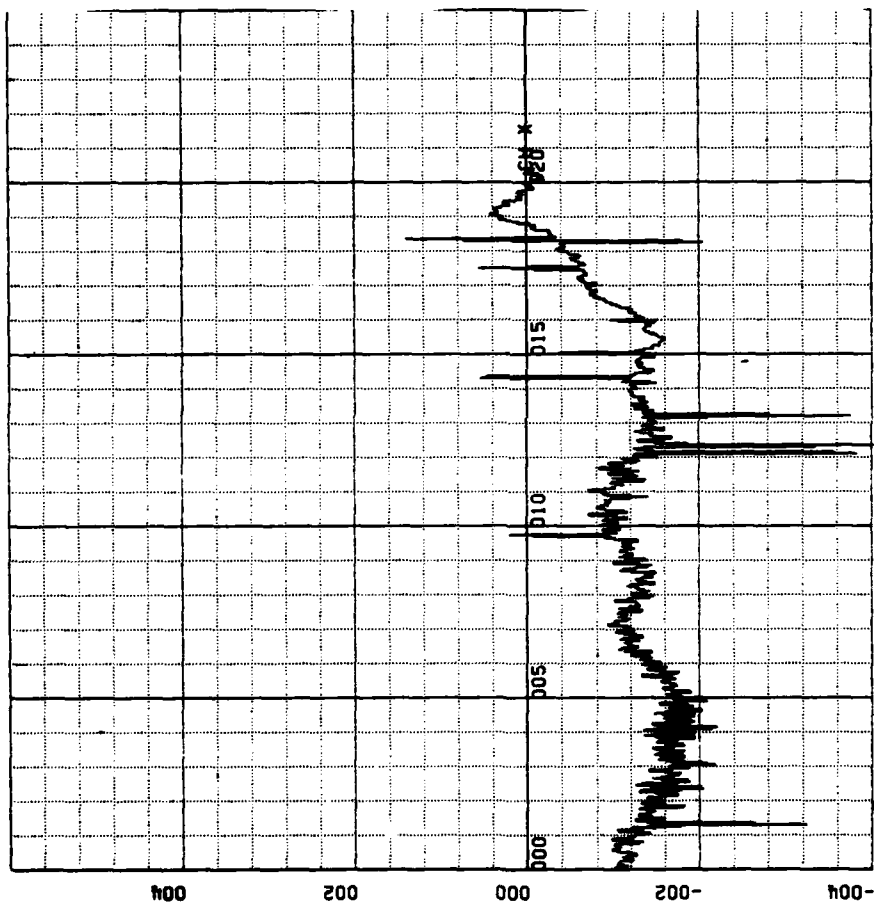


Figure 3.7. X Coil Voltage, 17 August 82, 1302-1336 Local.  
Amplitude (volts : 0.2 units/in) vs. Time (seconds : 500 units/in)

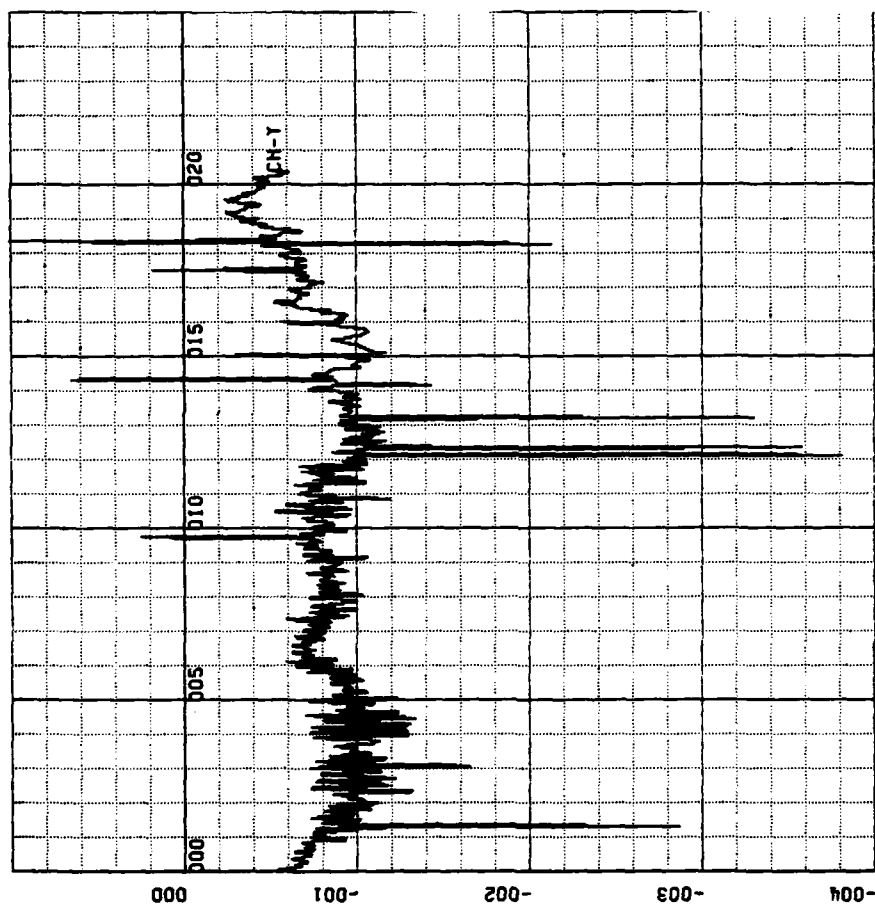


Figure 3.8. Y Coil Voltage, 17 August 82, 1302-1336 Local.  
Amplitude (volts : 0.1 units/in) vs. Time (seconds : 500 units/in)

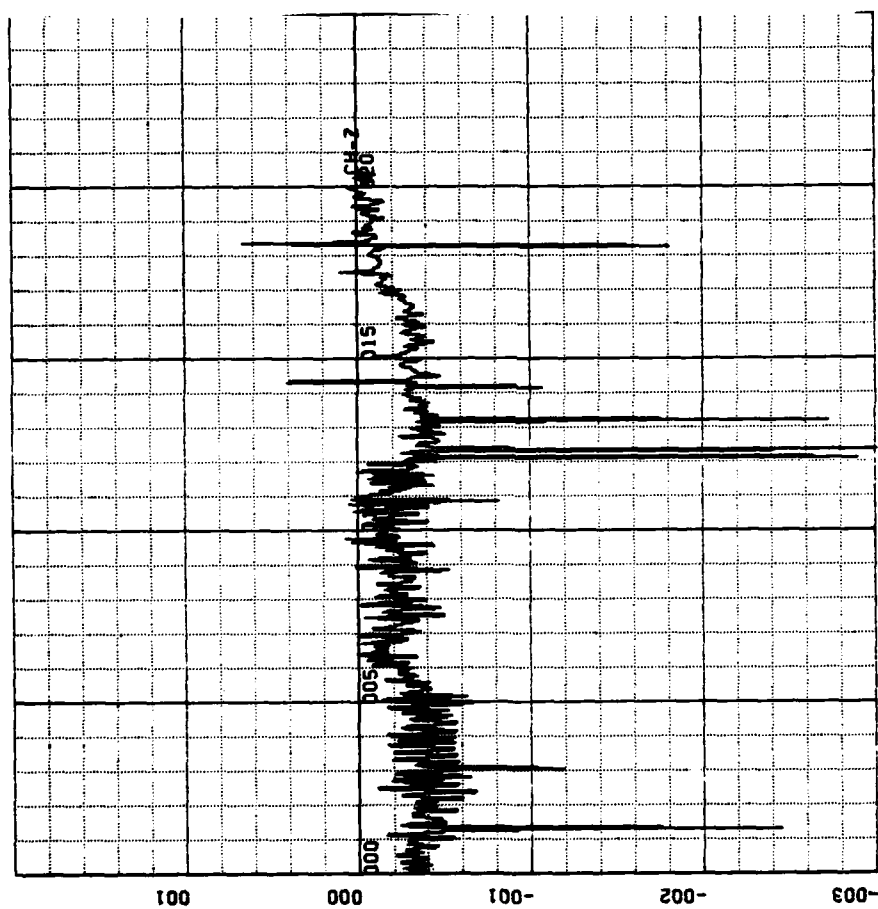


Figure 3.9. Z Coil Voltage, 17 August 82, 1302-1336 Local.  
Amplitude (volts : 0.1 units/in) vs. Time (seconds :500 units/in)

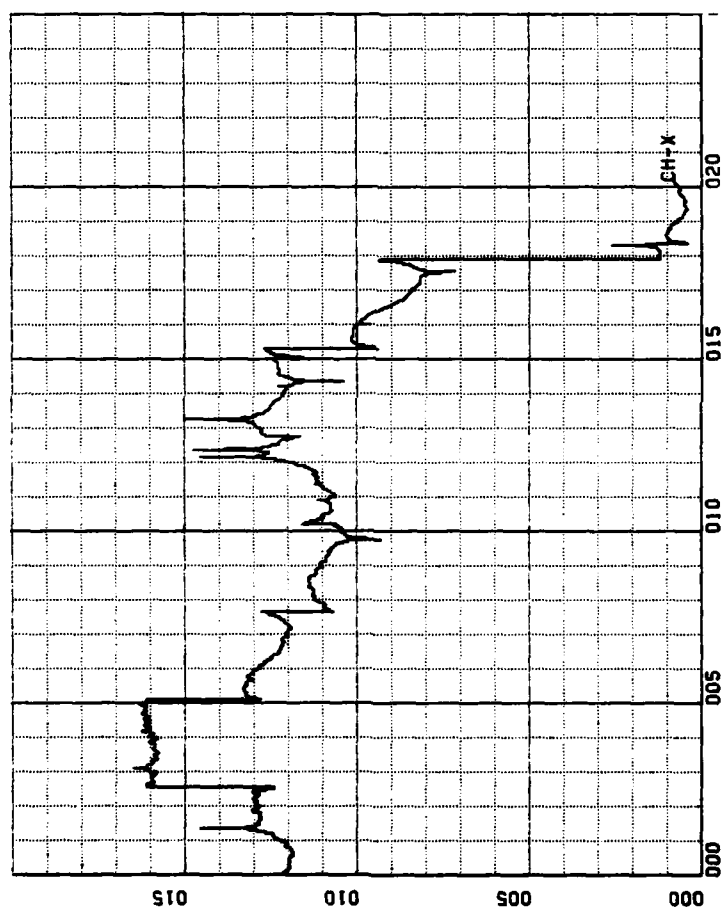


Figure 3.10a. X-Coil Magnetic Field, 17 August 82, 1302-1336 Local.  
 Amplitude (nanoteslas : 5 units/in) vs. Time (seconds : 500 units/in)  
 8 point smoothing

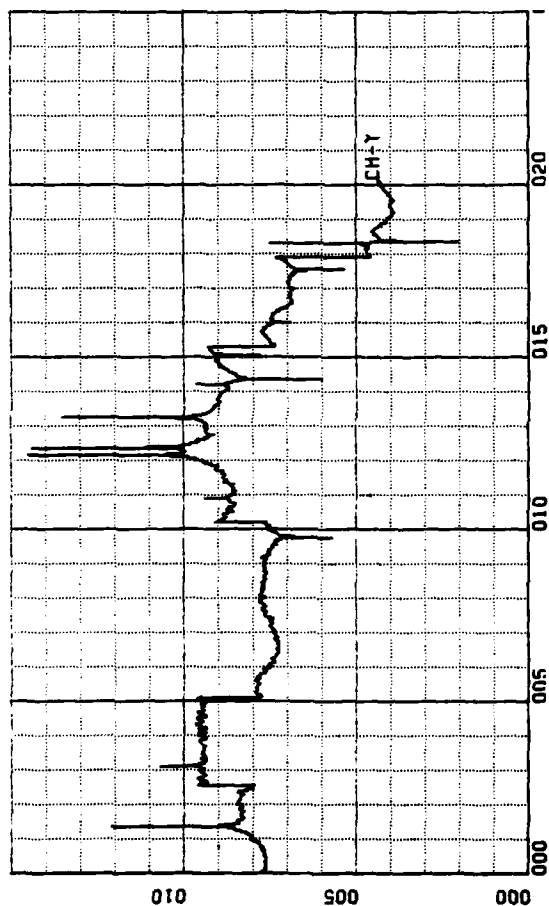


Figure 3.11a. Y-Coil Magnetic Field, 17 August 82, 1302-1336 Local.  
 Amplitude (nanoteslas : 5 units/in) vs. Time (seconds : 500 units/in)  
 8 point smoothing

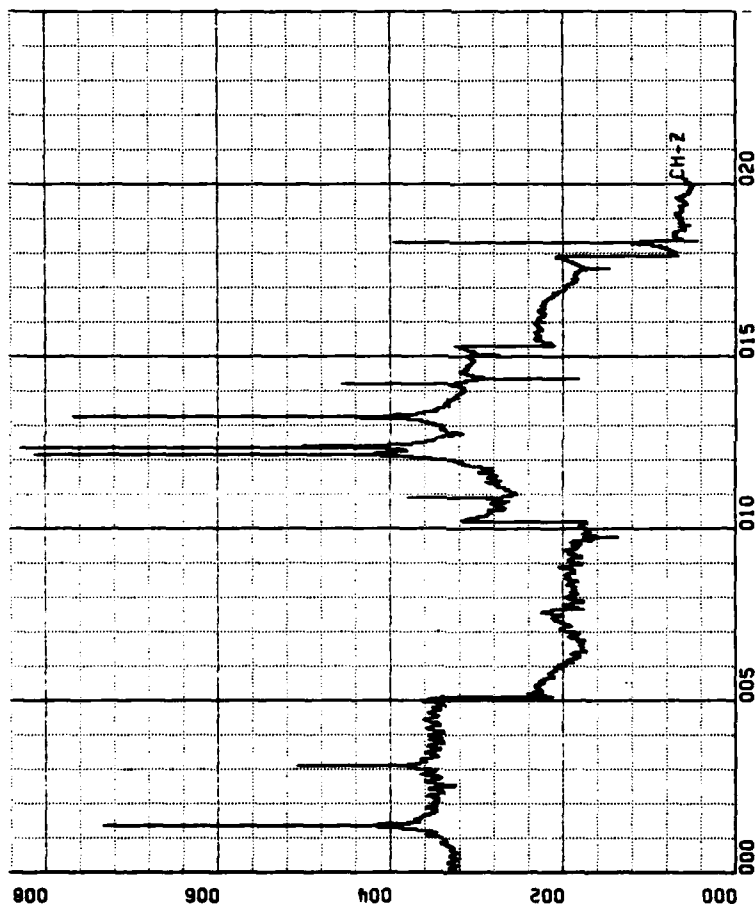


Figure 3.12a. Z-Coil Magnetic Field, 17 August 82, 1302-1336 Local.  
 Amplitude (nanoteslas : 2 units/in) vs. Time (seconds : 500 units/in)  
 8 point smoothing

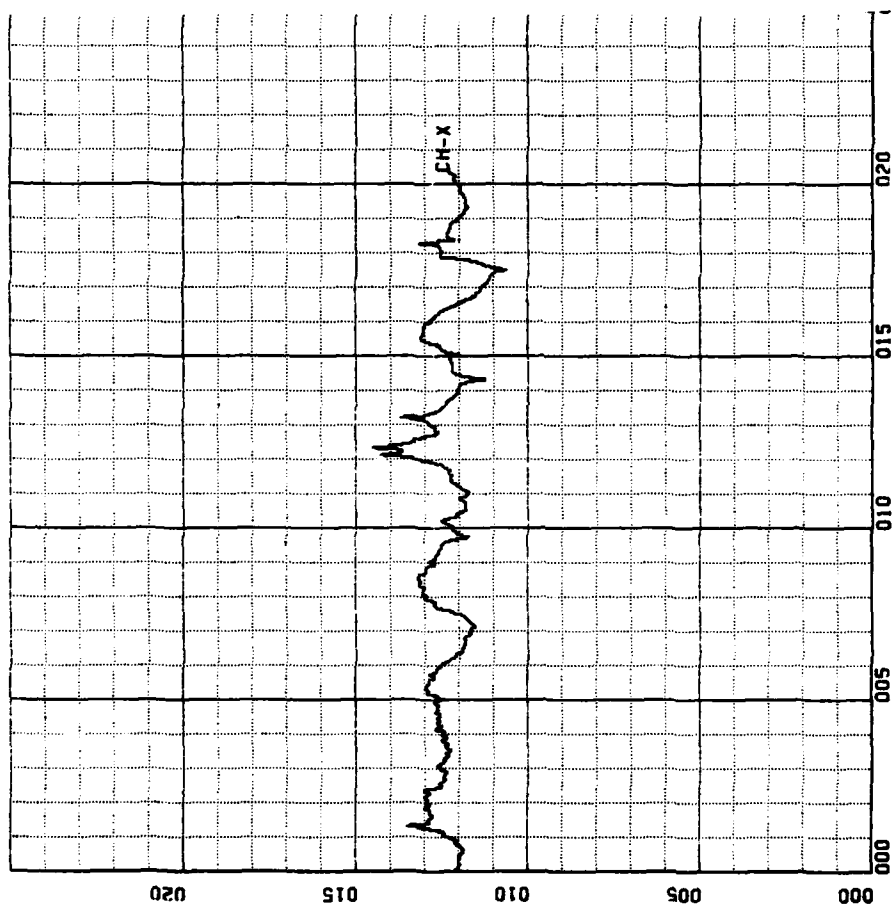


Figure 3.10b. X Coil Magnetic Field, 17 August 82, 1302-1336 Local.  
 Amplitude (nanoteslas : 5 units/in) vs. Time (seconds : 500 units/in)  
 144 point smoothing

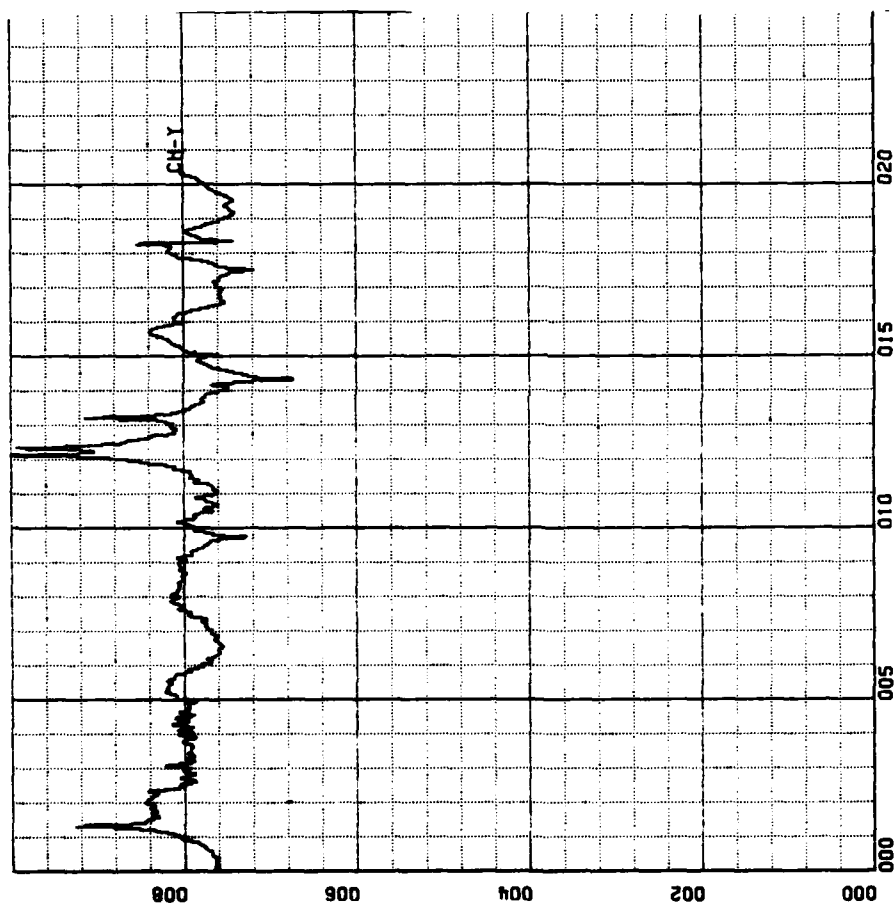


Figure 3.11b. Y Coil Magnetic Field, 17 August 82, 1302-1336 Local.  
 Amplitude (nanoteslas : 1 unit/in) vs. Time (seconds : 500 units/in)  
 144 point smoothing



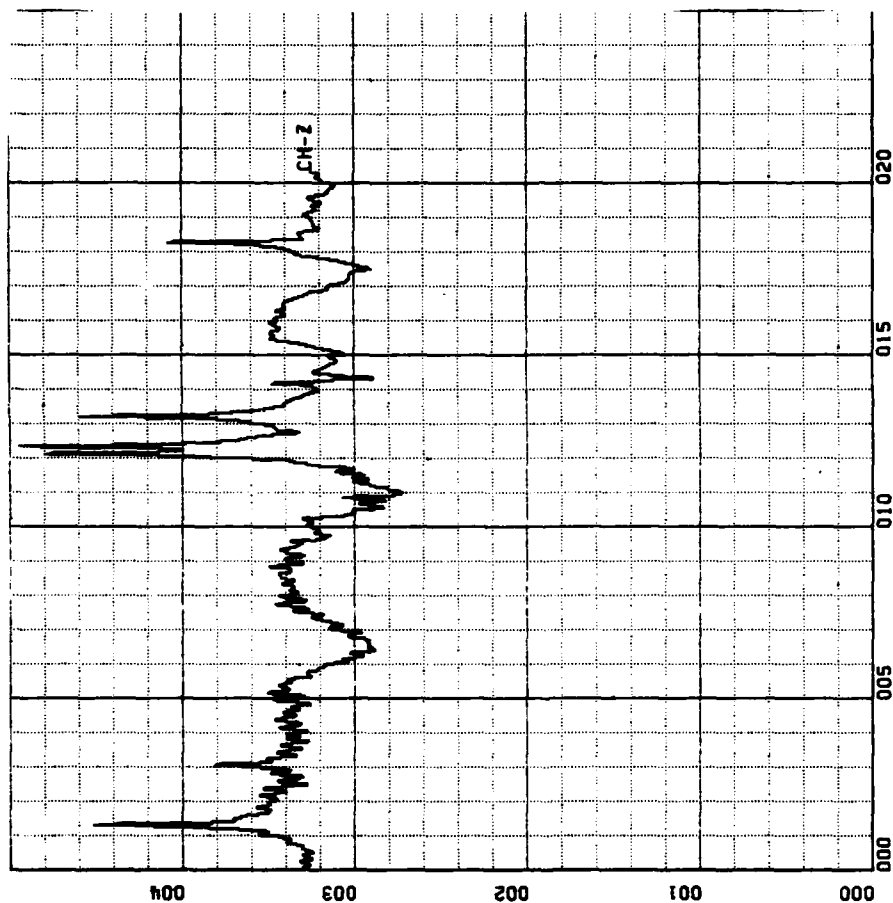


Figure 3.12b. Z Coil Magnetic Field, 17 August 82, 1302-1336 Local,  
 Amplitude (nanoteslas : 1 unit/in) vs. Time (seconds : 500 units/in)  
 144 point smoothing

should note that the transfer function as designed ignores phase information since it is just a least squares fit to data like that of Figure 2.2. Once the transfer function is applied, the reverse transform is performed. We obtain the complex absolute values of the magnetic field data (in nanoteslas) and place the data in new real arrays. To insure that there are no discontinuities between blocks of data, Figures 3.10a, 3.11a and 3.12a, all the blocks are connected to the first by adding or subtracting a constant to each element, Figures 3.10b, 3.11b, 3.12b. The data now undergoes the same 144 point double running average as the voltage to bring out fluctuations with periods of 10-45 seconds. Again DRAWP is used to plot the data. The computer program LVFTCl produces the smoothed magnetic field plots. It is provided in Appendix C.

## 2. Smoothed Magnetic Field Data Analysis

Again looking at the first 34 minutes of digital data tape GMDT 11, we see in the magnetic field data the same exceptional structures as seen in the voltage data, Figures 3.10-3.12. The glitches, however, do highlight one problem rather well. From Figures 3.7-3.9 we note that positive voltage spikes produce negative magnetic field spikes. This would indicate a  $\pi$  phase shift is introduced either in the transfer functions or in the digital Fourier transform. After investigating another digital tape GMDT 3A, 18 August 82, 0121-0251 local, we see another behavior. Figures 3.13-3.15

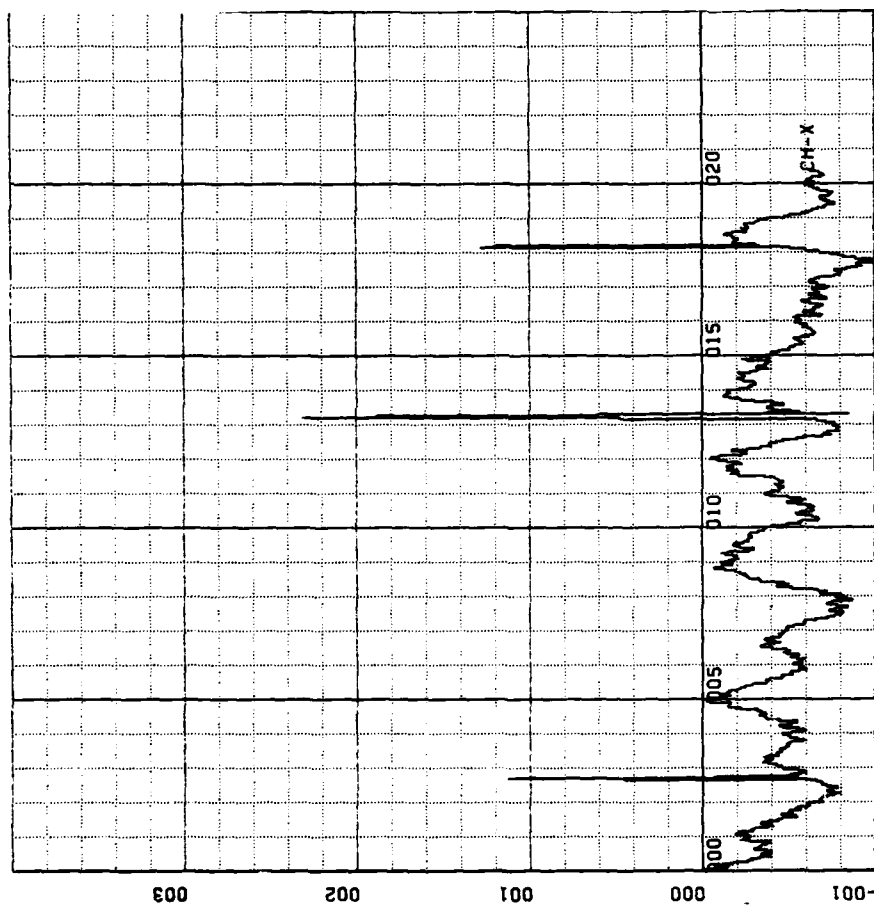


Figure 3.13. X Coil Voltage, 17 August 82, 2241-2315 Local.  
Amplitude (volts : 0.1 units/in) vs. Time (seconds : 500 units/in)

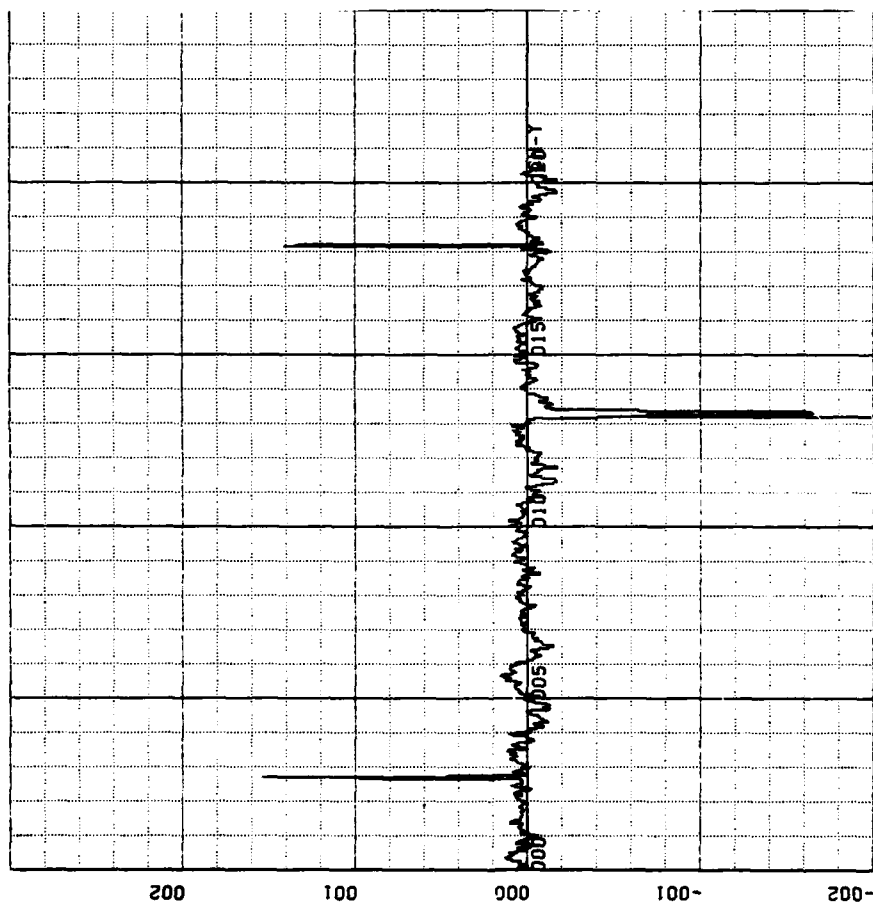


Figure 3.14. Y Coil Voltage, 17 Voltage 82, 2241-2315 Local.  
Amplitude (volts : 0.1 units/in) vs. Time (seconds : 500 units/in)

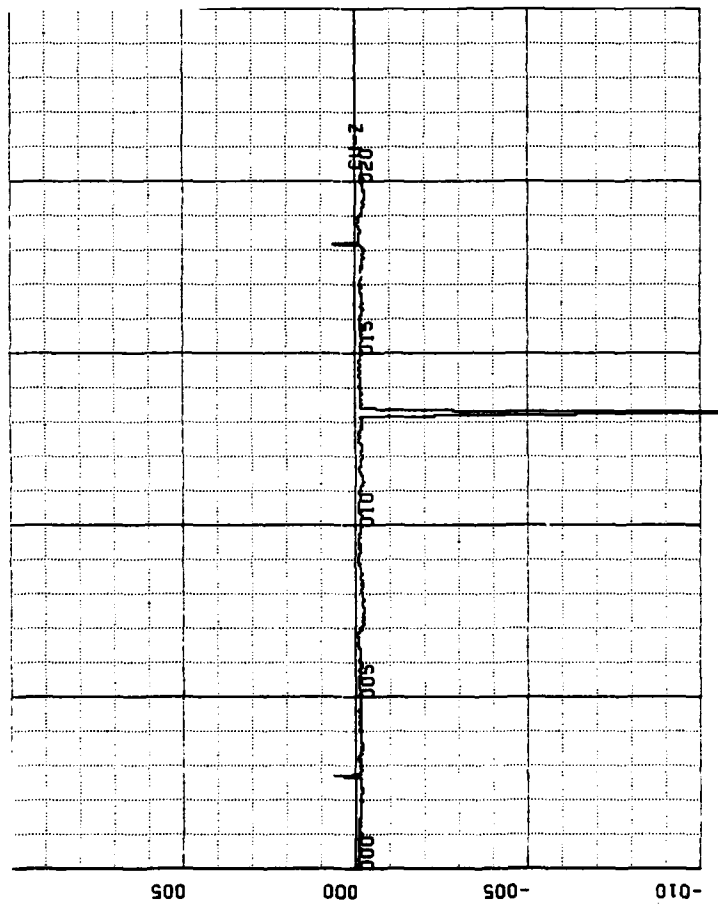


Figure 3.15. Z Coil Voltage, 17 August 82, 2241-2315 Local.  
Amplitude (volts : 0.5 units/in) vs. Time (seconds : 500 units/in)

are the smoothed voltages for the first 34 minutes of data on GMDT3A after a one minute tape advance. Figures 3.16-3.18 are the smoothed magnetic fields for the same time period. The X-coil voltages show three positive spikes while the X-coil magnetic field shows three negative spikes. This supports the theory of a pi phase shift. However, the Y-coil voltage shows two positive spikes and one negative spike, while the Y-coil magnetic field has three positive spikes. Thus it appears we have a rather arbitrary phase problem that may find its origin in the transfer functions that do not maintain the correct phase.

From Figures 3.16-3.18 we note exceptional features that do not correspond to voltage spikes. The exceptional features are separated by time periods of 256 seconds which is the size of the blocks analyzed. These features persist with the data block connection scheme and 144 point smoothing. Their origin is not understood. Some data blocks look like Figure 3.19 with the end points having about the same value. However, some have end points as illustrated in Figure 3.20. The varying end point values are also shown in Figures 3.10a, 3.11a and 3.12a. This may be a source of the large amount of hash between 2 hertz and 10 hertz seen in the PSD's.

After looking at the magnetic field data it was obvious a validation experiment was needed for the sensing system and software.

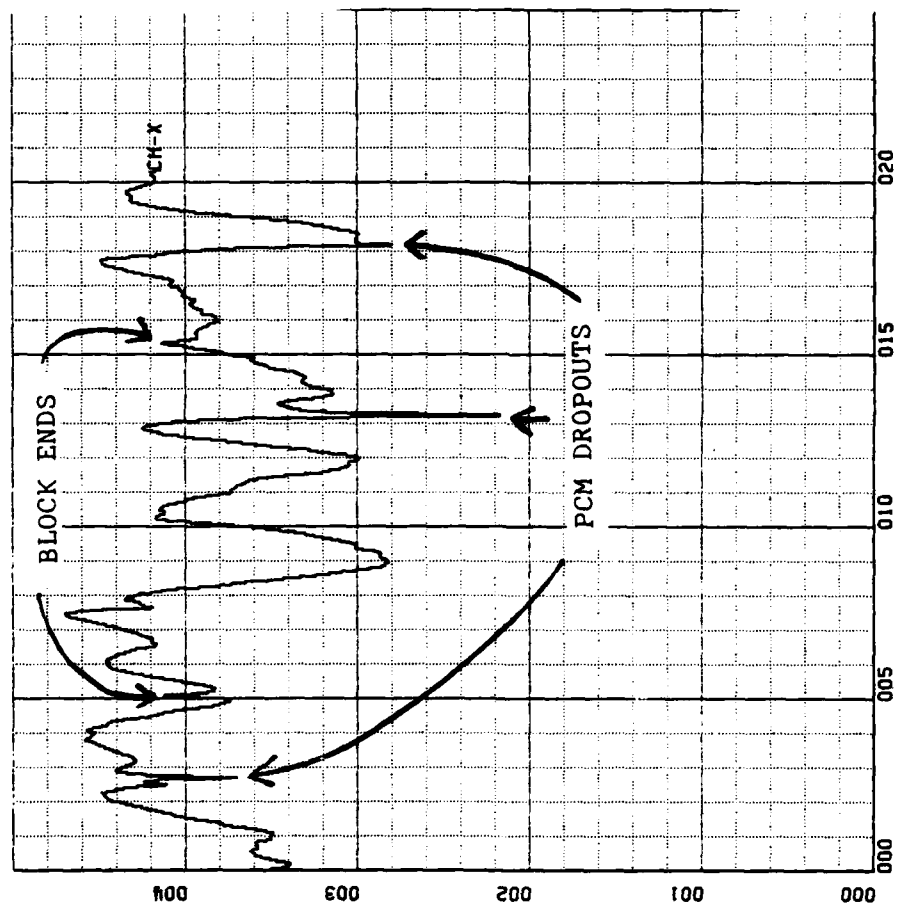


Figure 3.16. X Coil Magnetic Field, 17 August 82, 2241-2315, Local.  
Amplitude (nanoteslas : 1 unit/in) vs. Time (seconds : 500 units/in)

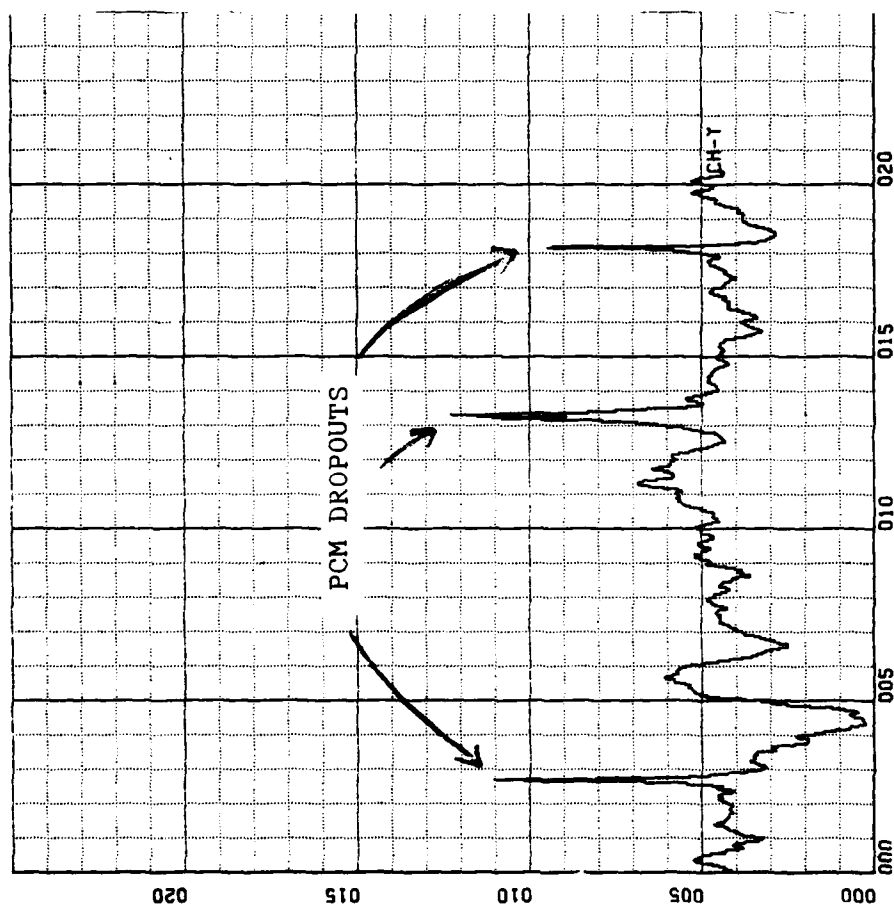


Figure 3.17. Y Coil Magnetic Field, 17 August 82, 2241-2315 Local.  
Amplitude (nanoteslas : 0.5 units/in) vs. Time (seconds : 500 units/in)



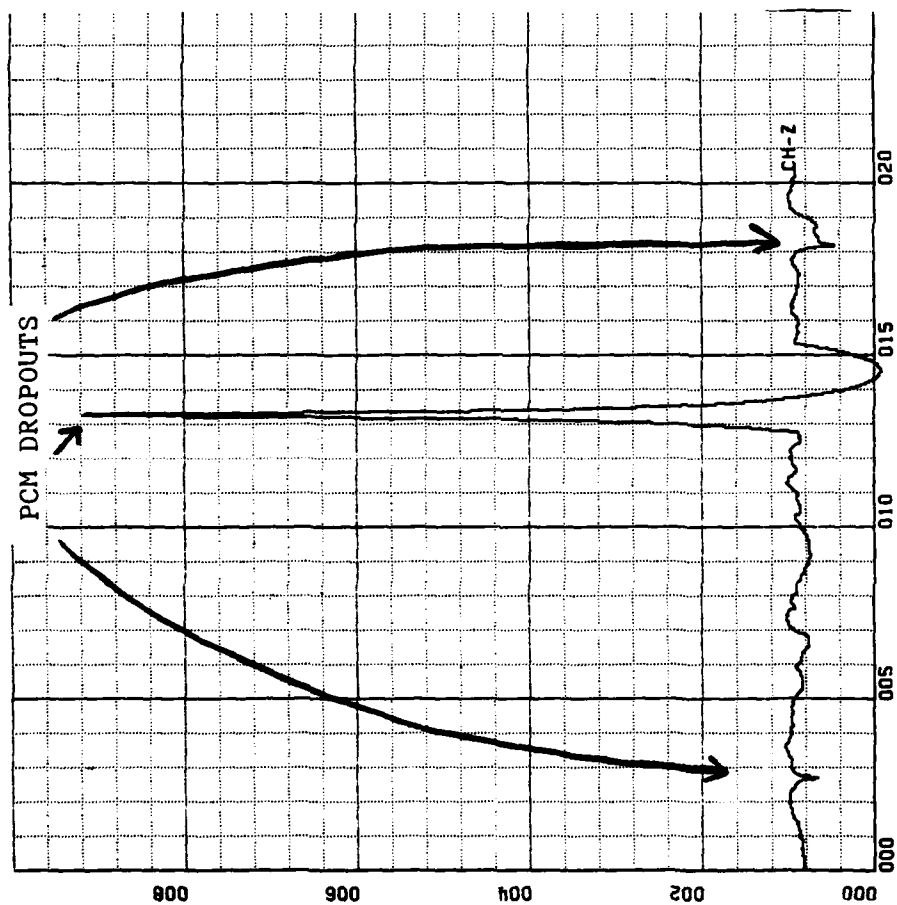


Figure 3.18. Z Coil Magnetic Field, 17 August 82, 2241-2315 Local.  
Amplitude (nanoteslas : 2 units/in) vs. Time (seconds : 500 units/in)



Figure 3.19. One Frame of Data with End Points Having the Same Value

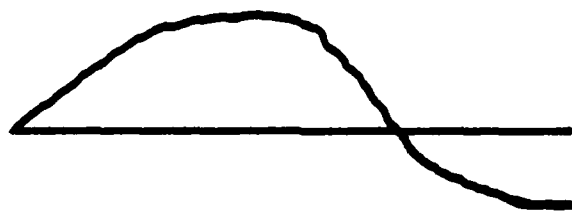


Figure 3.20. One Frame of Data with End Points Having Different Values

#### IV. SYSTEM AND SOFTWARE VALIDATION

##### A. EXPERIMENTAL APPARATUS

The inconsistencies in phase between the time series voltage and magnetic field plots prompted an experiment to validate the sensing system and software. The sensing apparatus consisted of the X-coil and a Schoenstadt fluxgate magnetometer. The sensing axis of both sensors were horizontal and oriented North-South. Figure 4.1 shows the test set-up. Instead of an on axis arrangement, the set-up shown was used because of limited resources. The fluxgate magnetometer is closer to the source since it has less sensitivity at the frequency of interest than the coils. Recorded on the usual X-channel was the output from the X-coil. The Y-channel contained data from the coil after passing through an additional Krohn-Hite model 3321 lowpass filter with a 10 hertz cutoff. On the Z-channel was the output from the fluxgate magnetometer. All three channels were recorded simultaneously and a 64 sample/second sample rate was used. An on-site chart recorder monitored the fluxgate and double filtered coil voltage output real time. The experiment produced two digital data tapes each approximately 46 minutes in length denoted GMTT1A and GMTT1B.

Artificial magnetic fields were introduced into the region by applying sinusoidal currents from a Wavetek signal generator to a cylinder (diameter = 0.13m) wrapped with 150 turns of wire. Location of the source is noted in Figure 4.1. The

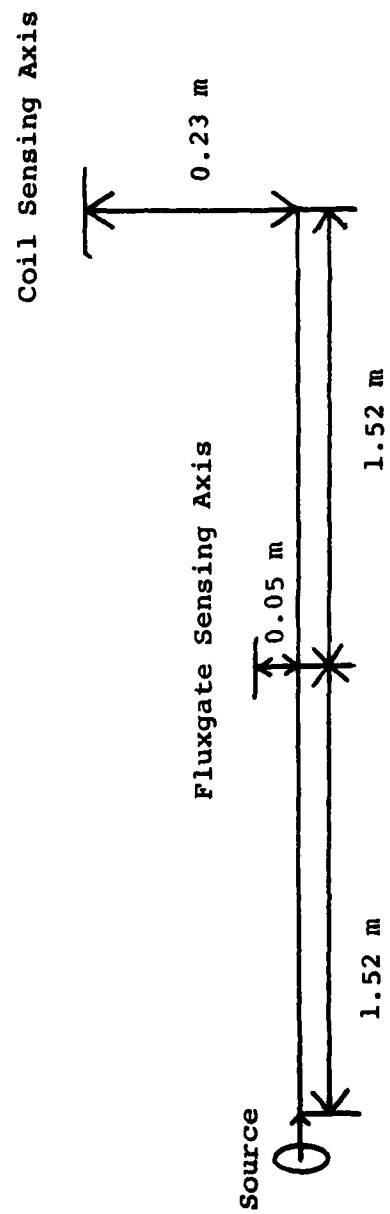


Figure 4.1. Test Arrangement

applied sinusoidal currents varied in frequency from 0.005 hertz to 10 hertz. For each frequency, two magnitude currents were applied to the source to demonstrate a linear response with amplitude.

The fluxgate magnetometer output is correct in phase and amplitude to at least 1 hertz. The transfer function between voltage and magnetic field for the fluxgate magnetometer is a constant of 10 nanoteslas/volt. Thus the fluxgate provides an excellent check for the coil transfer functions, the RD data stripping subroutine and the digital fourier transform.

## B. EXPERIMENT RESULTS

### 1. Voltage

From the real time chart record of voltage for the fluxgate and double filtered coil, we can check the computer generated voltages using VOLTR and VOLTS. Table 4.1 shows the chart record and computer generated voltages for the fluxgate and double filtered coil at various frequencies. Only the large amplitude oscillations are measured for the double filtered coil because of poor signal-to-noise, for the small amplitude oscillations.

Table 4.1 shows good agreement between the chart record and computer output for the double filtered coil. However, the fluxgate magnetometer voltages undergo a constant transformation of 0.831 from chart record to computer plot. This may be explained by a problem in the data stripping

Table 4.1. Coil and Fluxgate Voltage

FREQUENCY (HZ)	CHART RECORD VOLTAGE (V)			COMPUTER GENERATED VOLTAGE (V)		
	FLUXGATE		COIL	FLUXGATE		COIL
	<u>Large Amplitude Oscillation</u>	<u>Small Amplitude Oscillation</u>	<u>Large Amplitude Oscillation</u>	<u>Large Amplitude Oscillation</u>	<u>Small Amplitude Oscillation</u>	<u>Large Amplitude Oscillation</u>
0.1	2.45	0.78	0.90	2.00	0.60	0.90
0.09	2.45	0.80	0.76	1.98	0.60	0.83
0.08	2.45	0.78	0.69	2.00	0.60	0.70
0.07	2.44	0.70	0.66	2.00	0.60	0.68
0.06	2.46	0.77	0.50	1.97	0.60	0.50
0.05	2.45	0.79	0.40	2.20	0.75	0.40
0.04	2.41	0.78	0.40	2.15	0.70	0.37
0.03	2.50	0.82	0.30	2.02	0.65	0.33
0.02	2.50	0.76	0.20	2.03	0.60	0.31
0.01	2.50	0.78		1.96	0.57	

Double filtered coil and fluxgate magnetometer voltages,  
real time and computer generated.

algorithm. The present agreement between the chart record and computer generated voltages is shown in Table 4.2.

Another more serious problem became obvious during the examination of the computer generated voltage plots. For approximately the first 20 minutes of data recording the fluxgate magnetometer was not connected to the PCM board. Figures 4.2-4.4 show the two respective sensing devices. Figures 4.2 and 4.3 both contain "real" signal while Figure 4.4 does not contain "real" signal until the amplitude discontinuity indicating connection of the fluxgate magnetometer to the PCM board. Figures 4.2-4.4 indicate that "pick-up" is occurring probably between the channels at the PCM board. The amplitude of the cross-talk voltage is about 0.15 volts peak-to-peak at the frequency of 0.1 hertz. The amplitude of the "real" signal on the double filtered coil is 0.29 volts at 0.1 hertz. Thus 51 percent of the "real" signal is coupled to the disconnected channel. Coupling between channels of this magnitude raises serious questions about the computer generated data, especially for coherence. Discovering the amount of the channel pick-up if the channel is loaded requires further experimentation.

Figures 4.5-4.7 show an interesting feature of the coil data versus fluxgate magnetometer data. On the channels containing the coil output we see noise on top of the signal. This noise is not present on the channel containing the fluxgate magnetometer data. Since all three channels passed

Table 4.2. Percent Agreement Between the Chart Record  
and Computer Generated Voltages

<u>FREQUENCY (HZ)</u>	<u>FLUXGATE FIELD (%)</u>		<u>COIL FIELD (%)</u>	
	<u>Large Amplitude Oscillation</u>	<u>Small Amplitude Oscillation</u>	<u>Large Amplitude Oscillation</u>	<u>Large Amplitude Oscillation</u>
0.1	87	74	100	
0.09	87	72	94	
0.08	87	76	99	
0.07	87	84	98	
0.06	87	84	100	
0.05	87	97	100	
0.04	87	93	92	
0.03	87	84	94	
0.02	87	80	69	
0.01	86	80		



# 0.1 Hz with 60 Hz Aliasing

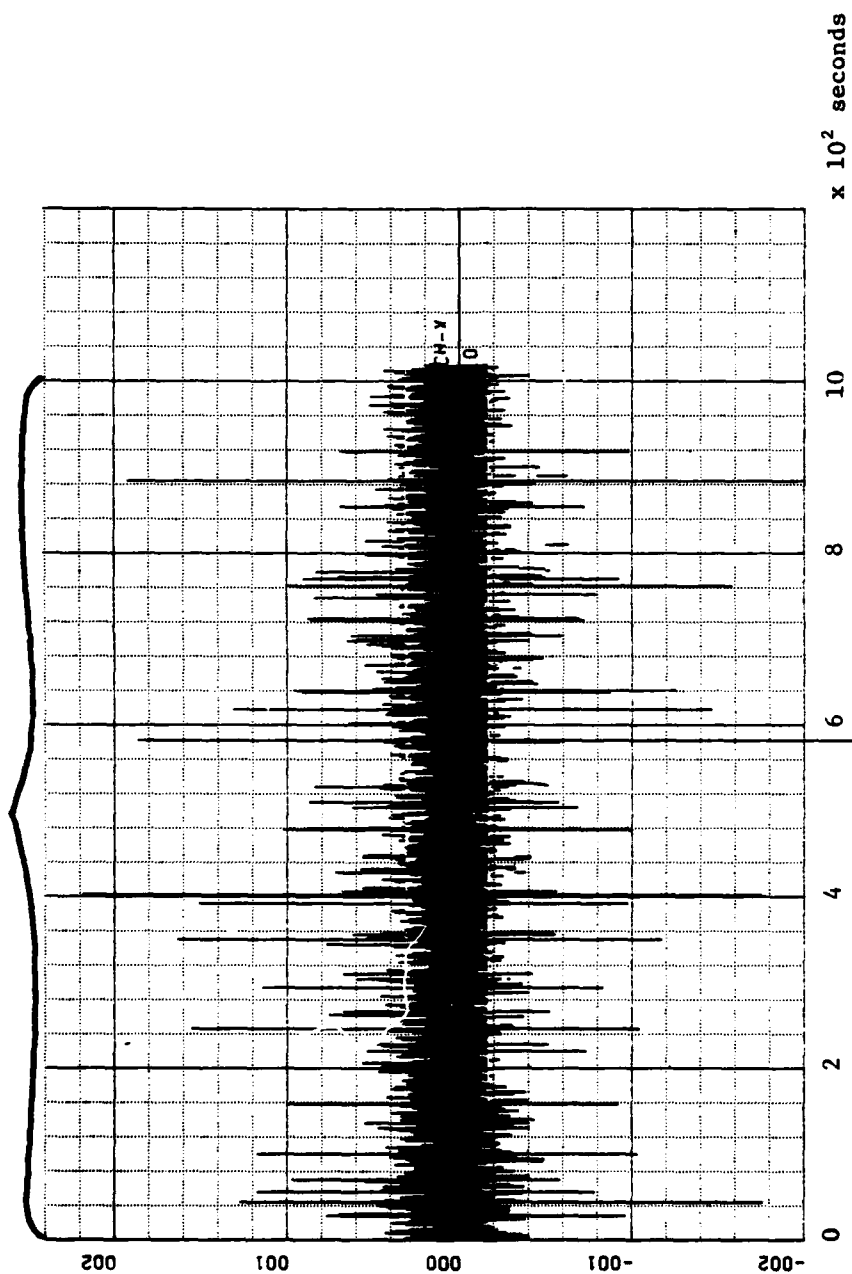


Figure 4.2. X-Coil Voltage, 26 April 83, 0931-0948 Local.  
Amplitude (volts : 1 unit/in) vs. Time (seconds : 200 units/in)

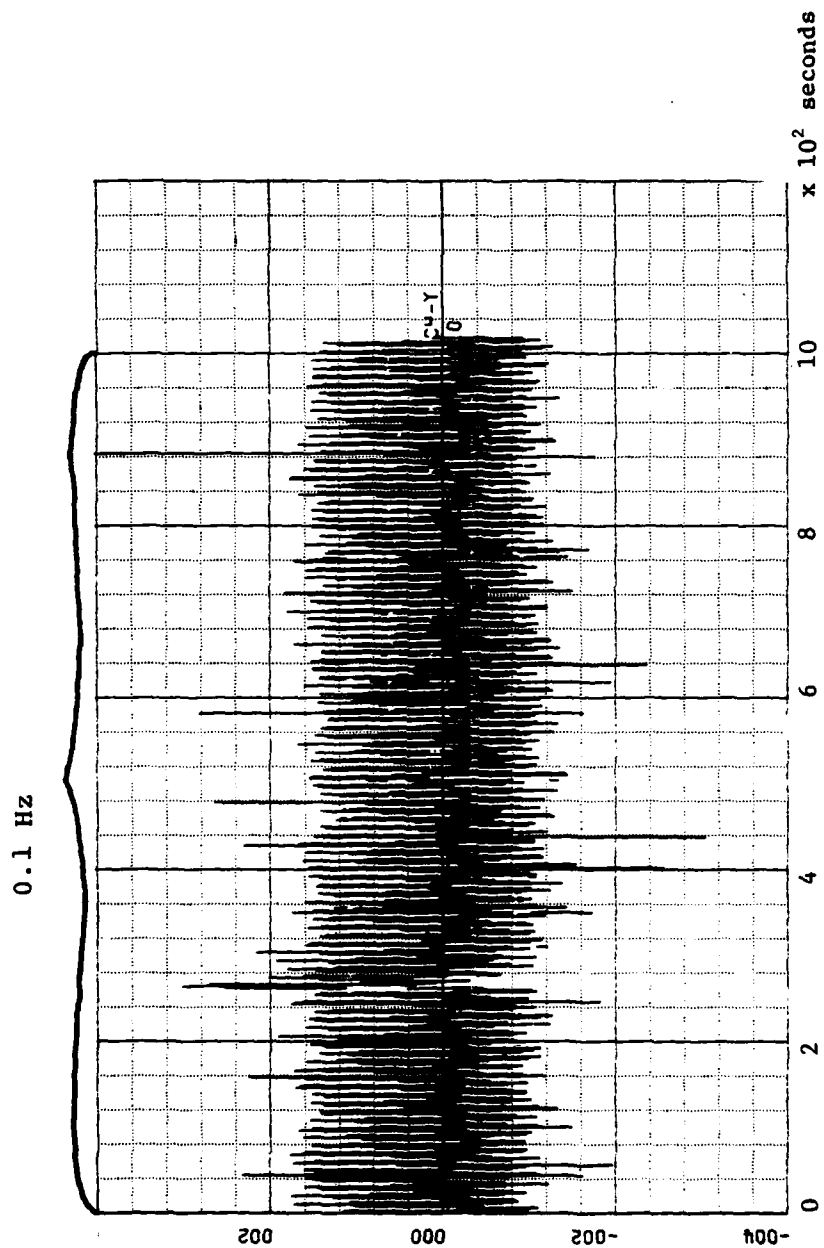


Figure 4.3. Filtered X-Coil Voltage, 26 April 83, 0931-0948 Local.  
Amplitude (volts : 0.2 units/in) vs. Time (seconds : 200 units/in)

AD-A132 443 AN ANALYSIS OF A PC-3 MICROPULSATION IN THE GEOMAGNETIC  
FIELD(U) NAVAL POSTGRADUATE SCHOOL MONTEREY CA  
K B STEVENS JUN 83

AN ANALYSIS OF A PC-3 MICROPULSATION IN THE GEOMAGNETIC  
FIELD(U) NAVAL POSTGRADUATE SCHOOL MONTEREY CA  
K B STEVENS JUN 83

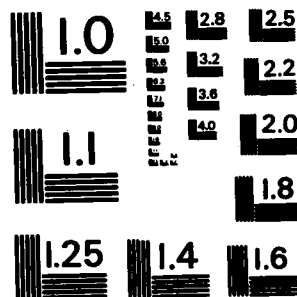
22

UNCLASSIFIED

F/G 8/14

NL

END  
DATE  
TIME  
4 3 4



MICROCOPY RESOLUTION TEST CHART  
NATIONAL BUREAU OF STANDARDS-1963-A

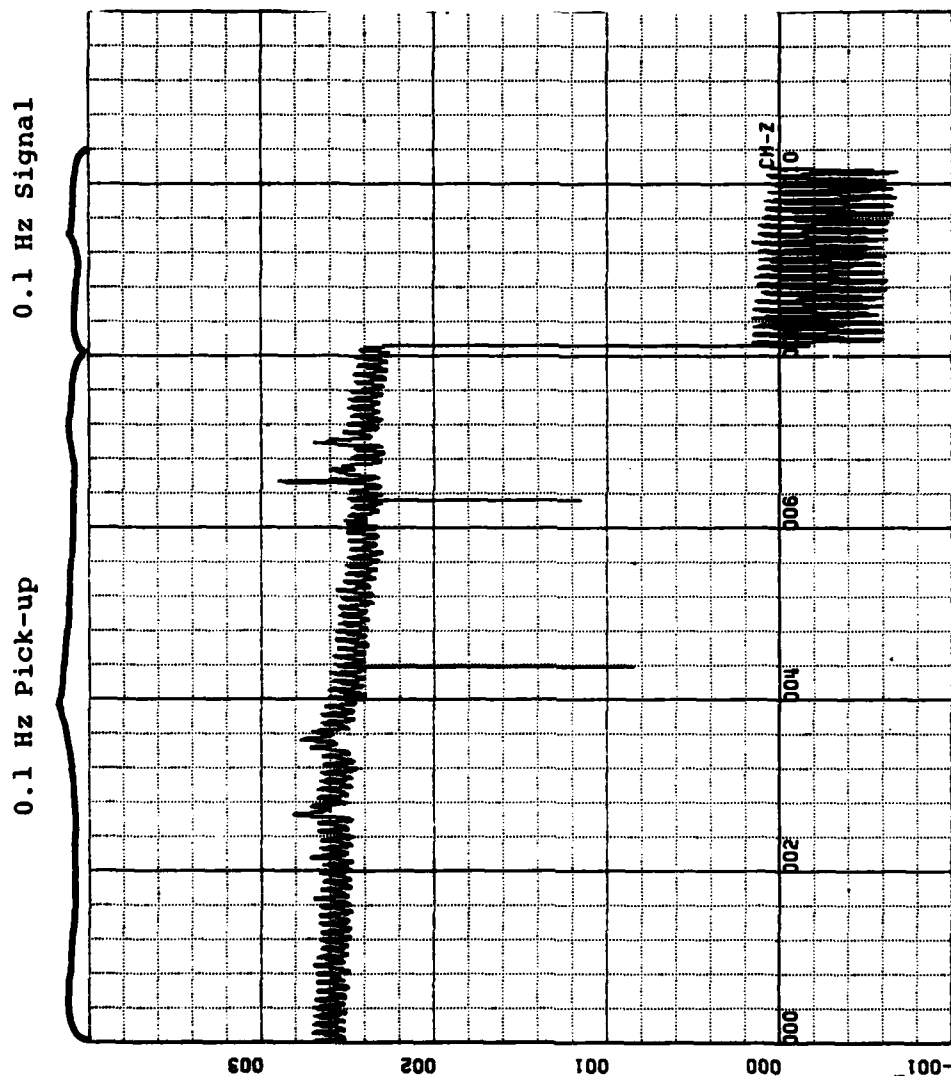


Figure 4.4. Fluxgate Voltage, 26 April 83, 0931-0948 Local.  
Amplitude (volts : 1 unit/in) vs. Time (seconds : 200 units/in)

through the PCM encoder and decoder, the noise is probably in the coil amplifiers or the coils themselves. An experiment to investigate the true origin of the noise should be done.

## 2. Magnetic Field

Given the dipole equation [Ref. 6] and the experimental arrangement in Figure 4.1, the ratio of magnitude of the magnetic field seen by the fluxgate to that seen by the coil can be calculated. From the geometry in Figure 4.1 the field at the coil would be a factor of 8 less than that seen by the fluxgate. This is because the source is a dipole and the field of a dipole falls off as  $1/R$ . Detailed consideration of the geometry gives a ratio of approximately 8.09. Table 4.3 contains the magnetic field measured at the fluxgate magnetometer. Using the ratio calculated from the geometry, the expected magnetic field amplitude at the coil is listed in Table 4.3.

A modified form of computer code LFVTC1 generated the magnetic field versus time plots for the test tapes. Table 4.3 shows the computer generated peak-to-peak magnetic field values read from the computer plots. From Table 4.3 it appears that the coil magnetic field amplitude is in error by a factor of approximately three (with exception to the low frequencies). One can conclude that a problem exists in the software.

Figures 4.8-4.9 show the magnetic field data for the second seventeen minutes of digital data tape GMTT1A. Figure 4.9 is the magnetic field measured by the fluxgate magnetometer

Table 4.3. Measured and Computer Generated Magnetic Field Magnitudes

FREQUENCY (Hz)	KNOWN FLUXGATE FIELD (mT)			EXPECTED COIL FIELD (mT)			EXPECTED RATIO FLUXGATE/COIL			COMPUTER COIL FIELD (mT)			ACTUAL RATIO FLUXGATE/COIL		
	LARGE AMPLITUDE OSCILLATION	SMALL AMPLITUDE OSCILLATION		LARGE AMPLITUDE OSCILLATION	SMALL AMPLITUDE OSCILLATION		LARGE AMPLITUDE OSCILLATION	SMALL AMPLITUDE OSCILLATION		LARGE AMPLITUDE OSCILLATION	SMALL AMPLITUDE OSCILLATION		LARGE AMPLITUDE OSCILLATION	SMALL AMPLITUDE OSCILLATION	
0.1	24.50	7.80		3.04	0.96		8.06	8.12		1.08	0.30		22.69	26.00	
0.09	24.50	8.00		3.03	0.99		8.09	8.08		1.00	0.35		24.50	22.86	
0.08	24.50	7.80		3.04	0.96		8.06	8.12		0.98	0.30		25.00	26.00	
0.07	24.40	7.00		3.02	0.87		8.08	8.05		0.98	0.32		24.89	21.88	
0.06	24.60	7.70		3.05	0.94		8.07	8.19		0.90	0.30		27.33	25.67	
0.05	24.50	7.90		3.03	0.98		8.09	8.06		0.76	0.35		32.23	22.57	
0.04	24.10	7.80		3.01	0.96		8.01	8.12		0.28	0.24		86.07	32.5	
0.03	25.00	8.20		3.09	1.01		8.09	8.12		0.32	0.14		78.13	58.57	
0.02	25.00	7.60		3.09	0.92		8.09	8.26		0.64	0.24		39.06	31.67	
0.01	25.00	7.80		3.09	0.96		8.09	8.12		0.40	0.14		62.50	55.71	

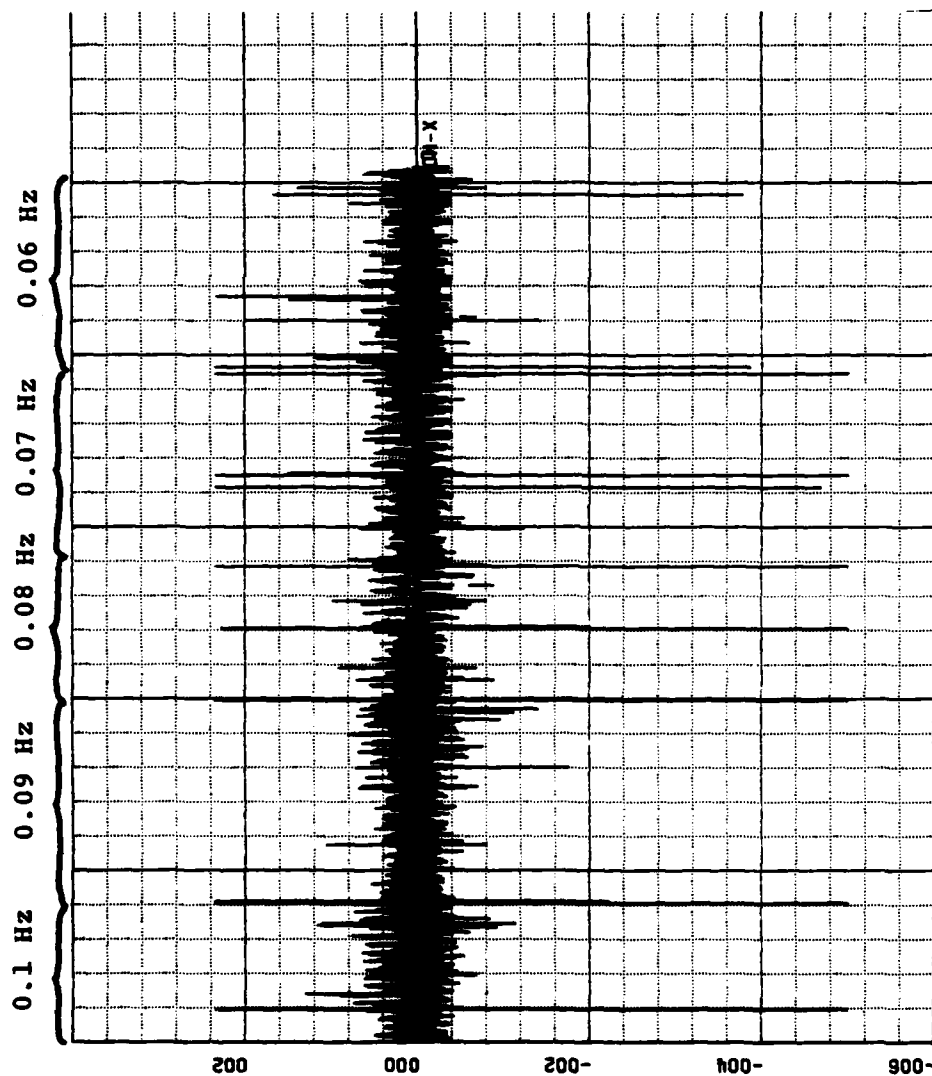


Figure 4.5. X-Coil Voltage, 26 April 83, 0948-1005 Local.  
Amplitude (volts : 2 units/in) vs. Time (seconds : 200 units/in)



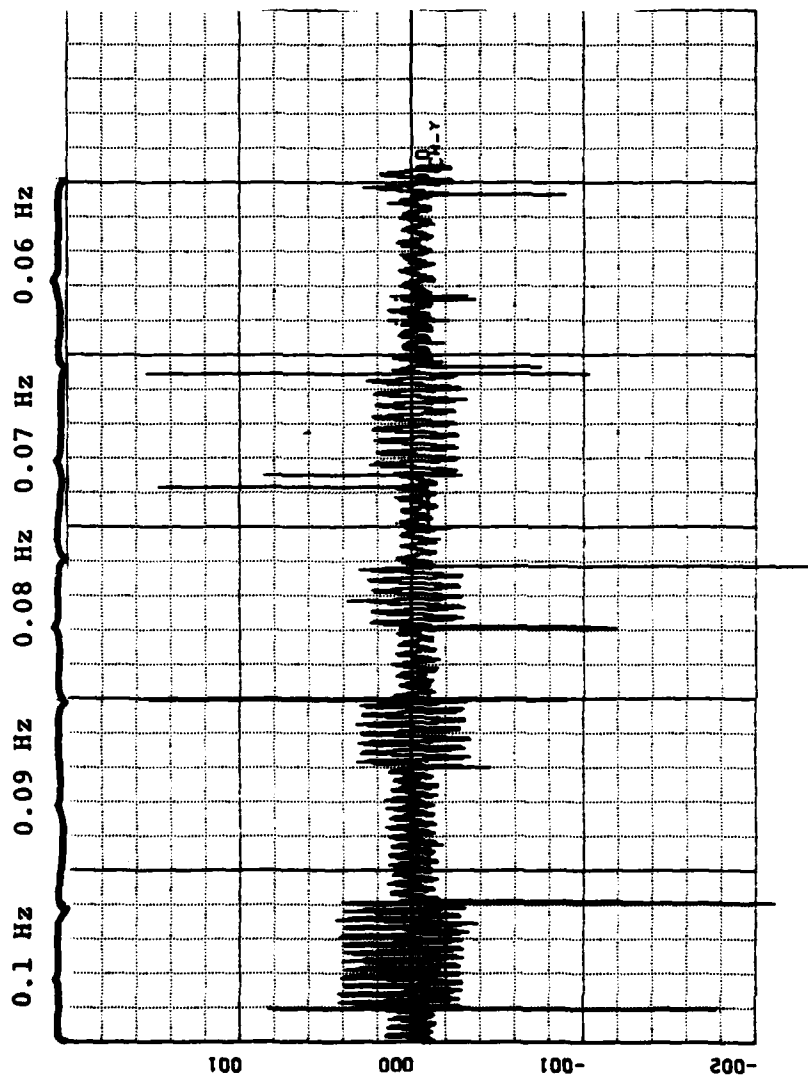


Figure 4.6. Filtered X-Coil Voltage, 26 April 83, 0948-1005 Local.  
Amplitude (volts : 1 unit/in) vs. Time (seconds : 200 units/in)

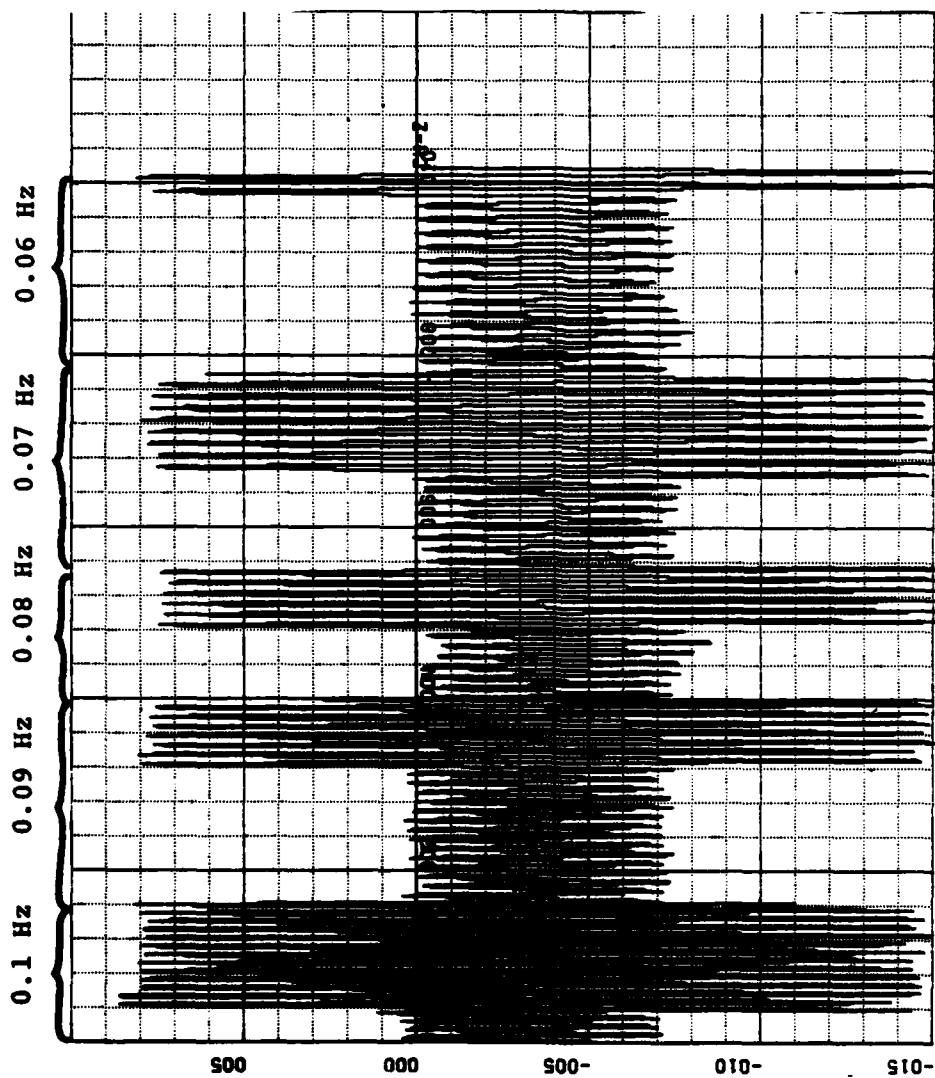


Figure 4.7. Fluxgate Voltage, 26 April 83, 0948-1005 Local.  
Amplitude (volts : 0.5 units/in) vs. Time (seconds : 200 units/in)

and Figure 4.8 is the magnetic field seen by the coil. For the coil we see discontinuities every 256 seconds corresponding to the block size of data. This indicates that the problems in the data block end points, as mentioned in Section III, do exist. It is not clear how to deal with this.

The first 300 seconds of Figures 4.8-4.9 is expanded in Figures 4.11-4.12. With the expanded data a phase difference between coil and fluxgate can be determined. By checking the phase difference, we can determine whether the phase independent transfer function is introducing error. For the 0.1 hertz field plotted in Figures 4.10-4.11 the coil lags the fluxgate by approximately 72 degrees. In Figures 4.12-4.13 we see that at 0.01 hertz the coil sensitivity has fallen and a reliable phase difference between the fluxgate and coil cannot be made. Figure 4.14 shows the relationship between phase angle and frequency.

The above experiment shows the advantages of having a real time "ground truth" record. With this, one can avoid "working in the blind". Computer products will have a check. Thus, a multi-channel chart recorder should be purchased to graph in real time the x, y, and z inputs to the PCM board. In addition, electronic circuitry should be developed and incorporated so that the chart records represent at least a low pass filtering of the coil voltages. Ideally, conversion of voltage to magnetic field could occur in real time at this point given the appropriate electronics.

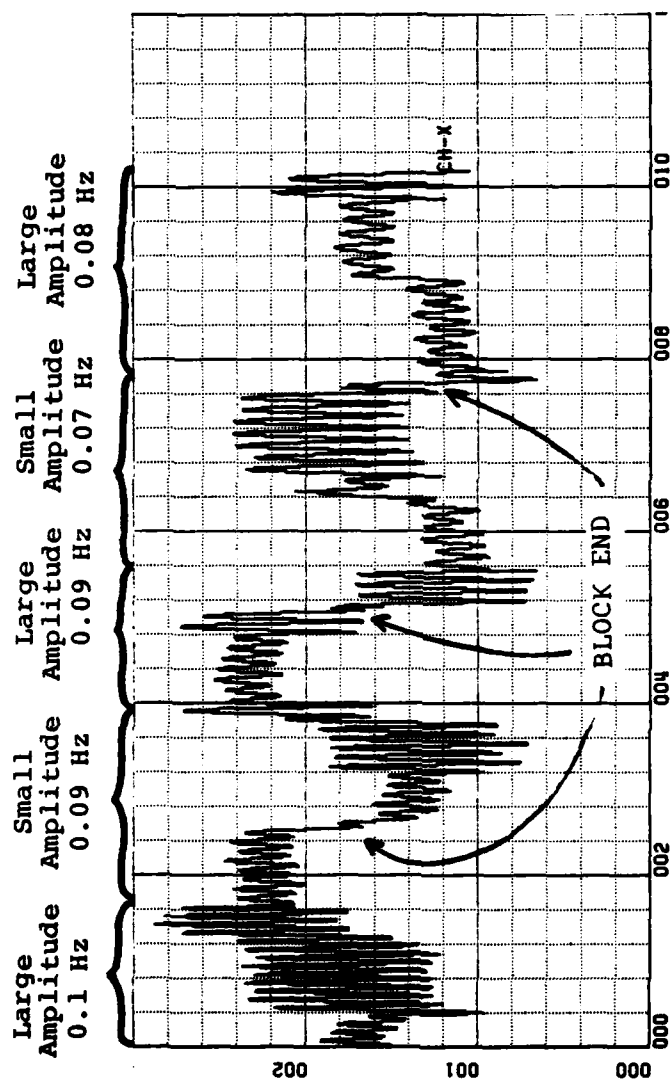


Figure 4.8. X-Coil Magnetic Field, 26 April 83, 0948-1005 Local.  
Amplitude (nanoteslas : 1 unit/in) vs. Time  
(seconds : 200 units/in)

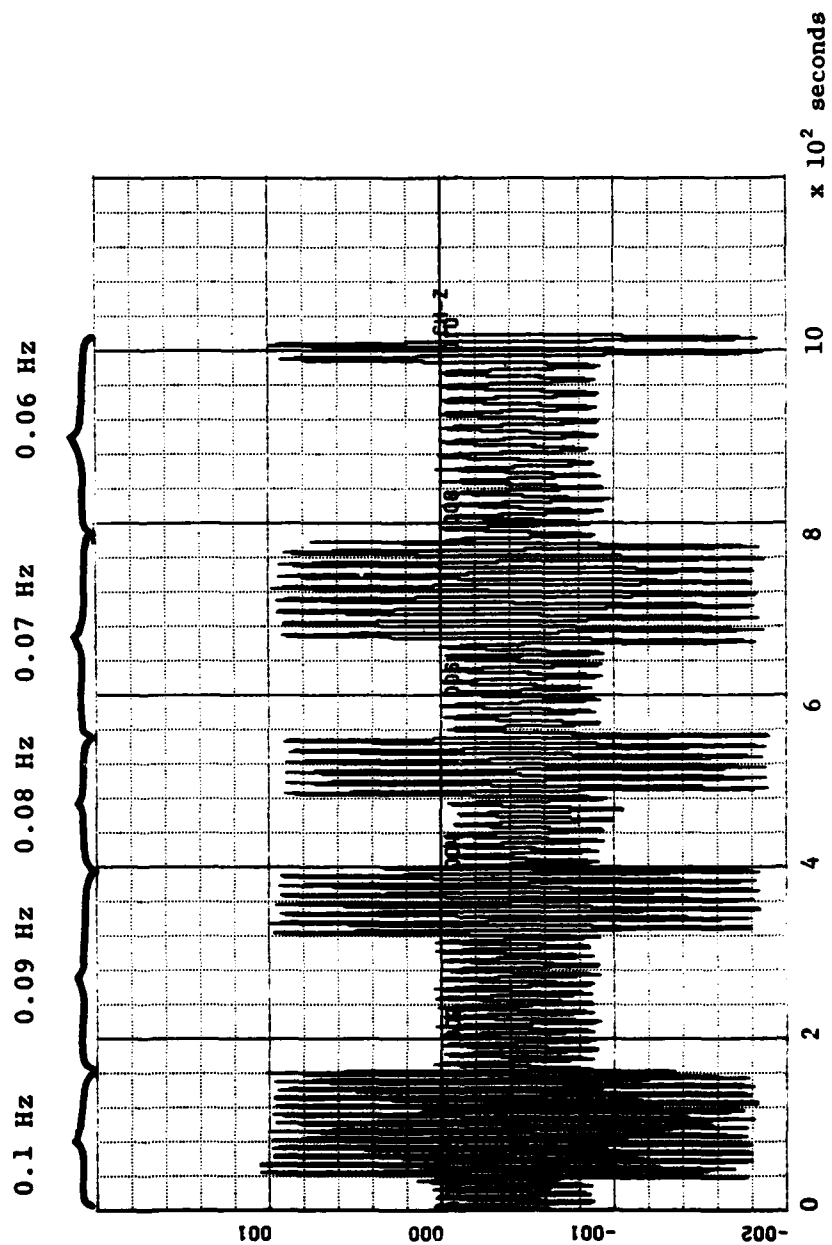


Figure 4.9. Fluxgate Magnetic Field, 26 April 83, 0948-1005 Local.  
 Amplitude (nanoteslas : 10 units/in) vs. Time  
 (seconds : 200 units/in)

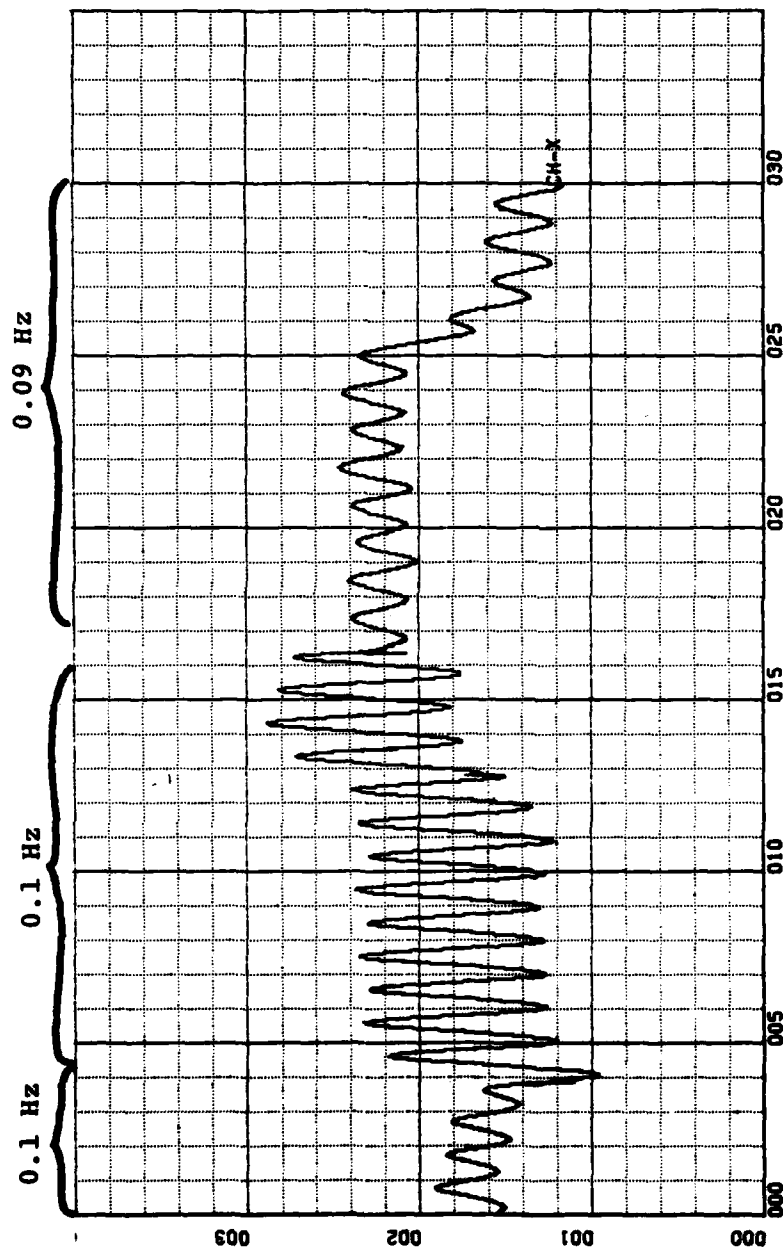


Figure 4.10. X-Coil Magnetic Field, 26 April 83, 0948-0953 Local.  
Amplitude (nanoteslas : 1 units/in) vs. Time (seconds : 50 units/in)

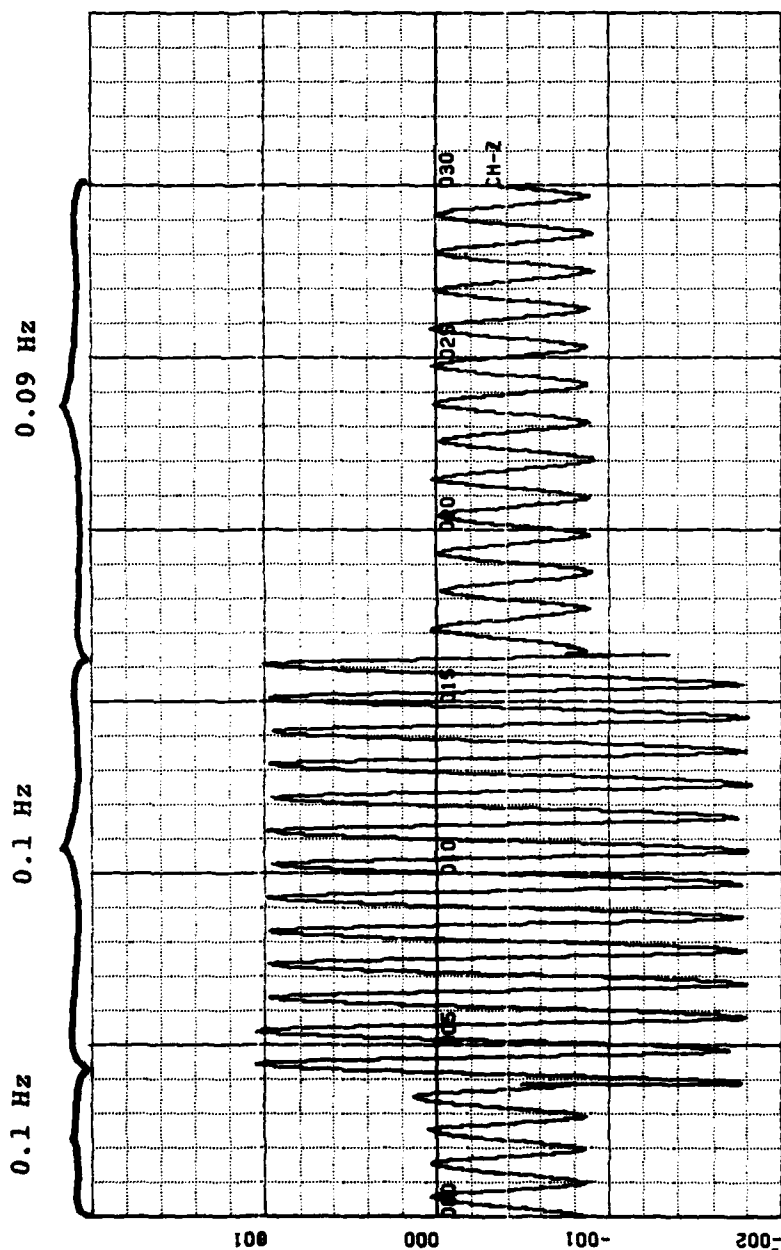


Figure 4.11. Fluxgate Magnetic Field, 26 April 83, 0948-0953 Local.  
Amplitude (nanoteslas : 10 units/in) vs. Time (seconds : 50 units/in)

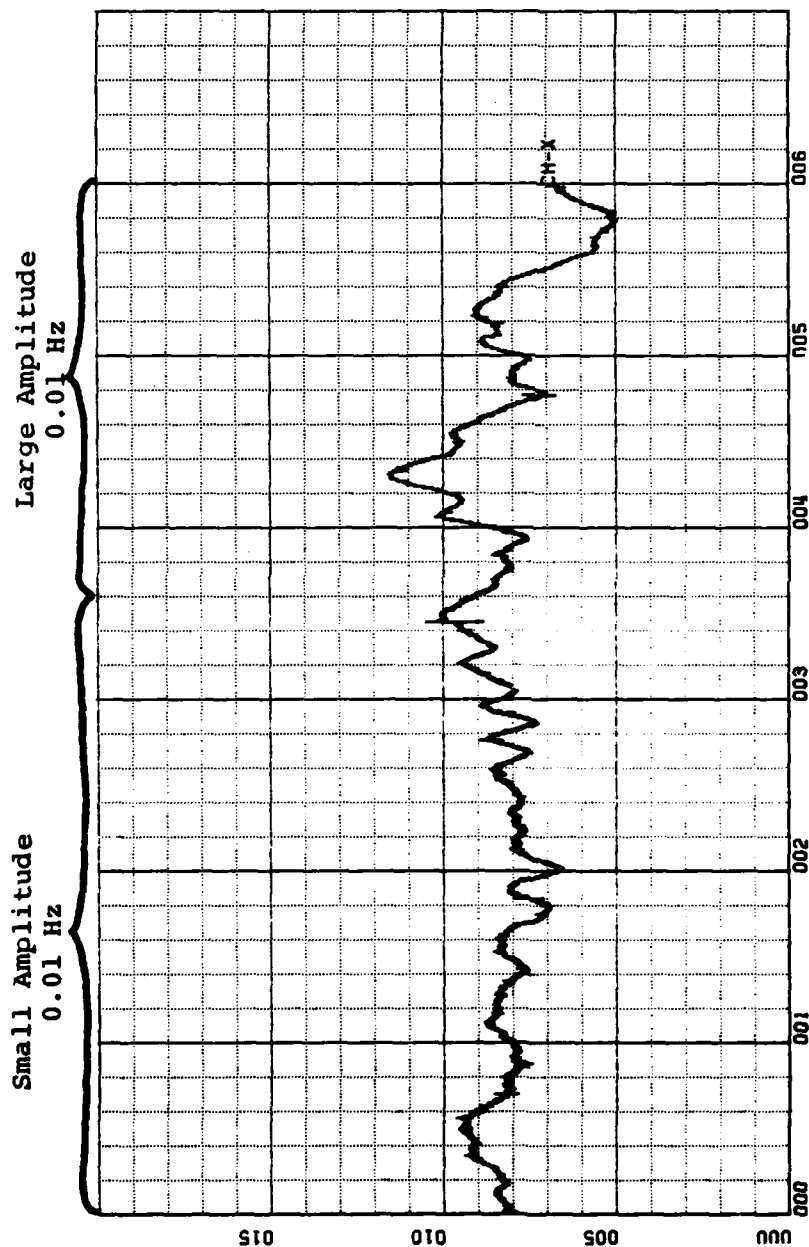


Figure 4.12. X-Coil Magnetic Field, 26 April 83, 1023-1033 Local.  
Amplitude (nanoteslas : 0.5 units/in) vs. Time (seconds : 100 units/in)



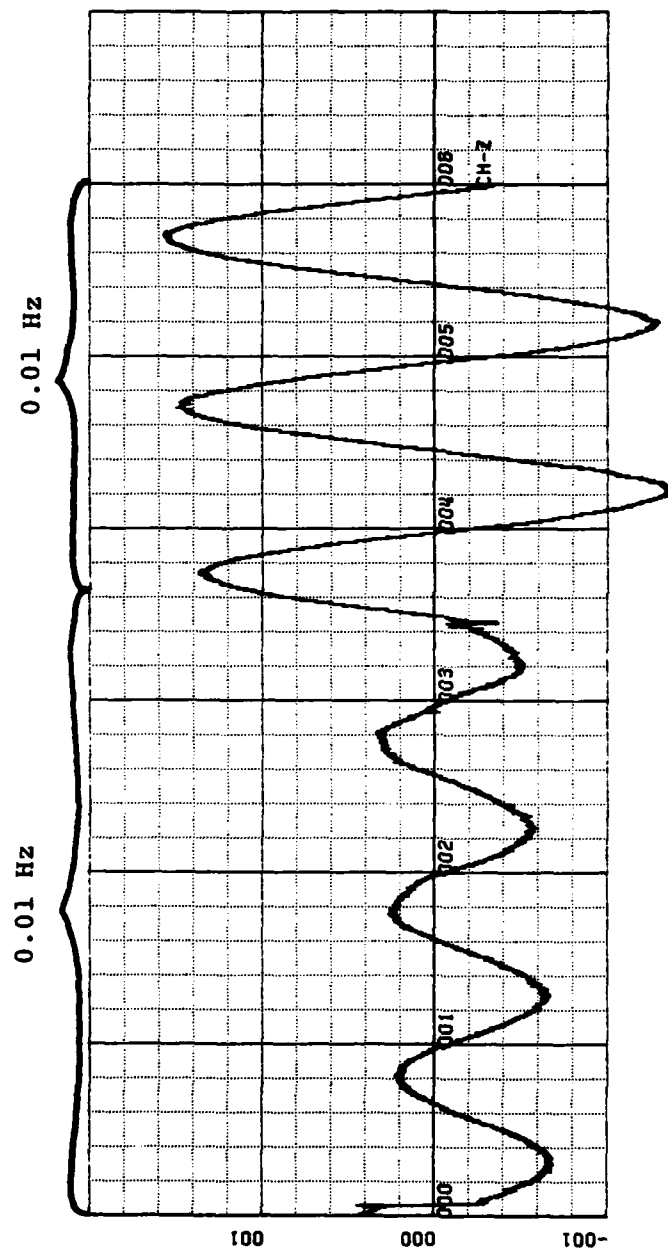


Figure 4.13. Fluxgate Magnetic Field, 26 April 83, 1023-1033 Local.  
Amplitude (nanoteslas : 10 units/in) vs. Time (seconds : 100 units/in)

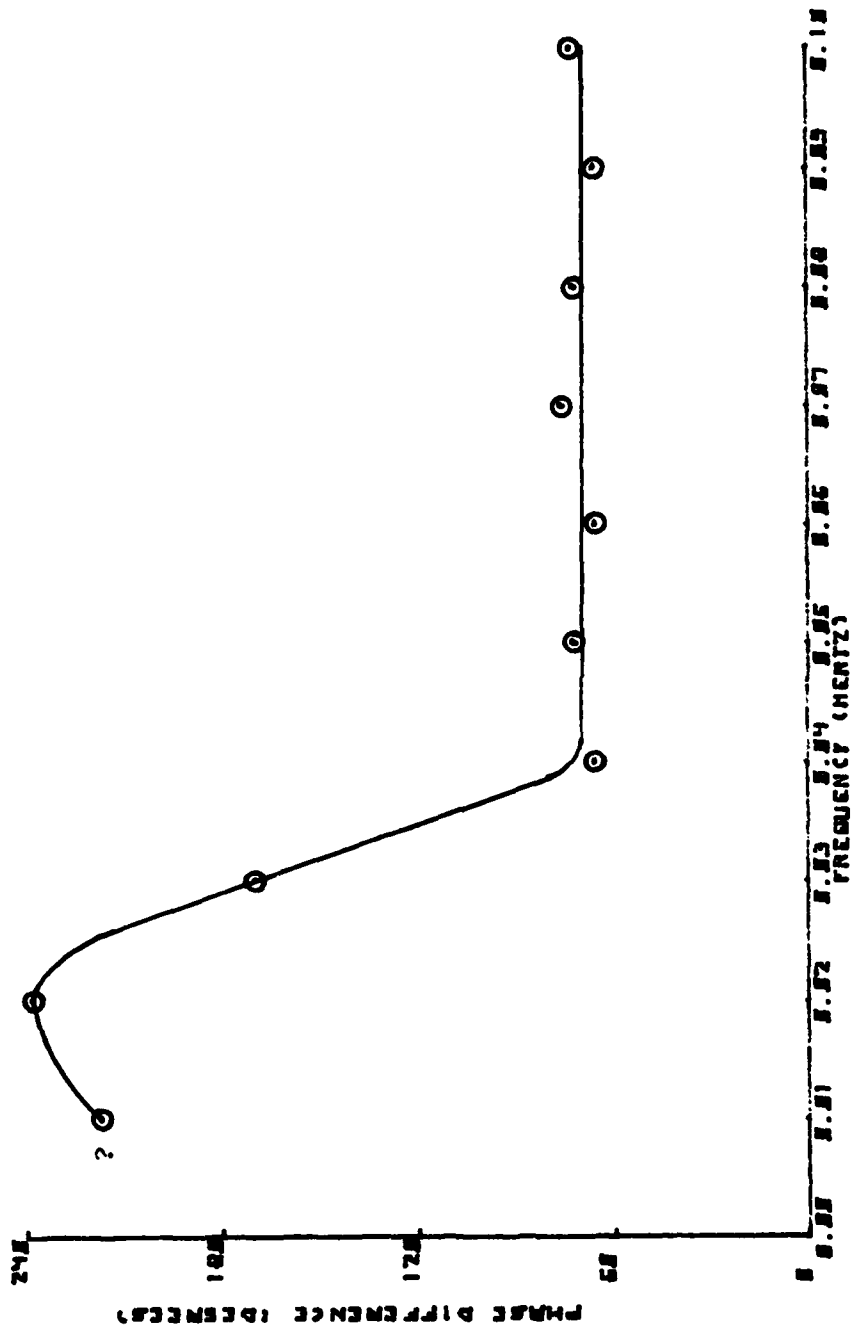


Figure 4.14. Phase Lag of Coil with Respect to Fluxgate

## V. MICROPULSATIONS

### A. THEORY

Currently there is no theory that completely models the observed micropulsations and geomagnetic noise. It is generally accepted that the generating mechanism for micropulsations is an interaction between the solar wind and the earth's magnetosphere [Ref. 5]. The observed micropulsations are classified by their period and regularity [Ref. 5]. Table 5.1 shows the micropulsation classification. The smoothing algorithm applied to the magnetic field data is designed to highlight micropulsations with periods between 10-45 seconds. Specifically we are interested in micropulsations classified as Pc 3. Pc 3 micropulsations are generally regular and have a more or less distinct period. Thus in the PSD plots we will be able to identify the micropulsation by an apparent anomaly at its frequency. Micropulsations have amplitudes of approximately 0.5 nT. This small amplitude is very small compared to a main magnetic field value of 50,000 nT, hence the term "micro" pulsations. Geomagnetic fluctuations are a combination of micropulsations and a general background noise. Micropulsation events grow out of the ever present background. The time series magnetic field plots will provide a means of obtaining the frequency of the micropulsation.

**Table 5.1. Micropulsation Classification**

<u>Notation</u>	<u>Period (seconds)</u>
Pc1	0.2-5
Pc2	5-10
Pc3	10-45
Pc4	45-150
Pc5	150-600

## B. MICROPULSATION DATA ANALYSIS

The first 1200 seconds of data after a 60 second tape advance on digital data tape GMDT 11, 17 August 82, 1301-1408 Local, may contain a micropulsation event. Figures 3.10-3.12 show the first 34 minutes of GMDT 11 after a 60 second advance. To determine whether the regular pulsations we see in the first third of Figures 3.10-3.12 (disregarding the suspicious "cusps") is a micropulsation, the scale must be expanded. Figures 5.1-5.3 show the regular pulsations on an expanded scale. From Figures 5.1-5.3 the period of the oscillation is calculated to be 17.2 seconds. Thus this section of data contains a type Pc 3 micropulsation.

Executing the computer code LANDXYZ [Ref. 1] on this section of data, we generate the PSD, coherence, degree of polarization, and ellipticity. Table 5.2 contains the amplitude, frequency, coherence, etc. for the micropulsation.

At the frequency of the micropulsation one would expect a good coherence, degree of polarization and ellipticity since the coil system is oriented arbitrarily with each coil sensing the micropulsation. The observed micropulsation exhibits a high coherence as shown in Table 5.2. The observed micropulsation has a high degree of polarization. Micropulsations are generally considered to be left-hand elliptically polarized [Ref. 5]. The observed micropulsation is elliptically polarized.

If the errors in phase and amplitude that were shown to exist in Section IV are constant, then that should not be a

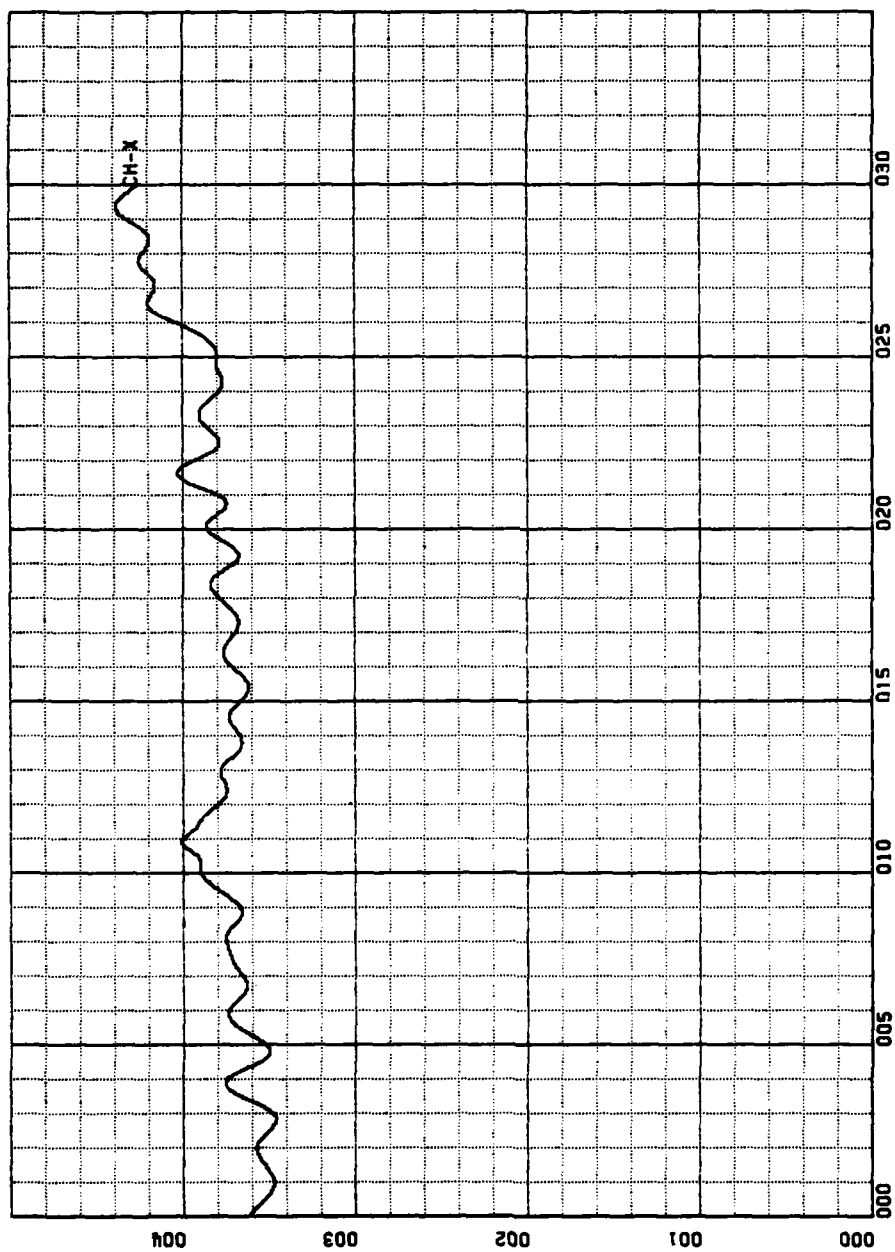


Figure 5.1. X-Coil Magnetic Field, 17 August 82, 1305-1310 Local.  
Amplitude (nanoteslas : 1 unit/in) vs. Time (seconds : 50 units/in)

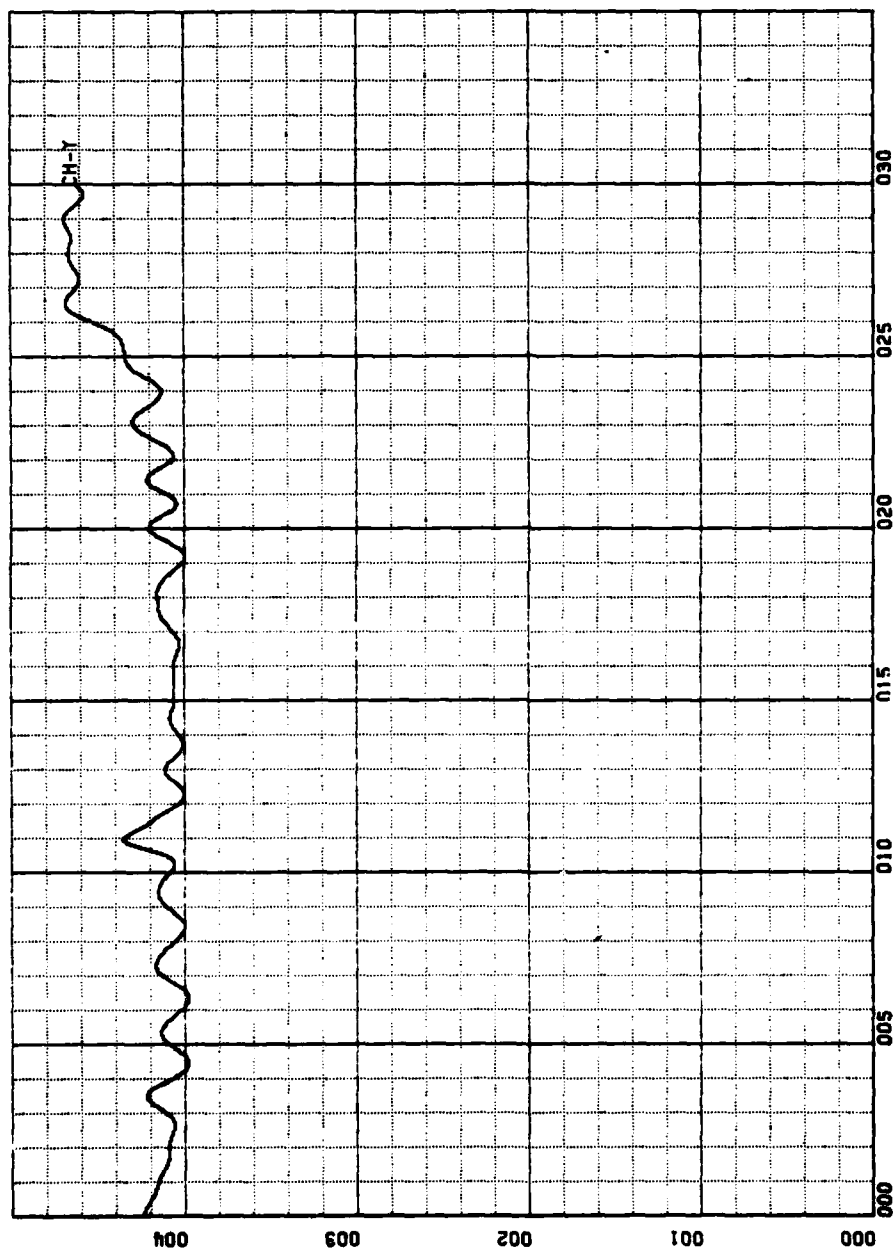


Figure 5.2. Y Coil Magnetic Field, 17 August 82, 1305-1310 Local.  
Amplitude (nanoteslas : 1 unit/in) vs. Time (seconds : 50 units/in)

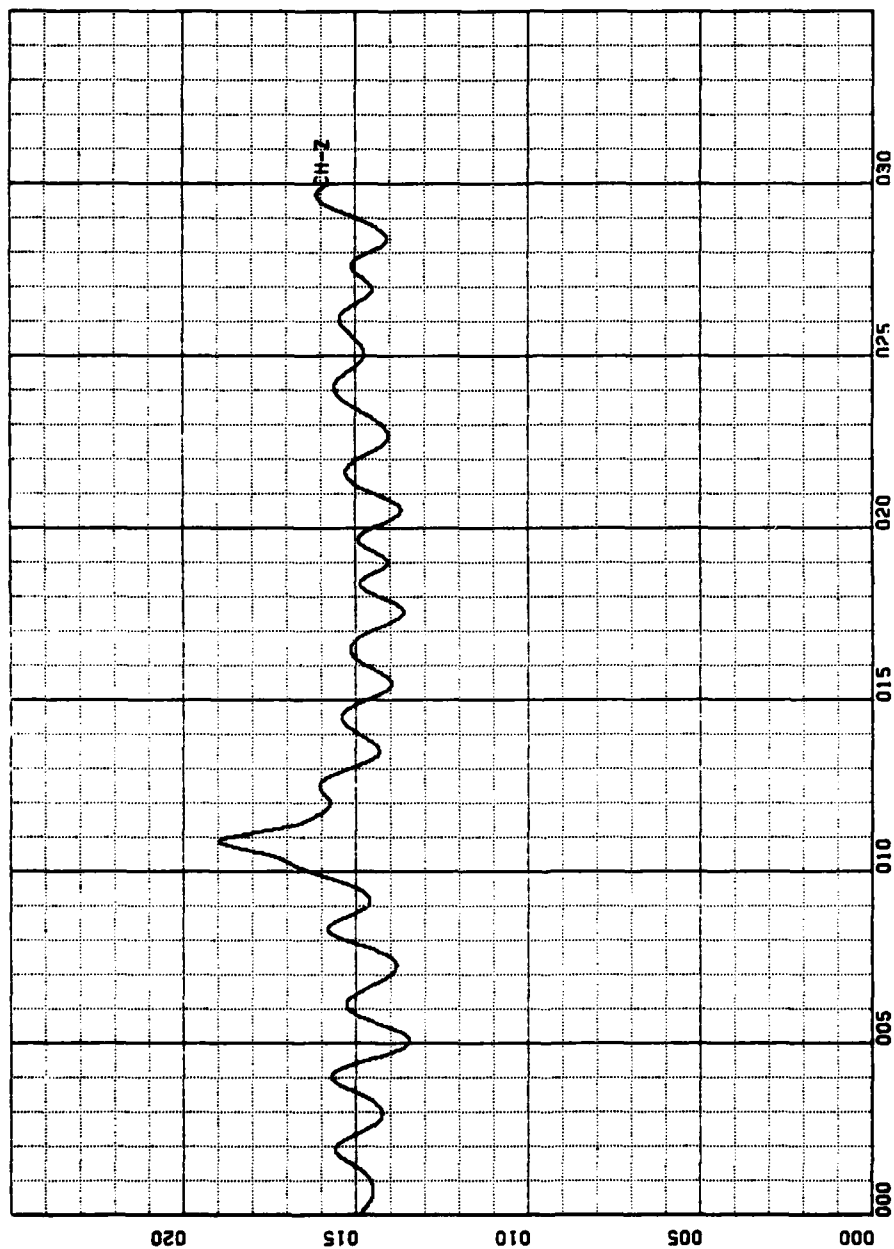


Figure 5.3. Z Coil Magnetic Field, 17 August 82, 1305-1310 Local.  
Amplitude (nanoteslas : 0.5 units/in) vs. Time (seconds : 50 units/in)



Table 5.2. Observed Micropulsation Properties

Frequency (Hz): 0.058

Peak-to-Peak Amplitude (nT): Amplitude  $= \sqrt{X^2 + Y^2 + Z^2} = 0.37$

PSD (dB) (Ref  $1 \text{ nT}^2/\text{Hz}$ ): X-Coil: -3dB

Y-Coil: -4dB

Z-Coil: 1.5dB

Coherence: X-Y Coils: 0.99

Y-Z Coils: 0.99

Z-X Coils: 0.99

Degree of Polarization: X-Y Plane: 0.99

Y-Z Plane: 0.99

Z-X Plane: 0.99

Ellipticity:

X-Y Plane: 0.45 (left hand)

Y-Z Plane: 0.10 (right hand)

Z-X Plane: 0.30 (left hand)

serious problem since we are dealing with a single frequency.  
Thus, the observed micropulsation exhibited definite structure  
decidedly different than the background.

## VI. CONCLUSIONS

A type PC-3 micropulsation event of peak-to-peak amplitude (0.37 nT) and period (17.2 seconds) was identified in a section of data. At the frequency of the micropulsation, the coherence between the three orthogonal coil sensors was about 0.99 for the xy-pair, 0.99 for the xz-pair, and 0.99 for the yz-pair. The degree of polarization was 0.99. The ellipticity was about 0.30.

The origin of the regular "hump"-like structure in the PSD's of previous coil data was found to be artificial and not representative in any way of natural phenomena in the geomagnetic field. Previous conclusions based on a frequency domain analysis of coil data characterized by a regular "hump" structure (strong or weak) in the PSD plots are known to be unsubstantiated.

Compared to a PSD frequency domain analysis of the data set, an analysis of geomagnetic field fluctuations in the time domain easily identifies data sets containing a micropulsation event. A double running average routine developed and applied to the time series data sets was found to be helpful in highlighting the micropulsation.

Detailed conclusions about the geomagnetic field from the coil measurements require a balance of analysis in the frequency and time domain.

An accurate reproduction of a time series plot for the geomagnetic field oscillations will require modification to the existing software.

Comparisons in the time or frequency domain between any pair of coils in the orthogonal system might be misleading as a result of cross talk between electrical inputs. The suspicion of cross talk is based on the observed pick-up on an unloaded input of the contents of an adjacent loaded and active input.

Further micropulsation studies should continue. This initial investigation of the coherence, polarization, and ellipticity features of micropulsation events shows promise that with more data, one might suggest novel physical mechanisms and models for the origin of micropulsations.

APPENDIX A  
VOLTR COMPUTER PROGRAM

Appendix A contains the VOLTR computer program that provides unsmoothed time series voltage plots. VOLTR uses the subroutine RD to strip voltage data off digital tapes. The integer voltage data is normalized to  $\pm 5V$  and plotted using the DRAWP subroutine.

```

//VGLISL JOB (1029,0129), STEVENS SMC 2670, CLASS=G
//*MAIN ORG=NPVMI,1029P,LINES=(65)
//*FORMAT PR,DNAME=PLOT,SYSVECTR,DEST=LOCAL
//EXEC PR,IXCLGP,PARM=LKED=LIST,MAP,XREF,REGION.GD=2048K
//FORT,SYNIN DD
INTEGER*2 IN(16)
C ARRAY IN IS USED IN READING DATA FROM TAPE
C REAL*4 XX(8192),YY(8192),ZZ(8192)
C THE ABOVE REAL*4 ARRAYS ARE USED TO ORDER INPUT DATA AND
C INITIALLY REPRESENT VOLTAGE - TIME SERIES INFORMATION.
C DIMENSION ZZ(165536),ZZY(165536),ZZV(165536)
C DIMENSION K,IS
C INTEGER*4 ITB(12)/12*0/
C REAL*4 RTB(128)/28*0.0/
C REAL ALAB(3)/CH-X,CH-Y,CH-Z/
C REAL*8 TITLE(12)
C EQUIVALENCE(TITLE(1),RTB(5))
C ARRAYS ITB,RTB,ALAB,AND TITLE ARE USED IN GENERATING
C THE VERTISATEC PLOTTER OUTPUT.
C DATA XX,YY/16384*0./
C DATA ZZ/8192*0./
C K=0
C IS=1
C DC 3 1 IN1=1,65536
C ZZ(1:IN1)=0.0
C ZZV(1:IN1)=0.0
C ZZV(1:IN1)=0.0
C TIME(1:IN1)=0.0
C 31 CCNT INUE
C THE NEXT FIVE LINES SERVE AS A TIME DELAY IN STARTING THE
C DATA ANALYSIS. ISEC IS THE NUMBER OF SECONDS DELAYED.
C ISEC=2048
C ITL=1 ISEC*32
C DC 55 JJ=1,ITL
C CALL KD(20,IN,200,IKEC,IRK)
C 55 CCNT INUE
C IFRAME=8192
C NR=8
C FNR=FLOAT(NR)
C DC 70 LI=1,NR
C THE DO LOOP ENDING WITH STATEMENT 70 ENABLES THE PROGRAM TO
C PROCESS A LARGE AMOUNT OF DATA BY REPEATING THE PROCESS IN
C BLOCKS.
C NR REPRESENTS THE NUMBER OF DATA SEQUENCES. ONE
C SEQUENCE CURRENTLY EQUALS 8192 DATA POINTS FOR EACH CHANNEL
C OR 256 SECONDS OF DATA.

```

VTH00010  
VTH00020  
VTH00030  
VTH00040  
VTH00050  
VTH00060  
VTH00070  
VTH00080  
VTH00090  
VTH00100  
VTH00110  
VTH00120  
VTH00130  
VTH00140  
VTH00150  
VTH00160  
VTH00170  
VTH00180  
VTH00190  
VTH00200  
VTH00210  
VTH00220  
VTH00230  
VTH00240  
VTH00250  
VTH00260  
VTH00270  
VTH00280  
VTH00290  
VTH00300  
VTH00310  
VTH00320  
VTH00330  
VTH00340  
VTH00350  
VTH00360  
VTH00370  
VTH00380  
VTH00390  
VTH00400  
VTH00410  
VTH00420  
VTH00430  
VTH00440  
VTH00450  
VTH00460  
VTH00470  
VTH00480

```

C C C THE DO LCCP ENDING WITH 60 READS THE DATA FROM THE PCM FRAME
C C C STRIPS OUT THE SYNC CODE, AND SORTS OUT THE DATA BY COIL
C C C CHANNEL.
C C C DO 60 JJ=1,IFRAME
C C C CALL RDI(20,IN,1000,IREC,IRR)
C C C XX(JJ)=IN(2)
C C C YY(JJ)=IN(3)
C C C ZZ(JJ)=IN(4)
C C C CCNT INUE
C C C N=8192
C C C FN=FLOAT(N)
C C C DELTAT=1./32.
C C C DO 20 J=1,N
C C C THE FOLLOWING CALCULATIONS NORMALIZE THE DATA TO +5V AND -5V.
C C C XX(JJ)=(XX(JJ)-1966.)*5./1966.
C C C YY(JJ)=(YY(JJ)-2085.)*5./2085.
C C C ZZ(JJ)=(ZZ(JJ)-2539.)*5./2539.
C C C XX IS THE X-COIL DATA, YY IS THE Y-COIL DATA,
C C C ZZ IS THE Z-COIL DATA
C C C NORTH-SOUTH COMPONENT (XX) AND THE VERTICAL COMPONENT (ZZ)
C C C CONTINUE
C C C DC 91 I3=1,8192
C C C ZZXI(I3)=XX(I3)
C C C ZZVI(I3)=YY(I3)
C C C ZZV(I3)=ZZ(I3)
C C C TIME2(I3)=(DELTAT*FLOAT(I3))+(256.0*FLOAT(K))
C C C I2=I3+1
C C C 91 CCNT INUE
C C C K=K+1
C C C 70 CCNT INUE
C C C VERSATEC PLOT OF V - TIME SERIES VOLTAGE
C C C NPIS=2048./DELTAT+1.
C C C NPIS DETERMINES NUMBER OF POINTS NECESSARY IN ORDER FOR
C C C THE 0 TO 2047 SECS RANGE TO BE PLOTTED.
C C C FOR THE FOLLOWING ITB AND KTB VALUES REVIEW THE WRITE-UP
C C C FOR THE SUBROUTINE PROCEDURE 'DRAWP'.
C C C ITB(3)=20
C C C ITB(4)=8
C C C ITB(7)=1
C C C ITB(12)=0.0
C C C RTB(1)=0.0
C C C RTB(2)=0.0
C C C RTB(3)=ALAE(1)
C C C READ(5,300C)ITILE
C C C CALL DRAWP(NPIS,TIME2,ZZXI,ITB,RTB)
C C C RTB(3)=ALAE(2)

```

```

VTH00490
VTH00500
VTH00510
VTH00520
VTH00530
VTH00540
VTH00550
VTH00560
VTH00570
VTH00580
VTH00590
VTH00600
VTH00610
VTH00620
VTH00630
VTH00640
VTH00650
VTH00660
VTH00670
VTH00680
VTH00690
VTH00700
VTH00710
VTH00720
VTH00730
VTH00740
VTH00750
VTH00760
VTH00770
VTH00780
VTH00790
VTH00800
VTH00810
VTH00820
VTH00830
VTH00840
VTH00850
VTH00860
VTH00870
VTH00880
VTH00890
VTH00900
VTH00910
VTH00920
VTH00930
VTH00940
VTH00950
VTH00960

```

VTH00970  
VTH00980  
VTH00990  
VTH01000  
VTH01010  
VTH01020  
VTH01030  
VTH01040  
VTH01050  
VTH01060  
VTH01070  
VTH01080  
VTH01090  
VTH01100  
VTH01110  
VTH01120  
VTH01130  
VTH01140  
VTH01150  
VTH01160  
VTH01170  
VTH01180  
VTH01190  
VTH01200  
VTH01210  
VTH01220  
VTH01230  
VTH01240  
VTH01250  
VTH01260  
VTH01270  
VTH01280  
VTH01290  
VTH01300  
VTH01310  
VTH01320  
VTH01330  
VTH01340  
VTH01350  
VTH01360  
VTH01370  
VTH01380  
VTH01390  
VTH01400  
VTH01410  
VTH01420  
VTH01430  
VTH01440

```

READ(5,3000)ITILE
CALL DRAMP(NPTS,TIME2,ZZV1,ITB,RTB)
RTB(3)=ALAB(3)
READ(5,3000)ITILE
CALL DRAMP(NPTS,TIME2,ZZV1,ITB,RTB)
ITB(3)=7
ITB(4)=5
ITB(12)=0
RTB(3)=ALAB(1)
READ(5,3000)ITILE
CALL DRAMP(NPTS,TIME2,ZZX1,ITB,RTB)
RTB(3)=ALAB(2)
READ(5,3000)ITILE
CALL DRAMP(NPTS,TIME2,ZZV1,ITB,RTB)
RTB(3)=ALAB(3)
READ(5,3000)ITILE
CALL DRAMP(NPTS,TIME2,ZZV1,ITB,RTB)
FORMAT(6AB)
3000 STOP
END
SUBROUTINE RD(IUN,IO,IKS,IKREC,IKQ)
THIS PROCEDURE FURNISHED BY DR. TIM STANTON,
DEPARTMENT OF OCEANOGRAPHY.
READ DATA FROM IUN, ALIGN , CHECK & RETURN
IUN=TAPE NUMBER, EG 20
IO=INTEGER*2 ARRAY, 16 LONG, (VALUES 0-4095, SUBTRACT 2048)*5
IRS= NUMBER OF RESINCS ALLUMED (ERRORS)
IKREC= COLNTER OF RECORDS (FRAMES OF DATA)
      BLOCK 512 BITS, 32 BITS = REGRD
      800 BPI TAPE UNLABLED
IKQ= NUMBER OF ACTUAL RESINCS (ERRORS)
INTEGER * 2 IO(16),IP(16)
DATA IKR /0/
IF (IKREC.EQ.0) IS=0
FOR MAT (16A2)
IF (IS.NE.0) GO TO 50
READ (IUN,20,END=900) IP
IS=IS+1
IF (IS.LT.17) GO TO 50
READ (IUN,20,END=900) IP

```

CCCCCCCCCCCCCCCC

20

40



```

50      IS=1
55      IREC=IREC+1
C      ICH=IMASK(IP(1S),3,0)+1
C      WRITE(6,55) ICH,IS,IUN,IREC
C      FORMAT('1' RESYNCH ICH,IS,IUN,IREC ',418)

      IF (ICH.NE.1) GO TO 40
      DO 100 I=1,16
      IQ(I)=ISHIFT(IP(1S),4)
      ICH=IMASK(IP(1S),3,0)+1
      IF (ICH.EQ.1) GO TO 80
      IER=IER+1
      WRITE(6,70) IUN,IREC,I,ICH,IER
      FORMAT('1' UNIT ',13,' RECORD ',16,'CHAN & DATA CH ',214,
$      ' ERRORS ',17)
      IF (IS.LI.17) GO TO 100
      READ (IUN,20,END=900) IP
      IS=1
      IREC=IREC+1
      CONTINUE
C
100      IF (IER.EC.0) GO TO 150
      IRR=IRR+1
      IF (IRR.LI.1RS) GO TO 120
      WRITE(6,110)
      FORMAT('1' STOPPED IN SUB RD BECAUSE GF IRR.GT.',16,' AT L110')
      IRQ=IRR
      STOP
      CONTINUE
120      WRITE(6,130) IREC,IRR
130      FORMAT('1' RESYNC AT FRAME ',16,' WITH TOTAL ERRORS ',17)
      IER=0
      IRQ=IRR
      GO TO 50
      CONTINUE
150      RETURN
900      WRITE(6,510) IUN,IREC
910      FORMAT('1' END OF UNIT ',13,' AT REC ',17)
      STOP
      END

FUNCTION ISHIFT(IN,NPLC)
      RETURNS SHIFTED VALUE OF I*2 WORD IN
      -VE LEFT,+VE RIGHT SHIFT
C
C
C      INTEGER * 2 IN
      IP=IN

```

VTH01450  
 VTH01460  
 VTH01470  
 VTH01480  
 VTH01490  
 VTH01500  
 VTH01510  
 VTH01520  
 VTH01530  
 VTH01540  
 VTH01550  
 VTH01560  
 VTH01570  
 VTH01580  
 VTH01590  
 VTH01600  
 VTH01610  
 VTH01620  
 VTH01630  
 VTH01640  
 VTH01650  
 VTH01660  
 VTH01670  
 VTH01680  
 VTH01690  
 VTH01700  
 VTH01710  
 VTH01720  
 VTH01730  
 VTH01740  
 VTH01750  
 VTH01760  
 VTH01770  
 VTH01780  
 VTH01790  
 VTH01800  
 VTH01810  
 VTH01820  
 VTH01830  
 VTH01840  
 VTH01850  
 VTH01860  
 VTH01870  
 VTH01880  
 VTH01890  
 VTH01900  
 VTH01910  
 VTH01920

VTH01930  
 VTH01940  
 VTH01950  
 VTH01960  
 VTH01970  
 VTH01980  
 VTH01990  
 VTH02000  
 VTH02010  
 VTH02020  
 VTH02030  
 VTH02040  
 VTH02050  
 VTH02060  
 VTH02070  
 VTH02080  
 VTH02090  
 VTH02100  
 VTH02110  
 VTH02120  
 VTH02130  
 VTH02140  
 VTH02150  
 VTH02160  
 VTH02170  
 VTH02180  
 VTH02190  
 VTH02200  
 VTH02210  
 VTH02220  
 VTH02230  
 VTH02240  
 VTH02250  
 VTH02260  
 VTH02270  
 VTH02280  
 VTH02290  
 VTH02300  
 VTH02310  
 VTH02320  
 VTH02330  
 VTH02340

```

30      IF (IP,LT,0) IP=IP+65536
        IF (NPLC,LT,0) GO TO 30
        ISHIFT=IP/(2**IABS(NPLC))
        RETURN
        ISHIFT=IP*(2**IABS(NPLC))
        IF (ISHIFT.GT.65535) ISHIFT=MOD(ISHIFT,65536)
        RETURN
        END
        FUNCTION IMASK(IN,IBL,IBR)
          MASK 1*2 WORD IN OUTSIDE BITS IBL & IBR
          INTEGER * 2 IN,IO
          IO=IN
          IF (IBR.EQ.0) GO TO 50
          IT=ISHIFT(IN,IBR)
          IO=IT
          IP=ISHIFT(IO,IBL-15-IBR)
          IO=IP
          IMASK=ISHIFT(IO,15-IBL)
          RETURN
          END
50
/*GO,SYSIN DD *
LA MESA VILLAGE, 17 AUG 82, 1324-1358 LOCAL
X COIL AMP IN VOLTS
LA MESA VILLAGE, 17 AUG 82, 2240-2314 LOCAL
Y COIL AMP IN VOLTS
LA MESA VILLAGE, 17 AUG 82, 1324-1358 LOCAL
Z COIL AMP IN VOLTS
LA MESA VILLAGE, 17 AUG 82, 1324-1358 LOCAL
X COIL AMP IN VOLTS
LA MESA VILLAGE, 17 AUG 82, 1324-1358 LOCAL
Y COIL AMP IN VOLTS
LA MESA VILLAGE, 17 AUG 82, 1324-1358 LOCAL
Z COIL AMP IN VOLTS
/*GO,FT20F001 DD UNIT=3400-4,VOL=SER=GMDT11,DISP=(OLD,KEEP),
//
// LABEL=(1,1,NL,1,IN)
// DCB=(RECFM=FB,LRECL=32,BLKSIZE=512,DEN=2)
//GO,SYSDUMP DD SYSOUT=A
//
//
  
```

APPENDIX B  
VOLTS COMPUTER PROGRAM

Appendix B contains the VOLTS computer program that provides smoothed time series voltage plots. VOLTS uses the subroutine RD to strip voltage data off digital tapes. The integer voltage data is normalized to  $\pm 5V$ . A double 144 point running average is applied to the data. The DRAWP subroutine plots the data.

```

//VLIS$IL JOB (1029,0129), 'STEVENS' SMC 2670', CLASS=G
//*MAIN OR G=NP GVM1=1029P, LINES=165)
//*FORMAT PR DDNAME=PLOT, SYSVECTR, DEST=LUCAL
// EXEC FR IXCLGP, PARM.LKED='LIST,MAP,XREF', REGION.GC=2048K
//FORT. SYSIN DD *
C      INTEGER*2 IN(16)
C      ARRAY * IN, IS USED IN READING DATA FROM TAPE
C      REAL *4 XX(8192), YY(8192), ZZ(8192)
C      THE ABOVE REAL*4 ARRAYS ARE USED TO ORDER INPUT DATA AND
C      INITIALLY REPRESENT VOLTAGE - TIME SERIES INFORMATION.
C      DIMENSION ZZXL(65536), ZZYL(65536), ZZVL(65536)
C      INTEGER K, 5, 15
C      REAL SUMX, SUMY, SUMZ, AVE1, AVE2, AVE3, AVE4
C      REAL GER*4 ITB(12)/12*0.0/
C      REAL *4 RTB(28)/28*0.0/
C      REAL ALAB(4)/CH-X, CH-Y, CH-Z, TOT, /
C      EQUIVALENCE(TITLE(1), RTB(5))
C      ARRAYS * ITB, RTB, ALAB, AND 'TITLE' ARE USED IN GENERATING
C      THE VERTSATEC PLOTTER OUTPUT.
C      DATA XX, YY, ZZ, 16384*0.0/
C      DATA ZZ/8192*0.0/
C      K=0
C      IS=1
C      SUMX=0.0
C      SUMY=0.0
C      SUMZ=0.0
C      DO 31 IN1=1, 65536
C      ZZXL(IN1)=0.0
C      ZZYL(IN1)=0.0
C      ZZVL(IN1)=0.0
C      TIME2(IN1)=0.0
C      CONTINUE
C      THE NEXT FIVE LINES SERVE AS A TIME DELAY IN STARTING THE
C      DATA ANALYSIS
C      ISEC=60
C      ITL=ISEC*32
C      DO 55 JJ=1, ITL
C      CALL RD(20, IN, 200, IREC, IRR)
C      CCNT INUE
C      IFRAME=8192
C      NR=8
C      FNR=FLOAT(NR)
C      DO 70 LI=1, NR
C      THE DO LOOP ENDING WITH STATEMENT 70 ENABLES THE PROGRAM TO
C      PROCESS A LARGE AMOUNT OF DATA BY REPEATING THE PROCESS IN
C      BLOCKS.

```

VTH00010  
 VTH00020  
 VTH00030  
 VTH00040  
 VTH00050  
 VTH00060  
 VTH00070  
 VTH00080  
 VTH00090  
 VTH00100  
 VTH00110  
 VTH00120  
 VTH00130  
 VTH00140  
 VTH00150  
 VTH00160  
 VTH00170  
 VTH00180  
 VTH00190  
 VTH00200  
 VTH00210  
 VTH00220  
 VTH00230  
 VTH00240  
 VTH00250  
 VTH00260  
 VTH00270  
 VTH00280  
 VTH00290  
 VTH00300  
 VTH00310  
 VTH00320  
 VTH00330  
 VTH00340  
 VTH00350  
 VTH00360  
 VTH00370  
 VTH00380  
 VTH00390  
 VTH00400  
 VTH00410  
 VTH00420  
 VTH00430  
 VTH00440  
 VTH00450  
 VTH00460  
 VTH00470  
 VTH00480

```

C C C C C C
      *NR* REPRESENTS THE NUMBER OF DATA SEQUENCES.
      1 SEQUENCE CURRENTLY EQUALS 8192 DATA POINTS FOR EACH CHANNEL
      OR 256 SECONDS OF DATA.

      THE DO LOOP ENDING WITH 60 READS THE DATA FROM THE PCM FRAME
      STRIPS OUT THE SYNC CODE, AND SORTS OUT THE DATA BY COIL
      CHANNEL
      DO 60 JJ=1,IFRAME
        CALL RD(20,IN,1000,IREC,IKR)
        XX(JJ)=IN(2)
        YY(JJ)=IN(3)
        ZZ(JJ)=IN(4)
      60 CONTINUE
      N=8192
      FN=FLOAT(N)
      DELTAT=1./32.
      DO 20 J=1,N
        XX(J)=XX(J)-1966.)*5./1966.
        YY(J)=YY(J)-2085.)*5./2085.
        ZZ(J)=ZZ(J)-2539.)*5./2539.
      20 CONTINUE
      *XX* IS THE X-COIL DATA, *YY* IS THE Y-COIL DATA,
      *ZZ* IS THE Z-COIL DATA
      *ZZ* IS THE SOUTH COMPONENT (XX) AND THE VERTICAL COMPONENT (ZZ)
      NORTH=0
      DO 91 I3=1,8192
        ZZ(I3)=XX(I3)
        ZZ(I3)=YY(I3)
        ZZ(I3)=ZZ(I3)
        TIME2(I3)=(DELTAT*FLCAT(I3))+(256.0*FLOAT(K))
        I5=I3+1
      91 CONTINUE
      K=K+1
      70 CONTINUE
      DO 73 L2=1,2
        Q=0
        DO 74 IS=1,65318
          SUMX=0.0
          SUMY=0.0
          SUMZ=0.0
          DO 75 J=1,144
            SUMX=ZZ(I3+(J-1)*144)+SUMX
            SUMY=ZZ(I3+(J-1)*144)+SUMY
            SUMZ=ZZ(I3+(J-1)*144)+SUMZ
          75 CONTINUE
          ZZ(I3)=SUMX/144.
          ZZ(I3)=SUMY/144.
          ZZ(I3)=SUMZ/144.
        73 CONTINUE
      70 CONTINUE
      C C C C C C

```

VTH00490  
 VTH00500  
 VTH00510  
 VTH00520  
 VTH00530  
 VTH00540  
 VTH00550  
 VTH00560  
 VTH00570  
 VTH00580  
 VTH00590  
 VTH00600  
 VTH00610  
 VTH00620  
 VTH00630  
 VTH00640  
 VTH00650  
 VTH00660  
 VTH00670  
 VTH00680  
 VTH00690  
 VTH00700  
 VTH00710  
 VTH00720  
 VTH00730  
 VTH00740  
 VTH00750  
 VTH00760  
 VTH00770  
 VTH00780  
 VTH00790  
 VTH00800  
 VTH00810  
 VTH00820  
 VTH00830  
 VTH00840  
 VTH00850  
 VTH00860  
 VTH00870  
 VTH00880  
 VTH00890  
 VTH00900  
 VTH00910  
 VTH00920  
 VTH00930  
 VTH00940  
 VTH00950  
 VTH00960



VTH01450  
 VTH01460  
 VTH01470  
 VTH01480  
 VTH01490  
 VTH01500  
 VTH01510  
 VTH01520  
 VTH01530  
 VTH01540  
 VTH01550  
 VTH01560  
 VTH01570  
 VTH01580

Z COIL AMP IN VOLTS  
 LA MESA VILLAGE, 17 AUG 82, 1302-1336 LOCAL  
 X COIL AMP IN VOLTS  
 LA MESA VILLAGE, 17 AUG 82, 1302-1336 LOCAL  
 Y COIL AMP IN VOLTS  
 LA MESA VILLAGE, 17 AUG 82, 1302-1336 LOCAL  
 Z COIL AMP IN VOLTS  
 7\*  
 //GO.FT20F001 00 UNIT=3400-4, VOL=SER=GMDT3A, DISP=(OLD,KEEP),  
 // LABEL=111NLINJ  
 // DCB=(RECFM=FB, LRECL=32, BLKSIZE=512, DEN=2)  
 //GO.SYSDUMP DD SYSOUT=A  
 //\*  
 //

## APPENDIX C

### LFVTC1 COMPUTER PROGRAM

Appendix C contains the LFVTC1 computer program that provides smoothed time series magnetic field plots. LFVTC1 uses the subroutine RD to strip voltage data off digital tapes. The voltage data is normalized to  $\pm 5V$ . The voltage data is fast fourier transformed using the FOURT subroutine. The transfer function is applied and forward transform taken. The resulting magnetic field data undergoes a double 144 point running average and is plotted using the DRAWP subroutine.





MAG00490  
MAG00500  
MAG00510  
MAG00520  
MAG00530  
MAG00540  
MAG00550  
MAG00560  
MAG00570  
MAG00580  
MAG00590  
MAG00600  
MAG00610  
MAG00620  
MAG00630  
MAG00640  
MAG00650  
MAG00660  
MAG00670  
MAG00680  
MAG00690  
MAG00700  
MAG00710  
MAG00720  
MAG00730  
MAG00740  
MAG00750  
MAG00760  
MAG00770  
MAG00780  
MAG00790  
MAG00800  
MAG00810  
MAG00820  
MAG00830  
MAG00840  
MAG00850  
MAG00860  
MAG00870  
MAG00880  
MAG00890  
MAG00900  
MAG00910  
MAG00920  
MAG00930  
MAG00940  
MAG00950  
MAG00960

```

TWOPI=6.2831853
COS60=COS(TWOPI/6.)
COS30=COS(TWOPI/12.)
D=16.75*TWOPI/360.
COSD=COS(D)
COSD1=COS(D190. - D)*TWOPI/360.)
D1 IS THE DECLINATION OR MAGNETIC VARIATION AT THE MAGNETOMETER
SITE
DO 31 IN1=1,65536
  ZZXI(IN1)=0.0
  ZZYI(IN1)=0.0
  ZZVI(IN1)=0.0
  ZZTI(IN1)=0.0
  TIME2(IN1)=0.0
31 CONTINUE
  THE NEXT FIVE LINES SERVE AS A TIME DELAY IN STARTING THE
  DATA ANALYSIS
  ISEC=60
  IYL=1 SEC*32
  DO 55 JJ=1,ITL
    CALL RD(20,IN,200,IREC,IRR)
55 CONTINUE
    IFRAME=8192
    NR=8
    FAR=FLOAT(NR)
    DO 70 LI=1,NR
      THE DO LOOP ENDING WITH STATEMENT 70 ENABLES THE PROGRAM TO
      PROCESS A LARGE AMOUNT OF DATA BY REPEATING THE PROCESS IN
      BLOCKS
      NR REPRESENTS THE NUMBER OF DATA SEQUENCES TO BE AVERAGED.
      I SEQUENCE CURRENTLY EQUALS 8192 DATA POINTS FOR EACH CHANNEL
      OR 256 SECONDS OF DATA.
      THE DO LCCP ENDING WITH 60 READS THE DATA FROM THE PCM FRAME
      STRIPS OUT THE SYNC CODE, AND SORTS OUT THE DATA BY COIL
      CHANNEL
      DO 60 JJ=1,IFRAME
        CALL RD(20,IN,1000,IREC,IRR)
        XX(JJ)=IN(2)
        YY(JJ)=IN(3)
        ZZ(JJ)=IN(4)
60 CONTINUE
      THE FOLLOWING SECTION GENERATES THE TIME AND FREQUENCY
      ARRAYS AND NORMALIZES THE INPUT PCM DATA TO VOLTAGE FORM
      IN PREPARATION FOR FAST FOURIER TRANSFORM TO THE FREQUENCY
      DOMAIN.
      N=8192
      FN=FLOAT(N)

```

MAG00970  
MAG00980  
MAG00990  
MAG01000  
MAG01010  
MAG01020  
MAG01030  
MAG01040  
MAG01050  
MAG01060  
MAG01070  
MAG01080  
MAG01090  
MAG01100  
MAG01110  
MAG01120  
MAG01130  
MAG01140  
MAG01150  
MAG01160  
MAG01170  
MAG01180  
MAG01190  
MAG01200  
MAG01210  
MAG01220  
MAG01230  
MAG01240  
MAG01250  
MAG01260  
MAG01270  
MAG01280  
MAG01290  
MAG01300  
MAG01310  
MAG01320  
MAG01330  
MAG01340  
MAG01350  
MAG01360  
MAG01370  
MAG01380  
MAG01390  
MAG01400  
MAG01410  
MAG01420  
MAG01430  
MAG01440

```

DELTAT=1./32.
DELTAF=1./ (FN*DELTAT)
DC 20 J=1,N
TIME(J)=DELTAT*FLOAT(J)
FREQ(J)=DELTAF*FLOAT(J)
XX(J)=(XX(J)-1966.*5./1966.
XX(J)=REAL(XX(J))
YY(J)=(YY(J)-2085.*5./2085.
YY(J)=REAL(YY(J))
ZZ(J)=(ZZ(J)-2539.*5./2539.
ZZ(J)=REAL(ZZ(J))
*XX* IS THE X-COIL DATA, *YY* IS THE Y-COIL DATA,
*ZZ* IS THE Z-COIL DATA, AND *TF* IS THE PROJECTION OF THE
NORTH-SOUTH COMPONENT (XX) AND THE VERTICAL COMPONENT (ZZ)
ON THE TCTAL GEOMAGNETIC FIELD VECTOR.
ON THE TCTAL GEOMAGNETIC FIELD VECTOR.
20 CONTINUE
DC 21 J=1,N
FREQ(J)=ALOG10(FREQ(J))
21 CONTINUE
THE NEXT FOUR STATEMENTS PERFORM AN FFT ON THE INPUT
TIME SERIES DATA. SEE THE WRITEUP ON 'FOUR' FOR
FURTHER INFORMATION.
CALL FOURT(XX,N,1,-1.0,WORK)
CALL FOURT(YY,N,1,-1.0,WORK)
CALL FOURT(ZZ,N,1,-1.0,WORK)
THE NEXT BLOCK OF STATEMENTS APPLY THE SYSTEM (VOLTAGE TO
B-FIELD) TRANSFER FUNCTION TO THE TRANSFORMED FREQUENCY
DOMAIN DATA. THIS BLOCK ENDS AT STATEMENT 9.
THE TRANSFER FUNCTION CONVERTS VOLTS TO NANOTESLAS (GAMMAS).
***WARNING*** THIS TRANSFER FUNCTIONS YIELDS AN INACCURATE
PHASE. USE A DIFFERENT TRANSFER FUNCTION IF PHASE INFORMATION
NEEDED.
DC 9 L=1,N
FREQ=FREQ(L)
IF (FREQ.LE.25.1) GO TO 1
XX(L)=XX(L)/28.
GO TO 8
1 IF (FREQ.LE.15.1) GO TO 2
XX(L)=XX(L)/(105.5-3.14*FREQ)
YY(L)=YY(L)/(181.32-7.588*FREQ)
ZZ(L)=ZZ(L)/(177.26-7.484*FREQ)
GO TO 8
2 IF (FREQ.LE.10.1) GO TO 3
XX(L)=XX(L)/(5.958*FREQ-30.97)
YY(L)=YY(L)/(7.166*FREQ-39.99)
ZZ(L)=ZZ(L)/(6.49*FREQ-32.35)
GO TO 8
3 IF (FREQ.LE.7.5) GO TO 4

```

MAGO1450  
MAGO1460  
MAGO1470  
MAGO1480  
MAGO1490  
MAGO1500  
MAGO1510  
MAGO1520  
MAGO1530  
MAGO1540  
MAGO1550  
MAGO1560  
MAGO1570  
MAGO1580  
MAGO1590  
MAGO1600  
MAGO1610  
MAGO1620  
MAGO1630  
MAGO1640  
MAGO1650  
MAGO1660  
MAGO1670  
MAGO1680  
MAGO1690  
MAGO1700  
MAGO1710  
MAGO1720  
MAGO1730  
MAGO1740  
MAGO1750  
MAGO1760  
MAGO1770  
MAGO1780  
MAGO1790  
MAGO1800  
MAGO1810  
MAGO1820  
MAGO1830  
MAGO1840  
MAGO1850  
MAGO1860  
MAGO1870  
MAGO1880  
MAGO1890  
MAGO1900  
MAGO1910  
MAGO1920

```

XX(L)=XX(L)/13.492*FRQ-6.31)
YY(L)=YY(L)/(4.252*FRQ-10.85)
ZZ(L)=ZZ(L)/(14.044*FRQ-7.89)
GO TO 8
4 IF (FRQ.LE.5) GO TO 5
  XX(L)=XX(L)/(2.6311*FRQ+0.14667)
  YY(L)=YY(L)/(3.012*FRQ-1.55)
  ZZ(L)=ZZ(L)/(3.184*FRQ-1.44)
GO TO 8
5 IF (FRQ.LE.3) GO TO 6
  XX(L)=XX(L)/(2.6311*FRQ+0.14667)
  YY(L)=YY(L)/(2.702*FRQ)
  ZZ(L)=ZZ(L)/(2.92*FRQ)
GO TO 8
6 XX(L)=XX(L)/(2.72*FRQ)
GO TO 7
8 CCNT INUE
9 IF (L)=(XX(L)*COSD + YY(L)*CUSD1)*COS60 + ZZ(L)*COS30
  CCNT INUE
  CALL FOURT(XX,N,1,1,1,WORK)
  CALL FOURT(YY,N,1,1,1,WORK)
  CALL FOURT(ZZ,N,1,1,1,WORK)
  DO 57 J=1,N
    XX(J)=XX(J)/FN
    YY(J)=YY(J)/FN
    ZZ(J)=ZZ(J)/FN
    TF(J)=TF(J)/FN
57 CCNT INUE
  ZY1(13)=CABS(YY(13))
  ZY1(13)=CABS(ZY1(13))
  ZY1(13)=CABS(ZY1(13))
  ZY1(13)=CABS(ZY1(13))
  CCNT INUE
56 THE NEXT 44 LINES OF CODE CORRECT DATA BLOCK END JUMPS.
  IF (K.NE.0) GO TO 36
  DO 66 IS=8048,8192
    SUMX=ZY1(13)+SUMX
    SUMY=ZY1(13)+SUMY
    SUMZ=ZY1(13)+SUMZ
    SUMT=ZY1(13)+SUMT
66 CCNT INUE
    CCNSTX=SUMX/144.
    CCNSTY=SUMY/144.
    CCNSTZ=SUMZ/144.
    CCNSTT=SUMT/144.
  DO 67 IS=1,8192

```

MAGO1930  
MAGO1940  
MAGO1950  
MAGO1960  
MAGO1970  
MAGO1980  
MAGO1990  
MAGO2000  
MAGO2010  
MAGO2020  
MAGO2030  
MAGO2040  
MAGO2050  
MAGO2060  
MAGO2070  
MAGO2080  
MAGO2090  
MAGO2100  
MAGO2110  
MAGO2120  
MAGO2130  
MAGO2140  
MAGO2150  
MAGO2160  
MAGO2170  
MAGO2180  
MAGO2190  
MAGO2200  
MAGO2210  
MAGO2220  
MAGO2230  
MAGO2240  
MAGO2250  
MAGO2260  
MAGO2270  
MAGO2280  
MAGO2290  
MAGO2300  
MAGO2310  
MAGO2320  
MAGO2330  
MAGO2340  
MAGO2350  
MAGO2360  
MAGO2370  
MAGO2380  
MAGO2390  
MAGO2400

```

ZZXI(I4)=ZXI(I5)
ZZVI(I4)=ZVI(I5)
ZZTI(I4)=ZTI(I5)
I4=I4+1
67 CONTINUE
36 CONTINUE
SUMX=0.0
SUMY=0.0
SUMZ=0.0
SUMT=0.0
DO 68 IS=1,144
SUMX=ZXI(I5)+SUMX
SUMY=ZVI(I5)+SUMY
SUMZ=ZTI(I5)+SUMZ
SUMT=ZTI(I5)+SUMT
68 CONTINUE
AVE1=SUMX/144.
AVE2=SUMY/144.
AVE3=SUMZ/144.
AVE4=SUMT/144.
DO 69 IS=1,8192
ZZXI(I4)=ZXI(I5)+{(CONSTX-AVE1)}
ZZVI(I4)=ZVI(I5)+{(CONSTY-AVE2)}
ZZTI(I4)=ZTI(I5)+{(CONSTZ-AVE3)}
ZZTI(I4)=ZTI(I5)+{(CONSTT-AVE4)}
I4=I4+1
69 CONTINUE
37 CONTINUE
TIME2(I5)={DELTA*FLOAT(I3)}+(256.0*FLOAT(K))
IS=IS+1
91 CONTINUE
70 CONTINUE
C THE FOLLOWING LINES OF CODE PERFORMS A DOUBLE RUNNING POINT
C AVERAGE ON THE DATA.
DC 73 L2=1,2
Q=0
DO 74 IS=1,65318
SUMX=0.0
SUMY=0.0
SUMZ=0.0
SUMT=0.0
DC 75 J=1,144
SUMX=ZZXI(I4+J)+SUMX
SUMY=ZZVI(I4+J)+SUMY

```



```

CALL DRAWP(NPTS,TIME2,ZZVL,ITB,KTB)
ITB(12)=1
RTB(3)=ALAB(4)
READ(5,3000)TITLE
CALL DRAWP(NPTS,TIME2,ZZTL,ITB,RTB)
FORMAT(6A8)
3000 STOP
      END
/*
//GO.SYSIN DC *
//LA MESA VILLAGE, 18 AUG 82, 1825-1859 LOCAL
//X COIL AMP IN NT
//LA MESA VILLAGE, 18 AUG 82, 1825-1859 LOCAL
//Y COIL AMP IN NT
//LA MESA VILLAGE, 18 AUG 82, 1825-1859 LOCAL
//Z COIL AMP IN NT
//LA MESA VILLAGE, 18 AUG 82, 1825-1859 LOCAL
//TCTAL FIELD AMP IN NT
//LA MESA VILLAGE, 18 AUG 82, 1825-1859 LOCAL
//X COIL AMP IN NT
//LA MESA VILLAGE, 18 AUG 82, 1825-1859 LOCAL
//Y COIL AMP IN NT
//LA MESA VILLAGE, 18 AUG 82, 1825-1859 LOCAL
//Z COIL AMP IN NT
//LA MESA VILLAGE, 17 AUG 82, 1825-1859 LOCAL
//TCTAL FIELD AMP IN NT
/*
//GO.FT20F001 DD UNIT=3400-4,VOL=SER=GMDT21,DISP=(OLD,KEEP),
//LABEL=(1,1,1,1)
//DCB=(RECFM=FB,LRECL=32,BLKSIZE=512,DEN=2)
//GO.SYSJUMP DD SYSOUT=A
//

```

#### LIST OF REFERENCES

1. Pogue, E. W., "Experimental Observations of Geomagnetic Micropulsations: Land and Sea", Master's Thesis, Naval Postgraduate School, Monterey, September 1982.
2. Gritzke, A. R. and Johnson, R. H., "Ocean Floor Geomagnetic Data Collection System", Master's Thesis, Naval Postgraduate School, Monterey, December 1982.
3. Fisher, J. T., "Coherence in the Horizontal Plane of the Geomagnetic Field in the Frequency Range of 0-10 Hz", Master's Thesis, Naval Postgraduate School, Monterey, December 1982.
4. Schweiger, J. M., "Evaluation of Geomagnetic Activity in the MAD Frequency Band (.04 to .06 Hz)", Master's Thesis, Naval Postgraduate School, Monterey, September 1982.
5. Jacobs, J. A., "Geomagnetic Micropulsations", p. 35-39, Springer-Verlay, 1970.
6. Jackson, J. D., "Classical Electrodynamics", p. 145-148, John Wiley and Sons, Inc., 1962.
7. Moose, P. A. and Thomas M. E., "Polarization Characteristics of Geomagnetic Fluctuations", Transactions American Geophysical Union, vol. 64, no. 18, p. 212, May 1983.



INITIAL DISTRIBUTION LIST

	<u>No. Copies</u>
1. Defense Technical Information Center Cameron Station Alexandria, Virginia 22314	2
2. Library, Code 0142 Naval Postgraduate School Monterey, California 93940	2
3. Dr. Otto Heinz, Code 61Hz Department of Physics Naval Postgraduate School Monterey, California 93940	2
4. Dr. Andrew R. Ochadlick Jr., Code 610C Department of Physics Naval Postgraduate School Monterey, California 93940	2
5. Dr. Paul Moose, Code 62Me Department of Electrical Engineering Naval Postgraduate School Monterey, California 93940	1
6. Dr. Michael Thomas Applied Physics Lab, JHU Submarine Technology Division Johns Hopkins Road Laurel, MD 20707	1
7. CPT Kurt B. Stevens 45 Tuscarora Street Addison, New York 14801	2
8. Office of Naval Research Attn: Mr. John G. Heacock Code 425 GG 800 N. Quincy Street Arlington, VA 22217	1
9. Naval Air Development Center Attn: Mr. Edward Yannuzzi Code 30 Warminster, PA 18974	1

10. Naval Air Systems Command  
Attn: Mr. Barry Dillon  
Code AIR-340J  
Washington, DC 20361

1

END

DATE  
FILMED

9 83